International Ocean Discovery Program Expedition 354 Preliminary Report Bengal Fan

Christian France-Lanord, Volkhard Spiess, T. Schwenk, Adam Klaus, R.R. Adhikari, S.K. Adhikari, J.-J. Bahk, A.T. Baxter, J.W. Cruz, S.K. Das, et al.

International Ocean Discovery Program Expedition 354 Preliminary Report

Bengal Fan

Neogene and late Paleogene record of Himalayan orogeny and climate: a transect across the Middle Bengal Fan

30 January–31 March 2015

Christian France-Lanord, Volkard Spiess, Adam Klaus,
and the Expedition 354 Scientists

IODP
INTERNATIONAL OCEAN DISCOVERY PROGRAM

Publisher's notes

Core samples and the wider set of data from the science program covered in this report are under moratorium and accessible only to Science Party members until 7 September 2016.

This publication was prepared by the International Ocean Discovery Program *JOIDES Resolution* Science Operator (IODP JRSO) as an account of work performed under the International Ocean Discovery Program. Funding for the program is provided by the following implementing organizations and international partners:

National Science Foundation (NSF), United States
Ministry of Education, Culture, Sports, Science and Technology (MEXT), Japan
European Consortium for Ocean Research Drilling (ECORD)
Ministry of Science and Technology (MOST), People's Republic of China
Korea Institute of Geoscience and Mineral Resources (KIGAM)
Australia-New Zealand IODP Consortium (ANZIC)
Ministry of Earth Sciences (MoES), India
Coordination for Improvement of Higher Education Personnel, Brazil

Disclaimer

Any opinions, findings, and conclusions or recommendations expressed in this publication are those of the author(s) and do not necessarily reflect the views of the participating agencies, Texas A&M University, or Texas A&M Research Foundation.

Portions of this work may have been published in whole or in part in other International Ocean Discovery Program documents or publications.

Copyright

Citation:

France-Lanord, C., Spiess, V., Klaus, A., and the Expedition 354 Scientists, 2015. Bengal Fan: Neogene and late Paleogene record of Himalayan orogeny and climate: a transect across the Middle Bengal Fan. *International Ocean Discovery Program Preliminary Report*, 353. http://dx.doi.org/10.14379/iodp.pr.354.2015

ISSN
World Wide Web: 2372-9562

May 2015

Expedition 354 participants

Expedition 354 scientists

Christian France-Lanord
Co-Chief Scientist
Centre de Recherches Pétrographiques et Géochimiques
Centre National de la Recherche Scientifique (CNRS)
BP 20, 15 Rue Notre-Dame-des-Pauvres
54500 Vandoeuvre les Nancy Cedex
France
cfl@crpg.cnrs-nancy.fr

Volkhard Spiess
Co-Chief Scientist
Department of Geosciences
University of Bremen
Klagenfurter Strasse
28359 Bremen
Germany
vspiess@uni-bremen.de

Tilmann Schwenk
Shorebased Scientist
Department of Geosciences
University of Bremen
Klagenfurter Strasse 28359
Bremen
Germany
tschwenk@marum.de

Adam Klaus
Expedition Project Manager/ Staff Scientist
JOIDES Resolution Science Operator
International Ocean Discovery Program
Texas A&M University
1000 Discovery Drive
College Station TX 77845
USA
aklaus@iodp.tamu.edu

Rishi R. Adhikari
Organic Geochemist
MARUM
University of Bremen
Leobener Strasse
28539 Bremen
Germany
radhikari@marum.de

Swostik K. Adhikari
Sedimentologist
Department of Geoscience
Shimane University
Matsue 690-8504
Japan
swostik_adhikari@hotmail.com

Jang-Jun Bahk
Sedimentologist
Petroleum and Marine Research Division
Korea Institute of Geoscience and Mineral Resources (KIGAM)
124 Gwahang-no
Yuseong-gu Daejeon 305-350
Republic of Korea
jjbahk@kigam.re.kr

Alan T. Baxter
Paleontologist (nannofossils)
School of Environmental and Rural Science
University of New England
Earth Sciences Building C02, Room 211
Armidale NSW 2351
Australia
alan.baxter@une.edu.au

Jarrett W. Cruz
Paleontologist (nannofossils)
Department of Earth, Ocean and Atmospheric Sciences
Florida State University
1806 Atkamire Drive
Tallahassee FL 32304
USA
Jwc09e@my.fsu.edu

Supriyo Kumar Das
Department of Geology
Presidency University
86/1 College Street
Kolkata 700073
West Bengal
India
sdas.geol@presiuniv.ac.in
das.supriyo.kumar@gmail.com

Petra Dekens
Paleontologist (foraminifers)
Department of Earth & Climate Sciences
San Francisco State University
1600 Holloway Avenue
San Francisco CA 94131
dekens@sfsu.edu

Wania Duleba
Paleontologist (foraminifers)
EACH/USP and Instituto de Geociencias
Universidade de Sao Paulo
Laboratorio de Micropaleontologia
Rua do Lago, 562
Sao Paulo, SP 05508-0800
Brazil
waduleba@gmail.com

Lyndsey R. Fox
Paleontologist (foraminifers)
School of Earth and Environment
University of Leeds
Leeds LS2 9JT
United Kingdom
eelrf@leeds.ac.uk

Albert Galy
Inorganic Geochemist
Centre de Recherches Pétrographiques et Géochimiques
Cenre National de la Recherche Scientifique (CNRS)
BP 20, 15 Rue Notre-Dame-des-Pauvres
54501 Vandoeuvre les Nancy Cedex
France
agaly@crpg.cnrs-nancy.fr

Valier Galy
Organic Geochemist
Department of Marine Chemistry and Geochemistry
Woods Hole Oceanographic Institution
360 Woods Hole Road, MS#4, Fye 107D
Woods Hole MA 02543
USA
vgaly@whoi.edu

Junyi Ge
Physical Properties Specialist
Institute of Vertebrate Paleontology and Paleoanthropology
Chinese Academy of Sciences
142 Xizhimenwai Street
Beijing
China
gejunyi@ivpp.ac.cn

James D. Gleason
Inorganic Geochemist
Department of Earth and Environmental Sciences
University of Michigan
2534 C.C. Little Building
1100 North University Avenue
Ann Arbor MI 48109-1005
USA
jdgleaso@umich.edu

Babu R. Gyawali
Paleontologist (nannofossils)
Department of Earth Science
Tohoku University
Aramaki Aza Aoba 6-3, Aoba-ku
Sendai 980-8578
Japan
gyawali.b@dc.tohoku.ac.jp

Pascale Huyghe
Sedimentologist
ISTerre
1381 rue de la Piscine
University Joseph Fourier
38041 Grenoble
France
pascale.huyghe@ujf-grenoble.fr

Guodong Jia
Organic Geochemist
Guangzhou Institute of Geochemistry
Chinese Academy of Sciences
511 Kehua Street, Tianhe District
Guangzhou 510640
China
jiagd@gig.ac.cn

Hendrik Lantzsch
Sedimentologist
University of Bremen
FB5, GEO, Room 2540
Klagenfurter Strasse
28359 Bremen
Germany
lantzsch@uni-bremen.de

M.C. Manoj
Sedimentologist
Marine Micropalaeontology
Birbal Sahni Institute of Palaeobotany
53 University Road
Lucknow, Uttar Pradesh 226007
India
manoj.mcm@gmail.com

Yasmina Martos Martin
Staff Scientist Trainee
International Ocean Discovery Program
1000 Discovery Drive
College Station TX 77845
yasmartos@gmail.com

Laure Meynadier
Paleomagnetist
Institut de Physique du Globe
Université Paris Diderot
Sorbonne Paris Cité
1 rue Jussieu
75005 Paris
France
meynadier@ipgp.fr

Yani M.R. Najman
Sedimentologist
Lancaster Environment Centre
Lancaster University
Lancaster LA1 4YQ
United Kingdom
y.najman@lancs.ac.uk

Arata Nakajima
Physical Properties Specialist
Department of Geology and Mineralogical Sciences
Yamaguchi University
1611-1 Yoshida
Yamaguchi
Japan
arata.nakajima@gmail.com

Camilo Ponton
Sedimentologist
Department of Earth Sciences
University of Southern California
3651 Trousdale Parkway, ZHS-117
Los Angeles CA 90089
USA
cponton@usc.edu

Brendan T. Reilly
Paleomagnetist
College of Earth, Ocean and Atmospheric Sciences
Oregon State University
104 CEOAS Administration Building
Corvallis OR 97331
USA
breilly@coas.oregonstate.edu

Kimberly G. Rogers
Sedimentologist
Institute of Arctic and Alpine Research
University of Colorado at Boulder
4001 Discovery Drive
Boulder CO 80303
USA
kgrogers@colorado.edu

Jairo F. Savian
Paleomagnetist
Departamento de Geologia
Instituto de Geociências
Universidade Federal do Rio Grande do Sul
Avenida Bento Gonçalves, 9500, Prédio 43126, Sala 206B
Campus do Vale, Agronomia
Porto Alegre 91501-970
Brazil
jairo.savian@ufrgs.br

Peter A. Selkin
Paleomagnetist
School of Interdisciplinary Arts and Sciences
University of Washington, Tacoma
1900 Commerce Street, Box 358436
Tacoma WA 98402
USA
paselkin@uw.edu

Michael E. Weber
Physical Properties Specialist
Geologisches Institut
Universität Kõln
Zuelpicher Strasse 49a
50935 Cologne
Germany
michael.weber@uni-koeln.de

Trevor Williams
Downhole Measurements and Physical Properties Specialist
Borehole Research Group
Lamont-Doherty Earth Observatory of Columbia University
PO Box 1000, 61 Route 9W
Palisades NY 10964
USA
trevor@ldeo.columbia.edu

Koki Yoshida
Sedimentologist
Department of Geology
Faculty of Science
Shinshu University
Asahi 3-1-1
Matsumoto 390-0812
Japan
kxyoshid@shinshu-u.ac.jp

Education and outreach

Diane Hanano
Education Officer
IODP-Canada
University of British Columbia
#2020 - 2207 Main Mall
Vancouver BC V6T 1Z4
Canada
dhanano@eos.ubc.ca

Lisa Strong
Education Officer
Lisa Strong, Video/Multimedia Producer
Strong Mountain Productions
Marin California 94965
USA
lisa@strongmountain.com

Siem Offshore AS Officials

Steve Bradley
Master of the Drilling Vessel

Wayne Malone
Offshore Installation Manager

Technical suport

Lisa Brandt
Chemistry Laboratory

James Cordray
Marine Computer Specialist

Lisa Crowder
Assistant Laboratory Officer

Benjamin Daniel
Marine Laboratory Specialist (temporary)

Seth Frank
X-Ray/Microbiology Laboratory

Timothy Fulton
Imaging Specialist

Clayton Furman
Schlumberger Engineer

Randy Gjesvold
Marine Instrumentation Specialist

Sandra Herrmann
Assistant Laboratory Officer

Michael Hodge
Marine Computer Specialist

Dwight Hornbacher
Applications Developer

Hannah Kastor
Curator

Zenon Mateo
Core Laboratory

Stephen Midgley
Operations Superintendent

William Mills
Laboratory Officer

Beth Novak
Paleomagnetism Laboratory

Sonja Storm
Marine Laboratory Specialist

Garrick Van Rensburg
Marine Instrumentation Specialist

Jean Wulfson
Publications Specialist

Hai Zhao
Applications Developer

Abstract

International Ocean Discovery Expedition 354 to 8°N in the Bay of Bengal drilled a seven site, 320 km long transect across the Bengal Fan. Three deep-penetration and an additional four shallow holes give a spatial overview of the primarily turbiditic depositional system that comprises the Bengal deep-sea fan. Sediments originate from Himalayan rivers, documenting terrestrial changes of Himalayan erosion and weathering, and are transported through a delta and shelf canyon, supplying turbidity currents loaded with a full spectrum of grain sizes. Mostly following transport channels, sediments deposit on and between levees while depocenters laterally shift over hundreds of kilometers on millennial timescales. During Expedition 354, these deposits were documented in space and time, and the recovered sediments have Himalayan mineralogical and geochemical signatures relevant for reconstructing time series of erosion, weathering, and changes in source regions, as well as impacts on the global carbon cycle. Miocene shifts in terrestrial vegetation, sediment budget, and style of sediment transport were tracked. Expedition 354 has extended the record of early fan deposition by 10 My into the late Oligocene.

Introduction

Of regions where tectonics and climate interact, southern Asia seems to illustrate their possible influences on each other more dramatically than any other region. The high elevation of the Tibetan Plateau and the rapid rise from the lowlands of northern India across the Himalaya profoundly affect both the average temperature structure of the atmosphere responsible for the seasonal winds and the distribution of precipitation that characterize the south Asian monsoon (Molnar et al., 2010; Boos and Kuang, 2011). Concurrently, monsoonal precipitation along the Himalaya generates one of the most important erosion fluxes of the planet. This surface mass transfer acts on the thermal structure and stress field of the mountain range and partly controls its morphology (Avouac and Burov, 1996). Finally, the erosion processes contribute to the global atmospheric CO_2 drawdown responsible for Cenozoic global cooling (Fig. **F1**) through organic carbon burial and silicate weathering. However, if the Tibetan Plateau and the Himalaya have influenced climate during Cenozoic time, the evidence suggesting such an influence is wholly inadequate to understand quantitatively how these geographical features have developed through time. This inadequacy is mostly due to the fact that direct records of the erosion of the mountain range are rare or limited in duration, so there is no consensus on the mass accumulation rate generated by the Tibet-Himalayan erosion to date (Métivier et al., 1999; Clift, 2006). Because of the lack of adequate sedimentary archives, the early stages of Himalayan evolution since the continental collision ~55 My ago to the Miocene are essentially unknown.

Expedition 354 was proposed to obtain data that can not only test hypothetical links between climate and tectonics but also provide new data not easily acquired but relevant for understanding a number of Earth processes. This expedition focuses on the erosional record of the Himalaya and on the development of the Asian monsoon over Cenozoic time. Because geology lacks the tools for determining paleoelevations except in unusual and ideal circumstances, the sedimentary record of material eroded from a mountain belt holds the least ambiguous record of its paleotopography. Approximately 80% of the material eroded from the Himalaya was deposited in the Bay of Bengal, which therefore hosts the most complete record.

Reconstructing accumulation rates from fan deposits is challenging because (1) the 2500 km length of the fan leads to variable thickness and onlap time from north to south and (2) the nature of fan deposition means that accumulation at a given location is highly discontinuous and hence cannot capture a regional trend of accumulation. For these reasons, this expedition is based on an east–west transect approach with a large number of holes covering younger timescales. As the transect crosses the fan at 8°N latitude (middle fan), Paleogene deposits, if they exist, are in reach of reasonable drilling depths. The transect is anchored on the western flank of the Ninetyeast Ridge with a deep hole located to recover the oldest fan deposits. From there, the transect extends west across the central axis of the fan and ends at Deep Sea Drilling Project (DSDP) Site 218 above the 85°E Ridge. To resolve characteristics of fan construction during the Quaternary, a spacing of ≈50 km between sites was chosen based on the typical width of channel-levee systems.

During Expedition 354, seven sites were drilled on an east–west transect at 8°N (Figures **F2**, **F3**, **F4**, **F5**, **F6**; Table **T1**), including

- One deep site to ~1200 meters below seafloor (mbsf) to recover a complete sequence of fan deposits, in particular to reach pre-fan deposits (Site U1451);
- Two sites to ~900 mbsf (Sites U1450 and U1455) complementing Site U1451 to provide a transect of three sites across ~300 km to recover Pliocene and upper Miocene sediment to study Neogene fan evolution and the impact of the monsoonal system on sediment supply and flux; and
- Four dedicated shallow sites to 200–300 mbsf to recover a complete terrigenous record of the Himalayan flux over the last 1–2 My, complemented by the shallow portion of the other three deep-penetration sites.

During Expedition 354, the original transect of six sites was complemented by a seventh, alternate site (U1454) west of Site 218 that extended the transect to ~300 km.

Expedition 354 builds on knowledge acquired during earlier drilling and seismic exploration of the Bengal Fan (DSDP Leg 22; Ocean Drilling Program [ODP] Leg 116; and R/V *Sonne* Cruises SO93 [Legs 1–3], SO125, SO126, and SO188 [Legs 1 and 2]) and on current studies of the tectonic, geologic, geomorphological, and sedimentological processes acting on the Himalaya, the floodplain and delta of the Ganga-Brahmaputra, and the Bengal Fan. This expedition is one part of an integrated effort for International Ocean Drilling Program (IODP) drilling syntectonic basins around the Himalaya to improve our knowledge of monsoon evolution and its interaction with Himalayan growth and erosion. This includes in particular IODP Expedition 353 (Indian Monsoon) and IODP Expedition 355 (Arabian Sea Monsoon) on the Indus Fan.

Background

Geological setting

The Bengal Fan covers the entire floor of the Bay of Bengal (Fig. **F2**), from the continental margins of India and Bangladesh to the sediment-filled Sunda Trench off Myanmar and the Andaman Islands and along the west side of the Ninetyeast Ridge. It spills out south of the Bay of Bengal at its distal end to ~7°S. Another lobe of the fan, the Nicobar Fan, lies east of the Ninetyeast Ridge, but it ap-

parently was cut off from its primary source of turbidites, the head of the Bay of Bengal, during the Pleistocene by convergence between the northern end of the Ninetyeast Ridge and the Sunda Trench. The northeastern edges of the fans are subducted, and some of the Tertiary turbidites cropping out in the Indo-Burman Ranges of Myanmar, the Andaman and Nicobar Islands, and the outer arc ridge off Sumatra are interpreted as old Bengal and Nicobar Fan sediments.

Following the initial bathymetric discovery of the fan extension by Heezen and Tharp (1966), the Bengal and Nicobar Fans were delineated and named by Curray and Moore (1974), who also noted two horizons in reflection and refraction seismic data that pass into unconformities over the exposed and buried hills of folded sediments in the southern part of the fan and over the Ninetyeast Ridge. They concluded that these two horizons are regional and used them to divide the sedimentary section into three units in the Bay of Bengal. The ages of these unconformities were tentatively determined to be uppermost Miocene and upper Paleocene to middle Eocene during Leg 22 (Moore et al., 1974; Shipboard Scientific Party, 1974) at Sites 218 and 217, respectively (Fig. **F2**). Curray and Moore (1974) interpreted the older unconformity as having been initiated by the India-Asia collision, with the pre-Eocene sedimentary unit consisting of pelagic sediment and terrigenous material derived from India before the collision. Hence, the upper two sedimentary units define the Bengal Fan sensu stricto. Curray and Moore (1974) associated the upper Miocene unconformity with intraplate deformation, probably correlated with a plate edge event. These tentative age assignments were further confirmed and refined by later drilling during ODP Legs 116 and 121 (Cochran, Stow, et al., 1990; Peirce, Weissel, et al., 1989), although the interpretation and significance of the older unconformity and the time of initiation of Bengal Fan deposition and progradation remain very controversial.

The older unconformity was drilled and sampled only on the Ninetyeast Ridge. Correlation of this unconformity off the ridge into the fan section is possible along some but not all seismic lines (e.g., Gopala Rao et al., 1994, 1997; Krishna et al., 1998; Schwenk and Spiess, 2009). Leg 22 sites sampled the older unconformity. DSDP Site 215 showed a hiatus from early Eocene to late Miocene (Fig. **F7**). DSDP Site 211, located at the eastern distal edge of the Nicobar Fan, showed a hiatus from some time after the Maastrichtian until the Pliocene. The overlying younger sections are interpreted as distal fan.

Eocene initiation of Bengal Fan deposition is also suggested by the geology of Bangladesh, the Indo-Burman Ranges of India and Myanmar, and the Andaman-Nicobar Ridge. Hydrocarbon exploration onshore and offshore from southeastern Bangladesh (e.g., Kingston, 1986) shows total sediment thicknesses calculated from gravity to be >20 km, apparently with the Eocene and Oligocene Disang Series of deepwater shales and turbidites overlying oceanic crust. These are in turn overlain by Neogene prograding deposits of the Bengal Delta and the Ganga-Brahmaputra (Jamuna) river system, the Meghna River, and their ancestral rivers. Some of these rocks are mildly metamorphosed and uplifted into the accretionary prism in the Indo-Burman Ranges, with some sparsely fossiliferous flysch units correlated with the Disang Series (e.g., Brunnschweiller, 1966; Bender, 1983; Najman et al., 2008). Similar turbidites, the Andaman Flysch or Port Blair Formation, are found in the Andaman and Nicobar Islands, again usually assigned to Eocene and Oligocene ages (e.g., Karunakaran et al., 1975; Acharyya et al., 1991) and interpreted to represent parts of the early Bengal Fan, some of which are incorporated into the Sunda arc accretionary complex.

The initiation of deposition and progradation of the Bengal Fan followed the collision of India with Asia and the formation of a large proto-Bay of Bengal. Continued convergence of the Indian and Australian plates with the Southeast Asian plate reduced the size of the bay and focused the source of turbidites into the present Bengal Basin, Bangladesh shelf, and the Swatch-of-no-Ground (SoNG) shelf canyon (Curray et al., 2003).

Fans grow by progradation, and the first sediments are deposited at the mouth of a canyon and at the base of the slope, typically the continental slope. With time, fans prograde farther from the original base of the slope. Our limited information suggests that the Bengal Fan has prograded, as shown in Figure **F7**. The oldest rocks interpreted as Bengal Fan in the Indo-Burman Ranges are early Eocene; the oldest such turbidites in the Andaman and Nicobar Islands are middle Eocene. Sites 215 and 211 revealed upper Miocene and Pliocene turbidites, respectively. Neither Site 218 nor the Leg 116 sites reached the base of the fan. The interpretation that the Eocene unconformity marks the base of the fan suggests that it may represent a hiatus of variable duration (Fig. **F7**).

Sediment delivery into the Bengal Fan originates from the SoNG (Kottke et al., 2003; Michels et al., 1998; Palamenghi, 2011), which represents the only feature of this kind today. Sediments from the Ganges, Brahmaputra, and Meghna Rivers are transported to the mouth and then westward by currents parallel to the delta front (Kudrass et al., 1998). Approximately one-third of the Himalayan material is stored in the floodplain, and a significant portion is constructing a prograding shelf sequence (Goodbred et al., 1999). The remaining portion, approximately one-third, enters the SoNG, for example, by coast-parallel currents, partially initiated by storm events (Kudrass et al., 1998), to be finally delivered to the Bengal Fan.

Mechanisms of this transport, which must be associated with the initiation of turbidity currents, are largely unknown. However, sediment physical data for 47 cores along the 3000-km-long transport path from the delta platform to the lower fan distinguish different turbiditic environments (Weber et al., 2003). One of the main characteristics of the Bengal Fan is channel-levee systems of remarkable size (e.g., Hübsher et al. 1989; compilation by Curray et al., 2003). They are believed to form from mostly unchannelized turbidity currents. If they are able to erode the seafloor to the degree that an incision forms, subsequent turbidity currents are confined. As a consequence, erosion is enhanced, the cross section of the turbidity current is further constrained, and turbulent energy can be maintained over very long distances. If sufficient fine-grained material is incorporated in the suspension cloud, spillover deposits can form a triangular-like shape because the sedimentation decreases with distance from the channel axis (levee), constructing a channel-levee system.

For the Bengal Fan, these turbidity current characteristics were described in detail along the active channel by Hübscher et al. (1997), Weber et al. (1997, 2003), and Schwenk et al. (2003, 2009). Work by Hübscher et al. (1997) and Schwenk and Spiess (2009) confirms an overall similarity of channel-levee complexes and their geometries, scales, and distribution downfan between 8°N and 16°N. Weber et al. (1997) shows that these levees can build up over several thousand years. Schwenk et al. (2003) further demonstrate that the evolution of these deep-sea channels led to a pronounced, meandering formation of cut-off loops and their subsequent fill. In this sense, the drilling transect well represents characteristics of Bengal Fan architecture, whereas the sediment delivery system will likely

reveal a pronounced spatial and temporal variability over relatively short time periods.

Interlevee sediments are assumed to represent a lobe of progradational coarse-grained silty to sandy facies with the channel termination upslope, as it may occur, for example, after a channel avulsion. Subsequently, levee units form after the establishment of a channel, which typically erodes into previously deposited units. At the early stage, wedge-shaped units of high reflectivity may form from coarser grain size because of limited channel depth. The wedge-shaped units of lower reflectivity are supposed to be caused by overspill and flowstripping from turbidity currents that pass through the channel, likely originating at the SoNG on the Bangladesh shelf. Levee sediments are supposed to be mostly composed of silty to clayey material with a tendency to fine upward with increasing levee height. Hemipelagic units form when sediment supply is shut down or distal, thus creating a layer of almost constant thickness throughout large areas of the fan.

So far, distal (Leg 116) and middle fan sediments were demonstrated to reflect Himalayan geological sources (Stow et al., 1990; France-Lanord et al., 1993) and were used to track the evolution of the erosion rate of the Himalayan range (Copeland and Harrison, 1990) and the paleovegetation of the basin (France-Lanord and Derry, 1994; Galy et al., 2010) and to scale the impact of Himalayan erosion on the long-term carbon cycle through silicate weathering and organic carbon burial (France-Lanord and Derry, 1997).

Seismic studies/site survey data

The original IODP proposal for this expedition (552) was based on a single 500 km long multichannel seismic line at 8°N (GeoB97-020/027), which was acquired during R/V *Sonne* Cruise SO125 in 1997 (Spiess et al., 1998) to gain a better understanding of the buildup of the fan with respect to channel-levee geometries and stacking patterns (Fig. **F3**). For stratigraphic calibration, this seismic profile crossed DSDP Site 218, where sediments were cored and dated to the middle Miocene at 773 mbsf.

To further support IODP Proposal 552, a dedicated presite survey during R/V *Sonne* Cruise SO188-1 was carried out in June–July 2006. This cruise collected multichannel seismic, swath bathymetric, and Parasound subbottom profiler data on crossing lines through Sites U1449, U1450, and U1451 (proposed Sites MBF-6A, MBF-2A, and MBF-3A, respectively). These additional data provided further understanding of the spatial variation of sediment structures, particularly the underlying complex structures of buried channels (Figures **F3**, **F8**). Shallow-penetration sediment cores were taken at selected sites to complement the data already available from Site 218 (Site U1455).

The long seismic reflection Profile GeoB97-020/027 (Fig. **F3**) was interpreted with respect to the presence of channels, channel-levee systems, and seismic stratigraphy (Schwenk and Spiess, 2009). Several major reflectors and unconformities were traced across the drilling transect, revealing increased average sedimentation rates as a function of distance from the basement ridges at 85°E and 90°E. Age constraints provided by correlation to Site 218 suggest that the shallow-penetration sites (U1449, U1452, U1453, and U1454) extend to near the Pleistocene/Pliocene boundary and the mid-depth penetration sites (U1450 and U1455) extend to at least 8 Ma. Our deepest penetration and easternmost site (U1451) was selected to provide prefan sediments by drilling through the regional Reflector P (Eocene unconformity).

For Expedition 354, these data were reprocessed to improve lateral resolution from 20 to 10 m and vertical resolution to a higher bandwidth through conservative filtering and advanced noise suppression. Data examples shown in this report originate from these new data sets, which are superior to the original data set used by Schwenk and Spiess (2003).

Swath bathymetric data were acquired during Cruise SO125 using a Hydrosweep DS System and during Cruise SO188-1 using a Simrad EM120 echo-sounder system. The total multibeam coverage width is now 19 km, increasing in those areas where crossing lines were shot. Although bathymetry reveals a clear picture of the recent or Quaternary channel systems in the area, this information only applies to the upper few tens of meters of the section, which is otherwise a mix of stacked older channels and interlevee sequences. Digital Parasound subbottom profiler data (4 kHz) were also routinely collected during both cruises.

Scientific objectives

Expedition 354 was designed to reconstruct the erosional history of the Himalaya and its bearing on the development of the Himalaya and Tibet as topographic features and to document the relationship between erosion and climate throughout long-term and short-term fluctuations of the Indian monsoon as recorded in the Bay of Bengal.

1. Calibration of Neogene to present changes

Although the Miocene to recent sedimentary records in the Bengal Fan suggest that since 18 Ma Himalayan erosion was comparable to the actual regime in many ways, tectonic and climatic changes have occurred that are both likely to have influenced sedimentation in the Bay of Bengal. This includes upper Miocene changes in accumulation rate, continental vegetation, and weathering intensity that are documented both in the continental basin and the Bengal Fan (e.g., Quade and Cerling, 1995; France-Lanord et al., 1993; Burbank et al., 1993; France-Lanord and Derry, 1994; Martinod and Molnar, 1995; Clift et al., 2008; Galy et al., 2010). The development of intense channel-levee deposition in the Bengal Fan starts appearing in the upper Miocene or Pliocene and is also the mark of major change in sediment delivery to the Bay of Bengal (Schwenk and Spiess, 2009). During the late Pliocene, global cooling led to the growth of ice sheets in the Northern Hemisphere, which appears to be related to a global increase in detrital sedimentation rate and grain size (Zhang et al., 2001). Although the reality of this change has been questioned (Willenbring and von Blanckenburg, 2010) the evolution to higher climate instability should prevent an equilibrium state of fluvial and glacial basins and trigger their erosion. Such changes were observed in the distal Bengal Fan around ~0.8–1 Ma when the 100 ky cycle became strong. This expedition documents this critical period in the Earth's most intense erosion system, as tectonic and climate changes have left signatures in accumulation rates, grain sizes, physical properties, clay mineralogy, isotopic ratios, organic carbon burial, and so on, that will be tracked with postexpedition studies.

First, to what extent are variations in accumulation rates, clay mineralogy, and grain sizes from ODP Sites 717–719 (Fig. **F8**) representative of other parts of the fan? Because those holes only recovered sediments from the most distal parts of the Bengal Fan within a growing syncline, sedimentation might have been affected both by the large distance from the source and by the barrier imposed by the surrounding anticlines. The decreases in accumulation rate and grain size at ~7 Ma and the synchronous increased percentage of smectite (Bouquillon et al., 1990) suggest that if the mon-

soon strengthened at that time, it apparently did so without creating a more energetic erosive system, as might be expected from the strong seasonal precipitation of the monsoon. Obviously, if we find the same pattern of low accumulation rates, small grain sizes, and a large percentage of smectite at 7–8 Ma in the holes cored at 8°N during Expedition 354, we must consider the possibility that if the monsoon strengthened at that time, it did so by decreasing, not increasing, erosion rates. If we find a sediment history different from that at Sites 717–719, it is possible that the sedimentary record at the distal edge of the fan does not record faithfully the changes input at the source of the fan.

The present-day monsoon, if named originally for the seasonally steady winds over the Arabian Sea, also evokes the image of heavy rain over the Indian subcontinent. We have no evidence to date, or perhaps conflicting evidence, showing that precipitation increased over the Ganga and Brahmaputra drainage basins and the Bay of Bengal at 7–8 Ma (Derry and France-Lanord, 1997; Dettman et al., 2001) despite enhanced Indian monsoon seasonality over this period (Zhisheng et al., 2001). Assessing paleomonsoon intensity is challenging and can be tracked with two approaches. First, the efficiency of sediment transport from the Himalaya to the Bay of Bengal is somewhat controlled by the seasonality and intensity of rainfall that trigger high river discharge (Lupker et al., 2011). This transport in turn exerts control on sediment fluxes to the Bay of Bengal that can be traced by accumulation rates. Second, $\delta^{18}O$ in planktonic foraminifers deposited in the Bay of Bengal in the late Quaternary is related to precipitation amounts (Duplessy, 1982). If these microfossils can be recovered, they will provide another tool to assess the strength of the monsoon.

The main reason for drilling more than one site at 8°N is to minimize the effects of (1) varying sedimentation rates associated with pronounced increases in the vicinity of the active channel over time and (2) the migration of the active channel, hence avoiding biases that one site (or a set of adjacent sites) might give. Although the main focus of these sites is on the changes near 7–8 Ma, obviously we will obtain a Himalayan erosion record over a longer period that will allow analysis of the Himalayan response to monsoon fluctuation over the early Miocene, as proposed by Ramstein et al. (1997) and Fluteau et al. (1999), or Oligocene (Licht et al., 2014).

In addition, we plan to study other temporal and spatial variations in the sediment over the last 7 My. Site 218 and sites cored during Leg 116 show changes that possibly reveal other variations in the erosion regime. Data from Kroon et al. (1991) show a dip in the abundance of *Globigerina bulloides* at ~5 Ma, which might indicate a lull in the monsoon, the temporary dominance of another upwelling-sensitive foraminifer (Kroon et al., 1991), or some other inadequacy of *G. bulloides* to measure monsoon strength. We also seek quantitative measures of the interaction between climate change and sedimentation associated with global cooling and the onset of Northern Hemisphere glaciation at ~2.7–3.3 Ma and with the change from precession and obliquity-dominated climate variations to the strong 100 ky cycle at 0.8–1.2 Ma. The latter change appears to be marked by changes in deposition rates, grain sizes, and clay mineralogy at Sites 717–719 (France-Lanord et al., 1993). Again, one objective is to decide how representative the results from Sites 717–719 are. The same proxies for monsoon strength and erosion will be available for study of this period. The results from Sites 717–719 reveal no evidence of a change in erosion rate at 2.7–3.3 Ma, in contrast with what might be expected if glacial erosion were important and increased at that time. Moreover, if the only important change in sedimentation rate, and hence presumably in erosion rate, occurred at 0.8–1.2 Ma, such a change would provide a clue to what kind of change was important. We anticipate being able to resolve temporal variations on the timescale of orbital variations, but obviously we must expect significant variations in sedimentation rates. Hence, the seven site transect approach was designed to resolve as completely as possible the time record for a given time slice.

The 7 Ma transition is also marked by an expansion of C_4 photosynthetic plants in the Himalayan basin (Quade et al., 1989). Although C_4 plant expansion may result from a global decrease in atmospheric pCO_2 (Cerling, 1997), studies suggest that PCO_2 was already low at that period (Pagani et al., 1999; Beerling and Royer, 2011). In the latter hypothesis, C_4 plant expansion would instead require an adaptation to more arid conditions in the floodplain. Sediments sampled during Leg 116 show close links among variations in clay mineralogy (smectite/illite ratio), total organic carbon, and $\delta^{13}C$ (C_3 versus C_4 plants) (Fig. **F9**) (France-Lanord and Derry, 1994; Freeman and Colarusso, 2001). These relationships suggest changes in sediment provenance, with a mountain end-member delivering material unaltered with low organic carbon content of C_3 type and a floodplain end-member delivering altered material with high organic carbon content of C_4 type. If confirmed by new drilling at the scale of the entire fan, such relations would favor the hypothesis of a regional climate change to dryer conditions. Combining these with more sophisticated molecular and isotopic biomarkers (e.g., Galy et al., 2011; Contreras-Rosales et al., 2014) will reveal more accurately the link between monsoon intensity and plant distribution as a function of sediment origin.

2. Forcing of the carbon cycle and climate

Drilling the Bengal Fan should allow investigation of the effect of Himalayan erosion on the global carbon cycle, which has been debated (e.g., Raymo and Ruddiman, 1992; France-Lanord and Derry, 1997; Galy et al., 2007; Goddéris and Donnadieu, 2009). Erosion tends to consume atmospheric carbon by two mechanisms. First, weathering of silicates produces fluvial alkalinity flux that can later precipitate as carbonate in seawater. Second, plant debris and organic carbon are transported with the particulate flux and can be buried in deep-sea sediment. Ultimately, both mechanisms will take up carbon from the atmosphere and store it over long periods in the sedimentary reservoir. Observation of modern fluxes of erosion and of Bengal sediments suggests that the Himalayan erosion mostly consumes atmospheric CO_2 through burial of organic carbon preferentially to silicate weathering. Nevertheless, it remains impossible to assess the magnitude of these processes at a global scale because past fluvial fluxes are unknown. Sediment volume and geochemistry can provide direct and interpretable records of these fluxes if their accumulation rates in the Bengal Fan can be determined with sufficient accuracy. Our transect of drill sites at 8°N was designed to document the regional scale of such fluxes during the Neogene that can be extrapolated throughout the entire fan. The deepest penetration Site U1451 was designed to allow exploration of weathering and carbon burial prior to the Neogene.

3. Sampling of the oldest sediment of the fan

Scenarios of the timing and geometry of the collision between India and the rest of Eurasia suggest that collision in the western Himalaya occurred between 50 and 55 Ma, and perhaps later (~45 Ma) in the eastern Himalaya, near Everest for example (Rowley, 1996, 1998). However, there are contrasting models for the slowdown of Indian plate motion and the geometry of the collision (e.g., Dupont-Nivet et al., 2010; Van Hinsbergen et al., 2011; Aitchison et al., 2007;

Zhang et al., 2012). When the Himalaya emerged as a mountain range, however, remains less certain. Extending the record of sedimentation back in time should allow determination not only of when erosion began but also of when erosion penetrated deep enough into the crust to expose rapidly cooled minerals. In particular, we should be able to determine cooling ages of minerals whose closure temperatures are different, and from the isotopic signature, we should be able to identify what rock of the Himalaya has eroded. Differences between cooling ages and stratigraphic ages will then allow estimates not only of when erosion began but also of when erosion exhumed rock from different depths (Copeland and Harrison, 1990; Corrigan and Crowley, 1992; Galy et al., 1996).

Determining when emergence of the Himalaya took place might not provide any surprises. Nevertheless, recall that all of the rock cropping out in the Himalaya was carried by the Indian subcontinent and scraped off it following collision with Eurasia. Thus, given India's convergence rate of ~50 km/My toward Eurasia since 45 Ma, if collision occurred at 45 Ma but erosion began only at 35 Ma, we might infer that as much as 500 km of intact lithosphere was subducted beneath southern Eurasia before a significant mountain range formed. Conversely, if deposition of rock with a Himalayan isotopic fingerprint began shortly after 45 Ma, we must infer that some off-scraping of Indian crust occurred early in the history of the collision to build the initial Himalaya. Finally, we can imagine a flux of sediment early in the history of the collision, but of Tibetan, not Himalayan, origin. This would suggest some not necessarily easily quantified subduction of India beneath southern Tibet before thrust faulting within India created the Himalaya.

The well-known increase in the $^{87}Sr/^{86}Sr$ ratio of seawater beginning at ~40 Ma (DePaolo and Ingram, 1985; Hodell et al., 1989) is commonly attributed to increased erosion and weathering in the Himalaya (Edmond, 1992; Galy et al., 1999; Krishnaswami et al., 1992). A strong Himalayan signature, not only beginning at ~38 Ma but also contributing a pulse near 18 Ma (Richter et al., 1992), should, therefore, be corroborated in the sedimentary record of Himalayan erosion. This would be supported if detrital silicates with high $^{87}Sr/^{86}Sr$ ratios increased both at ~40 Ma and near 18 Ma. By extending the sedimentary record in the Bay of Bengal through the Oligocene, we can examine the hypothesized correlation of the increased marine Sr isotopic ratio at 18 Ma with weathering of Himalayan rock rich in radiogenic strontium. If we can sample the early history of Himalayan erosion, we can test the assumption that the increasing Sr isotopic ratio beginning at ~38 Ma also results from weathering of Himalayan rock. The sensitivity of the seawater Sr isotopic budget to the Himalayan flux is so high (Galy et al., 1999) that the seawater evolution through time provides a unique system where erosion rate may be estimated using a proxy other than accumulation rates.

The Bengal Fan is one of the thickest sediment sections in the world, and it is far too thick to sample the very old section. The oldest part of the fan sampled to date was at Site 718 more than 2500 km from the present apex of the fan, where early Miocene sediment (~17 Ma) was recovered. Because of its southern position and great water depth, this site is not adequate to penetrate the "oldest" sediment derived from the Himalaya because the fan may not have prograded so far south (e.g., Curray, 1994). Our deepest proposed site (U1451; proposed Site MBF-3A) is located on the west flank of the Ninetyeast Ridge, ~1300 km from the thicker section of the fan, where the section is thinner and where a possible Paleocene–Eocene unconformity ("P" horizon) could be reached at a reasonable depth (Curray et al., 1982).

4. Fan architecture and spatial depocenter variability

Since the Pliocene, sedimentation in the Bengal Fan has been dominated by deposition in channel-levee systems (Schwenk and Spiess, 2009). During this period, it appears the fan was built by an accumulation of lenses corresponding to distinct channel-levee episodes intercalated by more slowly accumulating intervals of fine-grained sediment (Fig. **F3**). Channels carry a flux of sediment for a brief period, apparently only for approximately thousands of years, and then fill with sediment as portions are abandoned and a new channel is cut into the levee system or outside it. Thus, accumulation at any point is likely very irregular. In the upper fan, accumulation varies from rates >30 m/ky for periods as long as 3000 y (Hübscher et al., 1997; Michels et al., 1998; Spiess et al., 1998; Weber et al., 1997) to very low accumulation rates in intervening periods. Nd-Sr isotopic signatures and bulk mineralogical and geochemical properties demonstrate that sediment accumulated in levees is dominated by Himalayan material, whereas very low accumulation hemipelagic deposits have distinct isotopic signatures in the upper fan, showing that other sources are mixed with Himalayan flux (Pierson-Wickmann et al., 2001). Determining the distribution and typical lifetime of depocenters is vital for interpreting the older sedimentary record of the fan and assigning different types of sedimentary facies and successions found in deep drill holes to structural units. To address this objective, the six planned sites distributed over a 200 km transect were designed to obtain sufficient spatial resolution on the basis of a typical width of a channel-levee system on the order of ~50 km. The shallower, ~300 m penetration sites will record the stacking of more than two systems.

Expedition 354 was designed to significantly improve and refine the poor existing age constraints (currently based only on spot-cored Site 218) of the stratigraphic and structural elements identified in the seismic data. This improvement is especially critical for constraining the transition from early sheet-like turbidite deposition to the onset of channel-levee systems that occurred in the latest Miocene (Schwenk and Spiess, 2009). Because most surface channels reach this part of the fan, it is believed that this marks the start of the development of channel-levee systems on the Bengal Fan generally (Fig. **F3**). Two reasons might be responsible for the onset of the channel-levee systems: (1) the initial creation of a canyon as point source or (2) changes in grain size of the delivered sediments transported by turbidity currents to the fan. The three drill sites targeting recovery of late Miocene sediments (Sites U1455, U1450, and U1451) will prove whether there were changes in grain size (as interpreted from Leg 116 results) and whether the onset of the channel-levee systems represents the first margin setting with a canyon and probably associated delta. Additionally, because several levees will be penetrated, new insights about the lifetime of distinct channel-levee systems will be gathered, which is so far only known for the active channel in the upper fan (Weber et al., 1997).

Additional objectives

Although Expedition 354 has been designed principally to document (1) Himalayan evolution and interactions with Indian monsoon evolutions and (2) turbiditic fan construction, drilling the Bengal Fan will allow additional important objectives to be addressed. This includes fan hydrology, Bengal Basin deformation, and deep biosphere issues.

Fan hydrology and hydrochemistry

The Bengal Fan is a major sedimentary reservoir filled by continental material including clays and organic matter that are likely to

evolve during diagenesis. Pore water chemistry and O-H isotopic compositions documented on Leg 116 cores revealed a high variability of compositions that imply that low-salinity fluid is released through dehydration reactions probably deeper than in the cored sections and that fluid advection occurs under thermoconvective conditions at least in that portion of the fan (Boulègue and Barriac, 1990; Ormond et al., 1995). There are also indications for diverse diagenetic reactions that release significant amounts of Ca and Sr in the pore water reservoir. Pore water analyses, physical properties, and downhole measurements will constrain the magnitude of compaction, dehydration reactions, and possible fluid transfer. This will lead to refined estimates of geochemical fluxes from the fan to the ocean.

Bengal Basin deformation

Throughout the Neogene, the Bengal Basin underwent significant multiphase deformation that resulted in the folding of the plate between the Ninetyeast Ridge and the 85°E Ridge (Krishna et al., 2001). In addition to the Miocene and Eocene unconformities (Curray et al., 2003), site survey data revealed two additional regional unconformities. Using the Site 218 age control, these were dated as Pleistocene and Pliocene, respectively (Schwenk and Spiess, 2009). These unconformities are interpreted to be equivalent to unconformities found in the central Indian Ocean, which are related to deformation events of the ocean lithosphere there (Cochran, 1990; Stow et al., 1990; Krishna et al., 2001). Additionally, several faults were identified in the seismic data, especially above the western flank of the Ninetyeast Ridge. These faults terminate within Pleistocene sediments, which also suggests tectonic events at least until the Pleistocene. As Site 218 dating is poorly constrained, we expect Expedition 354 results to allow more precise dating of unconformities and fault terminations, which in turn will improve the understanding of deformation events in the Bengal Basin.

Deep biosphere

Deep biosphere objectives were not specifically planned as a primary objective of this expedition, but specific sampling was conducted to document bacterial activity near the surface of the fan and at depth. These samples will allow us to explore the impact of terrigenous flux on bacterial development. The Bengal Fan represents one of the largest fluxes of terrestrial matter to the ocean with relatively fast accumulation. The apparent high preservation of terrigenous organic matter is a peculiar aspect of Bengal Fan sedimentation (Galy et al., 2007). Microbial activity is intimately intertwined with diagenesis and organic carbon degradation. Because preservation and burial of organic matter is one crucial parameter of the impact of Himalayan erosion on the carbon cycle, there is high interest in studying these processes.

Operations plan/drilling strategy

The operations plan and drilling strategy developed for Expedition 354 is fully described in the *Scientific Prospectus* (France-Lanord et al., 2014). Because Expedition 354 started in Singapore and ended in Colombo, an east–west sequence of sites was the most efficient. However, to better initiate overall shipboard laboratory operations and to best address the specific concern about the best approach to core in a sand-rich environment, we decided not to start with the easternmost site (U1451; proposed Site MBF-3A), which is the most challenging, deepest penetration site. Instead, we decided to start drilling at a short 300 m penetration location (Site U1449; proposed Site MBF-6A) with the advanced piston corer (APC) system, followed by a 900 m penetration location (Site U1450; proposed Site MBF-2A), to determine the depth of APC penetration and quality of XCB coring. The initial operations and time estimates for Expedition 354 planned for 56 days of operations on a very tight schedule. Nevertheless, large uncertainties were expected because of potentially poor recovery in sands and uncertain penetration rates that could affect good core recovery, feasibility of wireline logging, and overall hole conditions in rapidly deposited and loose sands. For these reasons and based on scientific interest, Site U1454 (proposed Site MBF-7A) was added during the expedition as an alternate site to extend the transect west of Site U1455 (proposed Site MBF-1A; DSDP Site 218) to core the most recent levee sequence.

The initial coring plan and time estimate included using only APC/extended core barrel (XCB) at all sites, except for Site U1451 (proposed Site MBF-3A), where RCB coring would be needed for deep penetration. Time was allocated for only a single hole at each site to the total target depth. If coring conditions (recovery, core quality, and penetration rate) required, the half-length APC (HLAPC) would be used to obtain deeper high-quality cores, but the additional wireline time was not included in the pre-expedition time estimates. We also planned for orientation for all full-length APC cores, using nonmagnetic hardware as much as possible, and a basic program of formation temperature measurements. A second hole was planned at our deepest penetration site (Site U1451; proposed Site MBF-3A) consisting of rotary core barrel (RCB) coring through the Eocene unconformity estimated to be at ~1500 m. The option to stabilize this second hole with a preassembled reentry cone with 400 m casing was considered the best approach to achieve the deep coring and logging objectives, but the time to install it was not included in the pre-expedition time estimates.

Wireline logging was planned for our three deepest penetration sites (Sites U1451, U1450, and U1455; proposed Sites MBF-3A, MBF-2A, and MBF-1A, respectively). These were intended to consist of two logging runs (triple combination [triple combo] and Formation MicroScanner [FMS]-sonic tool strings) and a check shot (Versatile Seismic Imager [VSI]) if hole conditions allowed.

Sampling and data sharing strategy

The shipboard sampling strategy was defined with each laboratory group to obtain the necessary shipboard observations and analyses. Special care was taken to obtain data from the differing lithologies. Because the exact nature of recovered sediment and quality of recovery was somewhat difficult to predict, we decided that the Scientific Party had to take a conservative approach to define personal sampling and that the majority of sampling for personal research had to be deferred until after the expedition. However, we defined some sampling objectives to conduct groups of exploratory analyses to test and refine sampling strategies to prepare for postexpedition sampling. This included large volumes of samples of sand to test heavy mineral separation and critical grain size, samples for preliminary $\delta^{13}C$ of TOC analyses to determine the position of the C_3–C_4 transition in the deep sites, samples to determine the feasibility of high-resolution analyses and relative dating with foraminifer $\delta^{18}O$ of a levee sequence, samples to test terrestrial and oceanographic biomarkers, and samples to test the feasibility of optically stimulated luminescence (OSL) dating in Late Pleistocene cores. Some suites of samples were taken for grain size analyses in turbidites, nannofossil biostratigraphy, and high-resolution analyses

of specific hemipelagic horizons (including U-channels for paleomagnetism studies).

Site summaries

Site U1449

Site U1449 (proposed Site MBF-6A) is part of a six shallow hole transect designed to document turbiditic transport and deposition processes in the Middle Bengal Fan at 8°N since the Pliocene. Sediments will also be used to trace sources of eroded sediments in the Himalaya and reconstruct erosion rates to tie erosion response to climate change. Site U1449 is located at 08°0.419′N, 088°6.599′E, in a water depth of 3653 m. The main Hole U1449A penetrated to 213.5 m drilling depth below seafloor (DSF) and was cored by a combination of APC, HLAPC, and XCB. Hole U1449B was a single APC core from the mudline taken for microbiological studies.

Principal results

Different structural elements of the sedimentary fan, including a more than 40 m thick levee succession, interlevee turbidites, and sands and hemipelagic sequences were cored. General lithologic boundaries correlate well with downcore variability in all physical properties and could be attributed to major seismic facies types and reflectivity characteristics. Seismic and average core velocities are in close agreement, which confirms that the major lithologies were properly sampled and nonrecovered XCB sections likely contained unconsolidated sands.

Cored sediments allowed us to characterize the sedimentological, physical, and geochemical properties of the material delivered mostly through turbidity currents and likely originating from the source region of the Himalaya. Integration of lithology, physical properties, seismic facies, and geochronological data shows that sedimentation varies over several orders of magnitude between centimeters per thousand years for hemipelagic units, representing a complete absence of fan sedimentation, followed by episodes with much higher rates (>>10 cm/ky) when interlevee units form and levees build up rapidly.

High accumulation rates of turbiditic deposition in the lower 120 m of the hole since ~2 Ma were followed by a low-accumulation hemipelagic episode during the Pleistocene around 1 Ma. Intercalated levee and interlevee deposits then formed until 300 ky ago, when hemipelagic sedimentation dominated again.

Operations

Hole U1449A was drilled to total depth of 213.5 m DSF. The APC system penetrated 57.1 m of formation and recovered 52.37 m (92%). The HLAPC penetrated 71.9 m of formation and recovered 74.98 m (104%). The XCB system penetrated 83.5 m of formation and recovered only 2.03 m (2%). Because of low recovery with the XCB system and because most objectives were achieved, drilling was terminated before reaching the initially planned depth of 300 m to save time. Hole U1449B was a single APC core from the mudline taken for microbiological investigations and recovered 7.91 m of sediments.

This first Expedition 354 drilling experience in the fan sediments allowed us to refine the drilling strategy for subsequent drill sites. As expected, recovery of sands intercalated between muddy units was challenging, and the HLAPC proved to be particularly efficient for sampling both turbiditic sequences and loose sand intervals.

Lithostratigraphy

The predominant lithology is siliciclastic and composed of normally graded intervals of mica-rich quartz-dominant fine sand, silt, and clay of varying thicknesses (i.e., turbidites). The observed mineralogical assemblage is characteristic of sediments found in Himalayan rivers. Turbidite sequences are generally separated by clay- and silt-sized mottled pelagic and hemipelagic intervals containing foraminifers and by occasional glassy volcanic ash layers. Lithologic differences between siliciclastic units and variations in grain size and bed thickness reflect cycles of proximal turbidity current channel activity, including activation, flow-stripping, avulsion, and abandonment. Bioturbated pelagic and hemipelagic calcareous clay likely represent times of channel-levee inactivity and hence reduced deposition through the settling of suspended sediment from the pelagic zone.

Biostratigraphy

Calcareous nannofossils and planktonic foraminifers provide biostratigraphic constraints at Site U1449. Overall, the abundance and preservation of these microfossils is dependent on the type of lithology recovered. Coarser sandy intervals contain few to barren calcareous nannofossils and barren to <0.1% foraminifers, but abundance and preservation improve considerably in the pelagic and hemipelagic intervals. These intervals were discontinuous at this site because of the regular influx of turbidites and levee sedimentation. Biostratigraphic controls are based on 53 nannofossil and 34 planktonic foraminifer samples, which provide a total of six biomarker horizons and a lower Pleistocene age at the bottom of Hole U1449A.

Paleomagnetism

Of the 38 cores collected from Hole U1449A, 30 were studied, avoiding deformed or sandy intervals. Most cores were unoriented, so inclination was used for core-to-core comparison and declination data within each core, both from discrete samples and archive section halves. The upper 91 m core depth below seafloor (CSF-A) in Hole U1449A reveals normal polarity corresponding to the Brunhes Chron (<0.781 Ma). A pelagic deposit between 88 and 97 m CSF-A contains several magnetic polarity zones corresponding to the Matuyama Chron and the Jaramillo and Cobb Mountain Subchrons. Interpretation of the magnetic polarity beneath the hemipelagic unit is difficult, but at least two cores (354-U1449A-20H and 22H) have reverse magnetization. Correlation between multiple holes in the Expedition 354 transect, particularly in pelagic and hemipelagic intervals, is expected to clarify the interpretation of the magnetostratigraphy of Hole U1449A.

Physical properties

Acquired data allow three lithologic groups to be distinguished. Sand-dominated lithologies reveal high acoustic velocity (~1700 m/s), high wet bulk density (~2.1 g/cm^3), generally high magnetic susceptibility (~50–200 SI), and intermediate levels of natural gamma radiation (NGR) (~70 counts/s). Silty clay lithologies show intermediate values of acoustic velocity (~1550 m/s), wet bulk density (~2.0 g/cm^3), and susceptibility (30–100 SI) and the highest NGR levels (~90 counts/s). Hemipelagic lithologies are easily distinguished by their low acoustic velocity (~1500 m/s), low wet bulk density (~1.6 g/cm^3), very low magnetic susceptibility (0–20 SI), low NGR (~25 counts/s), and the lightest color. Detailed comparisons between lithology and physical properties on selected intervals con-

firm the predictive capabilities of the physical property data for high-resolution reconstruction of depositional processes. Also, the data show a particularly high variability in coarser grained intervals; thus, deviation from in situ properties cannot be excluded.

Geochemistry

Shipboard sampling allowed analysis of 39 interstitial water samples, including a detailed sampling of the upper 9 m in single-core Hole U1449B. Inorganic and organic geochemical analyses were acquired on 12 samples for major and trace elements and 37 samples for organic and inorganic carbon. Data from turbidite sediments exhibit geochemical compositions similar to those observed for sediments from Himalayan rivers and from the upper fan levees and shelf. A total of 31 samples were taken for postexpedition microbiological research.

Site U1450

Site U1450 (proposed Site MBF-2A) occupies a central position at 8°0.42′ N and 87°40.25′E in the east–west transect across the Bengal Fan at 8°N. It is located at equal distance from Site U1451 above the Ninetyeast Ridge and Site U1455 above the 85°E Ridge. The overall thickness of the fan reaches ~4 km in this location (Curray et al., 2003). Neogene sediment thickness decreases toward the two ridges, which is likely the result of ongoing deformation on both ridges during Neogene times (Schwenk and Spiess, 2009). At this central position of the transect, the upper Miocene and Pliocene–Pleistocene sections of the fan appear to be most expanded and were inferred to contain a higher resolution record, as well as accumulating, on average, coarser grained material. The shallow section at this site is one of the seven ~200 m thick sites of the 8°N transect that constrain the Middle Bengal Fan architecture in space, time, and sediment delivery rate during the Pleistocene. The deeper section at this site will document the delivery mechanisms of the fan and the climatically and tectonically influenced sediment supply from the Himalaya during the Neogene. Changes in the source regions in response to tectonic processes and climatic interactions in the Himalayan basin are expected to be reflected in the sediments' mineralogical and geochemical compositions and geochronological data and by integrating accumulation rates across the transect.

Principal results

HLAPC coring combined with 4.8 m advances with no coring was essential to combine sufficient recovery in difficult lithologies with reasonable drilling time to reach 812 mbsf. This approach proved to be particularly efficient in recovering loose sand that otherwise would have been washed out during RCB or XCB coring. Because of remarkably low lithification of the sediment formation, this HLAPC approach permitted piston coring to 550 mbsf, and seven HLAPC cores were taken deeper, with the deepest at 688 mbsf.

As at other transect sites, the sedimentary succession is dominated by turbidites of siliciclastic composition with detrital carbonate content between 5% and 10%. These turbidites have high accumulation rates (5–10 cm/ky) from the upper Miocene to lower Pliocene. From the Pliocene to Pleistocene, turbidite accumulation peaks around 20–25 cm/ky. These turbidites have close mineralogical and geochemical affinities with sand and silt sampled in the Ganges, Brahmaputra, and lower Meghna Rivers. They carry all the mineral characteristics and major element composition characteristics of river sediments derived from high-grade metamorphic rocks of the Himalayan range. The representation of sand (41%) in Site U1450 cores matches well the grain size spectrum expected from river-derived detrital material, and bias by turbiditic transport may be minor. As downhole logging at this site was not possible because of poor hole conditions, it remains difficult to estimate the exact proportion of sand, silt, and clay in this hole. Over the entire section, the mineralogical and chemical composition of the turbidites as the prevailing lithology appears almost uniform, but detrital carbonate content tends to gradually increase deeper than the Pliocene, reaching concentrations twice as high as in modern rivers. This increase suggests either an evolution in eroded lithologies and/or a change in weathering conditions. Another distinctive, more carbonate rich lithology is represented by about 10 relatively thin hemipelagic intervals composed of calcareous clays. These intervals correspond to periods of slow accumulation at the site when pelagic deposition is significant enough to be identified but is still diluted in variable proportions by a fine clay component. The affinity of this clay material with the fine-grain plume generated by surrounding turbidity currents assumed to originate from canyons and the slope offshore Bangladesh remains to be determined by geochemical and clay mineralogical approaches. These low-accumulation intervals allow precise geochronological work and will be important for evaluation of accumulation rates. Testing their continuity across the transect will be a key element for the integrated study of fan construction dynamics and long-term detrital sedimentary input utilizing seismic correlation across the transect.

Site U1450 represents a reference section for shore-based studies of the erosion of the Himalaya during the Neogene. The detrital sediments cored here present little evidence for evolution over the last 8 My, suggesting rather steady conditions of erosion in the Himalayan basin. This evolution would require a major mountain range undergoing fast erosion and a monsoonal climate that allows rapid transport to inhibit weathering of the sediment in the floodplain. Unlike in the distal fan cored during Leg 116 (Cochran, Snow, et al., 1989), Site U1450 sediments show no clear change in accumulation rate, grain size, and clay mineralogy from 7 to 1 Ma. This stability suggests that the smectite-rich fine turbidites recorded in the distal fan for this time period (Bouquillon et al., 1990) relate more to a change in the channel and turbidite routing to the distal fan than to a change in Himalayan erosion. Site U1450 also covers the interval of expansion of C_4 flora (i.e., savanna to the expense of forest) recorded in both the distal and the middle fan (Galy et al., 2010). Sediments recovered at Site U1450 will allow detailed studies of this process and its possible connection with climate changes or erosion conditions.

Operations

Site U1450 consists of two holes. Hole U1450A was cored to 687.4 mbsf using primarily the HLAPC system alternating with short (4.8 m) advances without coring. The APC and XCB systems were used in the shallow and deepest portions of the hole, respectively. Because of very low recovery at depth with the XCB system, we pulled out and planned for deeper penetration coring and logging in a second hole later in the expedition. Overall, 282.7 m of core was recovered for the 444.7 m cored in Hole U1450A. Hole U1450B was drilled without coring to 608.0 m DSF and RCB cored continuously from there to 811.9 mbsf. Coring in Holes U1450A and U1450B overlaps from 608.0 to 677.8 mbsf. This deeper section cored 203.9 m and recovered 46.7 m of sediment (23%). Downhole logging was attempted with a triple combo tool string. On the way down, the bottom of the tool string encountered an obstruction at

133.7 mbsf and was stuck, likely in a collapsing sand layer. After the tool string was released, a short section of logging was acquired and deep logging of the site was abandoned.

Lithostratigraphy

The overall dominant lithology for Site U1450 (84% of total recovered material) is siliciclastic and comprises fining-upward sequences of fine sand, silt, and clay (i.e., turbidites), as well as homogenized sands and mixed silt-clay layers. These turbidites carry major and trace minerals characteristic of Himalayan rivers and of high-grade metamorphic rocks of the Himalaya. Clay assemblages are illite and chlorite, which are indicative for the same rivers. Siliciclastic units alternate with at least 10 units of calcareous clay sediments (16% of total recovered material). The thickest continuous calcareous clay intervals are in lithostratigraphic Unit III and consist of 5.14 m in Core 354-U1450A-34F and 4.8 m in Core 36F. Sediments give way downhole in Hole U1450B to increasingly more lithified material (e.g., limestone and claystone) from 627.50 m CSF-A to the base of recovered material. Additionally, Site U1450 contains three volcanic ash layers. Recovered sediments from Site U1450 were divided into 24 lithostratigraphic units based on lithologic and paleontological characteristics obtained through macroscopic and smear slide analyses, as well as physical property measurements.

Lithologic differences between units and variations in grain size and bed thickness reflect cycles of proximal turbidity current channel activity and abandonment. Sand intervals may represent interlevee "sheet flows," whereas finer grained fractions are more likely preserved in levee deposits. Bioturbated calcareous clays represent times of local channel-levee inactivity with reduced and finer siliciclastic deposition that reflects a relative increase in the contribution of biogenic origin from the pelagic zone. Many intervals of calcareous clay material show repeated sequences of color-graded beds, which can be due to increased entrainment of siliciclastic material, changes in water column productivity, or changes in the oxidation/reduction horizons of pore water. In Hole U1450B, intervals dominated by calcareous and/or clayey material become increasingly lithified with depth, and many are intercalated with very thin to thin silt or siltstone layers. Plant fragments occur throughout the cored section, more commonly in silt and siltstone intervals, although a few sand-dominated units also contain macroscopic organic material. At the top of Hole U1450A is an 18 cm thick ash layer that presumably corresponds to the ~75 ka Toba volcanic eruption which produced widespread tephra deposits across the Bay of Bengal (e.g., Gasparotto et al., 2000).

Biostratigraphy

Calcareous nannofossil and planktonic foraminiferal biostratigraphic analyses conducted on Site U1450 samples resulted in identification of 18 biomarker events. These events were used to construct 4 foraminferal and 11 nannofossil biozones, providing excellent age control extending back to the late Miocene. The recovery of a late Miocene succession achieves one of the key objectives of this expedition and includes sediments that may contain the C_4 photosynthetic flora expansion (Galy et al., 2010).

The succession of biostratigraphic zones at this site appears continuous, as no significant nannofossil biostratigraphic hiatuses were observed, indicating that the fan has been accumulating sediments, albeit at highly variable accumulation rates, since the late Miocene.

Paleomagnetism

A preliminary paleomagnetic study was conducted on 36 of the 86 cores collected from Hole U1450A, comprising 108 archive section-half and 52 discrete sample measurements. Sandy and/or deformed intervals were not measured. Polarity zones corresponding to the Jaramillo and Cobb Mountain Subchrons were identified in a calcareous clay unit in Core 354-U1450A-36F (173.30–174.60 m and 175.70–175.90 m CSF-A, respectively). An additional pair of reversals was observed in Core 52F (248.38 and 248.51 m CSF-A), but the polarity chron to which they belong has not yet been identified. The thickness of the Jaramillo and Cobb Mountain polarity zones in Hole U1450A suggests an accumulation rate for the calcareous clay interval similar to that in Hole U1449A (~1.5 cm/ky).

Physical properties

Physical property data acquired on Site U1450 cores included density, magnetic susceptibility, *P*-wave velocity, NGR, and thermal conductivity. The data are mostly of good quality, but the results from disturbed and partially filled sections are less reliable, as described below.

Physical properties at Site U1450 primarily reflect lithologic variations, with downcore compaction having a relatively minor effect. Using the principal lithologic name from the core description, which assigned six types of lithologies, average physical properties were calculated. From the 319 m total core recovery (39.6%), sand accounts for 131 m (41%), silt for 46 m (14%), clay for 72 m (22%), calcareous clay for 45 m (14%), claystone for 13 m (4%), calcareous claystone for 6 m (2%), and limestone for 7 m, with additional thin ash layers. In general, sands and silts have the highest density and *P*-wave velocity; sands have the highest magnetic susceptibility; clays have the highest NGR, and calcareous clay generally has the lowest values in all measurements. Some of the sand-rich intervals were difficult to recover and were often fluidized, which sometimes resulted in incompletely filled core liners; these cores had the effect of giving unexpectedly low gamma ray density, magnetic susceptibility, and NGR values. Cores that had inflow of core material ("suck in") also likely have lower than expected values in these physical properties due to volume reduction.

Geochemistry

Detailed pore water measurements show that four hydrological units in the middle fan can be distinguished based on sulfate, phosphate, silica, magnesium, potassium, calcium, and alkalinity content. Carbonate contents of bulk sediments vary widely from 1.2 to 63.2 wt% $CaCO_3$, reflecting contrasting depositional environments and significant contributions from detrital carbonates. Turbiditic sediments have low carbonate content, with values roughly doubling (from an average of 3.8 to 7.3 wt%) around 600 m CSF-A. This transition occurring during the Pliocene most likely reflects a change in detrital carbonate supply. A similar change is also observed at Site U1451 and can be deduced from DSDP Site 218 total inorganic carbon (TIC) data (von der Borch, Sclater, et al., 1974). Overall, total organic carbon (TOC) content is low with an average value of 0.4 wt%. Within turbidites, TOC broadly covaries with Al/Si ratios—a proxy for sediment grain size and mineral composition—reflecting preferential association of organic matter with clays previously documented in both the modern Ganges-Brahmaputra river system and in active channel-levee sediments in the Bay of Bengal deposited over the past 18 ky (e.g., Galy et al., 2007). But the TOC budget is likely to be also affected by the frequent presence of

woody debris concentrated in the lower part of many turbiditic sequences. In turbiditic sediments, the major element composition (e.g., Fe/Si and Al/Si) closely matches the chemical composition observed in sediments from the actual Ganges-Brahmaputra river system for both the trend and the range of variation (e.g., Galy and France-Lanord, 2001). At the low end of Al/Si ratios, the lack of significant difference suggests that extreme sorting documented in rivers' coarse bed sediments is also generated by turbidity current at Site U1450. Conversely, the clay-rich end-member recovered at Site U1450 appears slightly more aluminous (and likely finer) than surface suspended sediments from the lower Meghna River.

Microbiological subsampling of sediments and pore water at Site U1450 included establishing a microbial cell counting method, with further processing of the samples to be performed following the expedition.

Downhole measurements

Five downhole measurements were taken in Hole U1450A with the advanced piston corer temperature tool (APCT-3), ranging from 4.6°C at 86.3 m DSF to 13.5°C at 318.1 m DSF. These return a geothermal gradient of 38°C/km, which appears to be in the expected range.

Stratigraphic summary

Lithologic and physical property results confirm the expectation that Site U1450 would contain a high proportion of sand in the recovered cores; it may be even higher in the formation. As at Site U1449, the match between these data sets and seismic facies and horizons will allow us to assign broad lithologic categories to the seismic units and thus extrapolate throughout the seismic data set and between Expedition 354 drill sites. These data also allow identification of major depositional processes, which can be integrated to reconstruct the stacking pattern and evolution of fan deposition.

As Site U1450 reaches back to 8 Ma at 812 m DSF, a precise seismic stratigraphy will be established postexpedition, based on major hemipelagic units and associated distinct seismic reflectors. These units and reflectors will be used to estimate accumulation for various subfan units in time slices on the order of several hundred thousand to millions of years, one of the main expedition objectives. Site U1450 is located in a key position between the two other deep penetration Sites U1451 and U1455.

Recovering material of sufficient quality was a challenge during Expedition 354, particularly at Site U1450 because of the high proportion of sand. It was unexpected that the consolidation state of sands apparently does not change much with depth. Although loose sand was recovered with the APC system to refusal depth (560 and 630 m DSF in Holes U1450A and U1450B, respectively), the XCB and RCB systems provided little or no recovery of sand. The sand proportion is likely underrepresented in cores from the deeper section of the site. Based on discrete sample measurements of density and porosity, a downhole trend of porosity loss is observed, but from lithologic observations we can infer that consolidation state is different for different grain sizes. Clay shows a gradual transition to claystone with depth, with increasing *P*-wave velocities and densities downhole. However, sand was not recovered in any more consolidated state within the entire 800 m cored section.

Based on biostratigraphic and paleomagnetic data, the upper Miocene to lower Pliocene portion of the site is characterized by a relatively uniform accumulation, averaging to 5–10 cm/ky. From the early Pliocene to the Pleistocene, fan accumulation has intensified (~20–25 cm/ky), accompanied by a transition from more silt- to sand-dominated lithologies. Fan deposition ceased at this site at 300 ka.

Site U1451

Site U1451 (proposed Site MBF-3A) is the easternmost site of the seven site Bengal fan transect and was the only one aimed to core the older portions of the fan. The site is located above the western flank of the Ninetyeast Ridge at 8°0.42′N and 88°44.50′E, in 3607.3 m water depth. Seismic data show that the overall fan section is condensed at Site U1451 compared to the axial part of the fan because of ongoing deformation along the Ninetyeast Ridge since the Miocene (Schwenk and Spiess, 2009). The drilling objective was to recover the complete fan section down to a seismic unconformity, which is believed to indicate the onset of fan deposition at this location. Site U1451 also contributes to the Miocene–Pliocene transect of three ~900 m deep holes to document Himalayan erosion and paleoenvironment. Finally, the upper section of the site is part of the seven site transect to investigate late Pliocene to recent depocenter migration and overall fan sedimentation.

Two holes were drilled at Site U1451, Hole U1451A to 582.1 m DSF and Hole U1451B to 1181 m DSF. Hole U1451A was advanced with the APC, HLAPC, and XCB systems. From 200 to 582.1 m DSF, 4.8 m intervals were drilled without coring between HLAPC cores to achieve overall coring depths. In Hole U1451B, a reentry cone with 400 m casing was drilled into the seafloor. Deeper than 400 m DSF, Hole U1451B was cored with the XCB system from 542.0 to 640.8 m DSF and then with the RCB system to 1181 m DSF. Wireline logging failed because of unstable hole conditions. Core recovery was 86% in Hole U1451A and 29% in Hole U1451B.

Principal results

Coring at Site U1451 returned a complete sedimentary record of the Bengal Fan construction to the Paleogene. It constrains the fan turbiditic onlap to the late Oligocene (around 26–28 Ma) and provides the longest continuous record of Himalayan erosion throughout the Neogene. The upper section, as part of the seven site transect at 8°N, documents a change since the Miocene to a higher proportion of hemipelagic clay–rich deposition, consistent with a position less exposed to fan deposition because of Ninetyeast Ridge deformation.

The recovered turbiditic record extends back to 25–28 Ma, which is marked by a transition from Paleogene pelagic limestones to early Neogene claystones and siltstones, intercalated into pelagic intervals. Although this old turbiditic record carries all characteristics of Himalayan erosion across the full grain size spectrum, including sands, the growth rate of the fan deposits remained overall relatively low, on the order of a few centimeters per thousand years. A distinct change is observed in the middle Miocene, when fan growth intensified by almost an order of magnitude (>10 cm/ky). In the Pliocene, coarser material is absent, and the time interval between the early Pliocene and early Pleistocene is characterized by accumulation of carbonate-rich hemipelagic units. During the Pleistocene, a higher fine-grained detrital input is observed, but only over the last ~0.4 My. Fan deposits dominate the lithology again. As at other Expedition 354 sites, hemipelagic sediments dominate the surficial deposition.

The Site U1451 record, combined with that of Site U1450, reflects steady conditions of Himalayan erosion and Himalaya geological and structural evolution as documented by the recovered sediments' relatively uniform chemical composition and clay mineral assemblages. This record will be further constrained and re-

fined with postexpedition studies, which will reveal information about sources, erosion rates, and evolution of weathering.

At first glance, the Neogene record appears remarkably stable through time. One notable exception to this is the detrital carbonate contents of the turbidites, which are markedly higher before 6–7 Ma. This reflects either a long-term change in the geological sources or a difference in the weathering regime. The petrology of the sand reveals that high-grade metamorphic rock fragments and minerals that are characteristic of modern river sediments have been present since the middle Miocene and were less abundant during the early Miocene and late Oligocene. Such trends are consistent with increasing exhumation of high metamorphic grade rocks through time, but confirmation by postexpedition studies are required. Turbiditic sediments deposited at Site U1451 since 28 Ma reflect detrital archives similar in many aspects to those of recent fan deposits or to modern river sediments. Nonetheless, fan clastic deposition is not only restricted to turbidites, but deposition of detrital clays is prevalent in hemipelagic intervals during the Neogene and likely represents deposition associated to fan activity. Similar conditions of distal fan activity may also have been involved in the formation of the early Miocene and Oligocene claystones recovered, which have accumulation rates similar to Pleistocene hemipelagic units.

From seismic data, the early history of fan deposition at Site U1451 is associated with a change in depositional style above a seismic unconformity. This unconformity was likely cored at the bottom of the hole, recovering Eocene and Paleocene limestones and containing a 16–18 My hiatus. The structurally disturbed unit immediately overlying the unconformity is an Oligocene/Eocene limestone and claystone unit injected by sand and silt (injectites). On top, parallel strata are onlapping, which clearly indicates turbiditic sedimentation. Tilting of these Miocene strata with respect to the modern stratification indicates, however, tectonic deformation associated to the Ninetyeast Ridge, which has affected fan deposition to a minor degree at Site U1451 since the Miocene.

The well-represented hemipelagic deposition at Site U1451 during the last 6 My provides an excellent opportunity to develop a stratigraphic framework for the entire transect based on high-resolution biostratigraphy, oxygen isotopes, and perhaps cyclostratigraphy. This chronology can be tied into the seismic stratigraphy and will provide ages throughout the Pliocene–Pleistocene part of the transect, as hemipelagic units were confirmed to be prominent and easily traceable horizons.

The Miocene section reveals pronounced parallel stratification in seismic data, which seems to be related to the different consolidation behavior of sands, silts, clays, and hemipelagic units. Carbonate-bearing and clay units show a much more rapid lithification, whereas sand remains unconsolidated. This might explain why sand is not well represented in rotary cores. The stratification of the Miocene section, which is similar across the 8°N drill site transect, may in turn indicate a different mode of deposition with less channelized transport and more widespread distribution of turbiditic deposits. Whether this change in deposition is linked to an overall change in sediment transport or grain size has to await further detailed analysis that carefully considers the potential sampling bias.

Operations

Hole U1451A extends from the seafloor to 582.1 m DSF and was advanced by the APC, HLAPC, and XCB systems. Deeper than 200 m DSF, 4.8 m intervals were drilled without coring after most HLAPC cores in order to stay within the operation time frame. Formation temperature measurements (APCT-3) were made to 406.4 m DSF, the deepest piston core formation temperature measurement ever obtained. Hole U1451A cored 394.9 m and recovered 337.80 m of core (86%).

In Hole U1451B, a reentry cone with 400 m of casing was drilled into the seafloor. This assembly was intended to stabilize the hole for deep coring and logging operations. XCB coring in the upper 600 m was stopped because of failures of XCB cutting shoes. Hole U1451B was reentered a second time, and RCB coring penetrated to 1181 m DSF. RCB coring penetrated 627.6 m and recovered 180.86 m (29%). Wireline logging failed because of unstable hole conditions, probably due to collapse of the sand formation around 500 m.

Lithostratigraphy

Recovered sediments from Site U1451 were divided into 23 lithostratigraphic units based on lithologic and microfossil characteristics obtained through macroscopic and smear slide analyses, as well as physical property measurements. The overall lithology of the expedition's deepest hole is comparable to that described at other sites, with the exception of the Oligocene–Eocene section, which is lithified and was not penetrated at the other sites. The dominant lithology at Site U1451 is mica- and quartz-rich sand, silt, and clay turbidites, carrying high-grade metamorphic minerals in some intervals. Units of turbidites are separated by bioturbated nannofossil-rich calcareous clays and occasionally calcareous ooze. Five volcanic ash layers with fresh glass shards were identified in nonturbiditic intervals shallower than 154 m CSF-A, including the Toba ash layer, which is present at 2.6 mbsf in Hole U1451A.

Hemipelagic calcareous clay intervals of variable carbonate content, observed between 50 and 190 m CSF-A, are common throughout the Pleistocene and Pliocene. These intervals are intercalated with intermittent sand and mud turbidites representing intervals of rapid deposition during the Late Pleistocene. During the Miocene and late Oligocene, calcareous clay deposition is reduced and the record is dominated by turbiditic sediments. The latter contains numerous sand-rich layers to 520 m CSF-A (about 9 Ma). Downhole, the proportion of sand decreases. This observation is likely biased by the change in coring technique from the HLAPC system in Hole U1451A to the RCB system in Hole U1451B, as the RCB system was believed to be unable to recover loose sand. The turbidite units from 190 m CSF downhole mark an extended period of proximal channel or turbidite activity at this site from late Oligocene to late Miocene (~6 to 28 Ma). Deeper than this interval, calcareous and clastic sediments become increasingly lithified. Green to brown claystones are interbedded with light green and yellow calcareous claystones and limestones. Within the calcareous claystone sequences, breccias of calcareous claystone clasts in a siltstone and sandstone matrix are interpreted to be postdepositional intrusions or injectites. The lowermost ~100 m of Hole U1451B contains foraminiferal limestones, mottled calcareous claystones, and claystones reflecting the prefan paleooceanographic environment and much reduced influence of fan sedimentation. The transition from turbidites to limestone around 1100 m CSF-A marks the last occurrence of any significant fan deposition at this site. The present lithostratigraphic section therefore captures the complete sedimentary record of fan deposition to the onlap of the fan onto late Oligocene lime-

stones. This sedimentary record extends existing oceanic archives of the Himalayan erosion by about 10 My.

Biostratigraphy

Calcareous nannofossils and foraminferal biostratigraphic analyses at Site U1451 resulted in the identification of 39 biomarkers and the construction of 31 biozones, providing a comprehensive and detailed age model for the long-term development of the Middle Bengal Fan from the Paleogene to recent. Furthermore, the transition from probably Himalayan-derived turbiditic sediments to pelagic-dominated sedimentation is constrained to the late Oligocene.

The uppermost 120 m of Hole U1451A (lithostratigraphic Units I–III) is a sequence of turbiditic sands and muds with minor intercalated hemipelagic layers. Six biomarkers were identified within this sequence, providing good age control for Pleistocene fan development at this site. A thick (66 m) pelagic sequence was recovered in Cores 354-U1451A-23F through 29F (lithostratigraphic Unit IV) and contains eight biomarkers. This sequence represents more than 3 My of pelagic sedimentation, with little turbiditic influence. Deeper than lithostratigraphic Unit IV, 450 m of turbidite-dominated sedimentation, present from Core 354-U1451A-30F to the base of the hole, was deposited in approximately 3.5 My, based on four biomarkers observed in this sequence. The accumulation rates of ~1 and >10 cm/ky in the pelagic sequence and the turbidite-dominated sequence, respectively, suggest that the majority of fan development occurred in Miocene and Pleistocene and is more restricted in the Pliocene. The first occurrence of *Catinaster coalitus* was observed at the base of Hole U1451A (midpoint = 575.60 m CSF-A) and the top of Hole U1451B (590.06 m CSF-A) and provides tight age control for the overlap succession of the two holes.

The Oligocene/Miocene boundary was recovered and lies between Samples U1451B-54R-CC and 55R-CC. This boundary is identified by the last occurrence of *Reticulofenestra bisectus* and *Zygrhablithus bijugatus* (nannofossil Zone NP25). A major change from turbidite-dominated to pelagic-dominated sedimentation occurs between Cores 354-U1451B-62R and 63R (nannofossil Zone NP24).

Because of intense recrystallization and preservation issues, the depositional age of the limestones are difficult to constrain. Samples 354-1451B-71R-CC and 72R-CC contain *Morozobella aragonensis*, which is a marker species for foraminifer Zone E9 (43.6–52.3 Ma). The radiolarian species *Thyrsocyrtis rhizodon* was observed in Sample 354-U1451B-69R-CC, confirming an Eocene age for these sediments.

There appears to be a significant hiatus of 16–18 My between Samples 354-U1451B-71R-CC and 72R-CC. Sample 354-U1451B-72R-1, 0–1 cm, contains *Discoaster multiradiatus* and *Fasciculithus* spp., which are biomarkers for nannofossil Zone NP10. Sample 354-U1451B-73R-CC represents a gap zone marked by the absence of *D. multiradiatus* and places the base of Site U1451 in the Paleocene (Thanetian). Confirming the presence and extent of this hiatus will be the subject of postexpedition research.

Paleomagnetism

Paleomagnetism of 269 archive section halves and 93 discrete samples from Site U1451 allowed us to identify 12 polarity reversals in Hole U1451A, mostly in calcareous clay deposits. We place the boundary between the Brunhes and Matuyama Chrons at 72.24 m CSF-A in Hole U1451A. A calcareous ooze deposit in Hole U1451A contains polarity zones corresponding to the Jaramillo and Cobb Mountain Subchrons (80.35–81.78 and 83.10–83.44 m CSF-A, respectively), allowing us to correlate the interval with similar lithostratigraphic units at Sites U1449 and U1450. Several reversals between 140 and 163 m CSF-A in Hole U1451A are interpreted as the Gauss and Gilbert Chrons and their subchrons. Reversals at 108.30 and 218.70 m CSF-A in Hole U1451A have not yet been linked to the geomagnetic polarity timescale. Multiple declination changes were observed in Hole U1451B, most related to rotation during the coring process. None have yet been identified unambiguously as polarity reversals.

Physical properties

Physical property data were acquired at Site U1451 for all Hole U1451A and Hole U1451B cores, including density, magnetic susceptibility, *P*-wave velocity, NGR, and thermal conductivity. The data from APC cores are mostly of good quality. However, the whole-round logger data from cores obtained through RCB drilling—the majority of Hole U1451B—underestimate density, magnetic susceptibility, and NGR because the cores typically do not completely fill the liner cross section and in situ values are therefore underestimated.

Hole U1451A recovered core material from 0 to 579 m CSF-A, and Hole U1451B recovered core material from 542 to 1175 m CSF-A. The total core recovery at Site U1451 was 518.66 m (51%). Physical properties at Site U1451 primarily reflect lithologic variations but also show downcore compaction and lithification documented by decreasing porosities and increasing densities and *P*-wave velocities, specifically in the lowermost Cores 354-U1451B-65R through 73R. Based on the principal lithologic name from the core description, average physical properties were determined for 10 lithologies. The most common principal lithology is calcareous ooze (~120 m), followed by clay (~96 m), sand (~84 m), and silt (~74 m). Claystone (~65 m), limestone (~41 m), and siltstone (~21 m) make up the lower part of Hole U1451B. Volcanic ash occurs only in limited intervals (totaling 0.57 m), and siliceous ooze is absent. Physical property measurements follow the following general trends: limestones have the highest average density and *P*-wave velocity; sands have the highest magnetic susceptibility; volcanic ashes, clays, and claystones have the highest NGR, and calcareous oozes generally have the lowest values in all measurements. Some of the sand-rich intervals were difficult to recover and were often fluidized, which sometimes resulted in incompletely filled core liners; this resulted in anomalously low whole-round measurements (gamma ray attenuation [GRA] density, magnetic susceptibility, and NGR values). The same is true for most of the lithified intervals drilled with the RCB system, where GRA values significantly underestimate moisture and density values.

Geochemistry

Detailed pore water measurements distinguish five hydrological units based on sulfate, phosphate, silica, magnesium, potassium, calcium, and alkalinity content. The deepest unit bears distinct characteristics due to the strong influence of the limestones. It is characterized by a strong rise in calcium content although alkalinity remains low and constant, buffered by pressure-dissolution and recrystallization of the carbonate-rich lithology and an upward diffusion/advection of interstitial water.

Throughout Site U1451, the carbonate content of bulk sediments varies widely from 0.2 to 96.6 wt% $CaCO_3$, reflecting contrasted depositional environments, including significant contributions from detrital carbonates. Turbiditic sediments have

low carbonate content in the upper section (Pleistocene) with values roughly doubling around 150 m CSF-A. This sharp transition occurs during the early Pliocene and is followed by gradually increasing carbonate content to 700 m CSF-A. These trends in carbonate content of the turbiditic sediments most likely reflect a change in detrital carbonate supply, which correlates with observations at Site U1450. Turbiditic sediments are absent deeper than 1097 m CSF-A (mid-Oligocene), and limestone—at times almost pure ($CaCO_3$ > 97 wt%)—becomes the dominant lithology. Hemipelagic clays are present throughout the entire record and are characterized by highly variable carbonate content, often indistinguishable from that of turbiditic sediments. Major and trace element concentrations (e.g., CaO and Sr) measured via hand-held X-ray fluorescence (XRF) suggest that turbiditic and hemipelagic sediments consist of distinct binary mixings between carbonate and silicate end-members. The contrasted composition of the silicate fraction of hemipelagic clays is further supported by their frequent depletion in K and enriched Fe compared to turbiditic clays. In turbiditic sediments, the major element composition (e.g., Fe/Si and Al/Si) closely matches the chemical composition observed in sediments from the actual Ganges-Brahmaputra river system.

Overall, TOC content is low, with an average value of 0.3 wt%. Within turbidites, TOC broadly co-varies with Al/Si ratios—a proxy for sediment grain size and mineral composition—reflecting preferential association of organic matter with clays previously documented in both the modern Ganges-Brahmaputra river system and in active channel-levee sediments in the Bay of Bengal deposited over the past 18 ky (e.g., Galy et al., 2007). Clay-rich turbiditic sediments are often characterized by significant organic carbon depletion compared with sediments from the modern Ganges-Brahmaputra river system and the active channel-levee system at 17° N. However, the TOC budget is likely to be also affected by the frequent presence of woody debris concentrated in the lower part of turbiditic sequences.

Microbiological subsampling of sediments and pore water at Site U1451 included establishing a microbial cell counting method, with further processing of the samples to be performed following the expedition.

Site U1452

Site U1452 (proposed Site MBF-5A) is located in the center of the seven site transect drilled during Expedition 354. Site U1452 is located in a relatively flat environment with a smooth morphology. Topographic expressions of channels are absent in the vicinity of the site. The seismic profile at this site reveals a prominent, >20 km wide and up to 40 m thick levee, the top which is at only ~5 mbsf.

At this site, we focused on coring the upper levee to provide a detailed record of this type of depositional system. Two holes were cored through this levee to allow high-resolution sedimentological, geochemical, and micropaleontological investigations. A single mudline core in Hole U1452A was devoted to the detailed study of the hemipelagic deposition during the last glacial cycle and to the Toba ash. Hole U1452B was cored to 217.7 mbsf for the study of the Upper Pleistocene section. Finally, Hole U1452C was cored to 41.3 mbsf to provide a more complete record of the levee and to allow more extensive sampling.

Principal results

Coring at Site U1452 contributed to the Pleistocene transect of seven sites, which is one of the primary Expedition 354 objectives. The levee sequence recovered will allow detailed integrated sedimentological and geochemical investigations. On such rapidly accumulated sediments, $\delta^{18}O$ measurements on planktonic foraminifers are expected to document the evolution in the sediment source region on glacial–interglacial timescales. This section is also important for the understanding of channel and levee formation. Site U1452 cored the fine-grained levee, as was done deeper in Site U1449, but also penetrated the coarser basal unit. Physical properties seem to indicate a progradation and the transition from sand deposition, through erosion, to levee construction.

The successful interpretation of seismic facies types with respect to grain size allowed coring strategies to target specific horizons. Hemipelagic layers, after being identified in several previous sites, were used to establish a preliminary Pleistocene seismic stratigraphy. Also, coring targeting these layers was successful and provided an improved chronology even when HLAPC coring was alternating with short 4.8 m advances without coring.

A hemipelagic unit deposited from ~0.8 to ~1.2 Ma between 166 and 190 m CSF marks a period when fan deposition was diverted to other parts of the fan and only clays were supplied to this area; this was also observed at our other sites to the east (Sites U1449, U1450, and U1451). Fan sedimentation intensified between 800 and 300 ka, as represented by sheeted sands and the levee. These sheeted sands and the levee grew by 100 m in 500 ky, equivalent to an average sedimentation rate of 20 cm/ky. The end of this intense period of fan sedimentation at 300 ka is constrained by the basal age of the surficial hemipelagic unit.

Operations

Hole U1452A was a single APC mudline core (Core 354-U1451A-1H) that recovered 8 m of sediments including the mudline. Hole U1452B consisted of oriented APC coring to 41.4 mbsf and continued coring with the HLAPC system. From 71.1 to 142.4 mbsf, we alternated 4.7 m long HLAPC cores with 4.8 m intervals drilled without coring. In this interval, seven HLAPC cores (354-U1452-14F through 26F) penetrated 32.9 m and recovered 21.41 m of core (65%). The eight 4.8 m advances without coring penetrated 38.4 m, nearly continuous HLAPC coring to 217.7 m. Nine 4.8 m advances without coring were intercalated with cores in units predicted to be sandy. Overall recovery is 79% for this hole.

Hole U1452C was continuously cored from the seafloor to 41.3 m CSF-A to obtain a more complete record of the uppermost levee sequence down to the sand layer at the base of the levee. All APC cores were oriented, and core recovery in this hole was 81%.

Lithostratigraphy

Drilling at Site U1452 intentionally targeted a Pleistocene-aged levee identified in the pre-expedition seismic data. The lithology and structures of sediments recovered indicate we captured the initiation and cessation of an entire levee sequence (8–40 mbsf), from prelevee sand sheets (40–167 mbsf) to calcareous clays (>167 mbsf), marking the initiation of turbiditic deposition levee-building at this location. The prelevee sand sheets are turbiditic sands dominated by mica- and quartz-rich sand characteristic of sediments found in Himalayan rivers. These sands were likely deposited as interlevee sheet flows originating from a nearby channel. The hemipelagic calcareous clay unit extends to 190 mbsf and overlies interlevee sand-rich turbidites.

The sediments at this site document the channel system shifting across the fan. Initially, the proximal channel sand deposition reduced and was succeeded by increased deposition of hemipelagic nannofossil-rich calcareous clays. Overlying this calcareous inter-

val, a very thick (~160 m) section of levee deposits (i.e., sand and mud turbidites) reflects activation of a nearby channel and the associated levee building that forms the top of the section. The levee deposits are overlain by a relatively thin unit of bioturbated calcareous clay, representing the end of proximal channel activity and in turn a decrease in siliciclastic input. The surficial calcareous clay unit at the top of the levee contains a glassy volcanic ash layer presumably from the Toba eruption that occurred at ~75 ka.

Biostratigraphy

Biostratigraphic control at Site U1452 is limited, but four tie points were observed and help to constrain levee development during the Pleistocene. Although the foraminiferal biomarker *Globorotalia tosaensis* (0.61 Ma) was found in Holes U1452B and U1452C (at 8.97 and 23.29 m CSF-A, respectively), its first occurrence was found at a shallower depth than the nannofossil biomarkers *Emiliania huxleyi* (0.29 Ma) and *Pseudoemiliania lacunosa* (0.44 Ma), indicating that this foraminifer was either reworked or has a longer extent in the Indian Ocean. Cores 345-U1452B-33F through 37F are dominated by hemipelagic calcareous clay, are abundant in nannofossils, and contain abundant to barren foraminifers. Interestingly, fragmentation of planktonic foraminifers was higher in the hemipelagic sediments than in the turbiditic sediments. The nannofossil biomarkers agree well with the magnetic polarity reversals found at Site U1452.

Paleomagnetism

As was observed in the upper parts of Sites U1449 through U1451, sediments at Site U1452 recorded the Brunhes/Matuyama boundary (184.10 m CSF-A) and both boundaries of the Jaramillo and Cobb Mountain Subchrons (186.00–187.20 and 188.33–188.61 m CSF-A, respectively). Relative to the seafloor, these are the deepest instances of these polarity transitions identified on our transect to date. Also similarly to Sites U1449 to U1451, the Jaramillo and Cobb Mountain Subchrons occur within an interval of hemipelagic sedimentation at Site U1452. The Brunhes/Matuyama Boundary is associated with an ash layer, believed to be from Toba. Microtektites, likely from the Australasian Microtektite Event dated at 790 ka, were found deeper than the Brunhes/Matuyama boundary, further supporting the identification of this polarity transition.

Physical properties

Physical property data were acquired on all cores from Holes U1452A and U1452B, including density, magnetic susceptibility, *P*-wave velocity, NGR, and thermal conductivity. The physical property data are mostly of good quality and reflect lithologic variations. Using the principal lithologic name from the core description to assign five lithologies (sand = ~46 m, silt = ~27 m, clay = ~33 m, calcareous clay = ~26 m, and volcanic ash), we calculated their minimum, maximum, and average physical properties. Average wet bulk densities are rather uniform for terrigenous sediment (sand, silt, and clay), ranging from 1.89 to 2.03 g/cm^3, calcareous clay has lower average densities (1.72 g/cm^3), and volcanic ash has substantially lower wet bulk densities (1.54 g/cm^3). Average *P*-wave velocities are highest in sand (1697 m/s) and lowest in clay and in calcareous clay (~1525 m/s). Average magnetic susceptibilities are also highest in sand (107×10^{-5} SI), followed by silt (80×10^{-5} SI) and clay (58×10^{-5} SI). The lowest values occur in calcareous clay (22×10^{-5} SI). Average NGR is high throughout the terrigenous components sand, silt, and clay (around 65 counts/s) and lower in calcareous clay (45 counts/s). Average thermal conductivity is highest in silt (1.63 W/[m·K]) and lowest in calcareous clay (1.18 W/[m·K]).

Geochemistry

Detailed pore water measurements distinguish two hydrological units based on sulfate, phosphate, silica, magnesium, potassium, calcium, and alkalinity content. Carbonate contents of turbiditic sediments vary from 0.6 to 7.4 wt% $CaCO_3$. Similar carbonate contents were measured in upper Pliocene and Pleistocene turbiditic sediments recovered at Sites U1449, U1450, and U1451. A 4.6 m thick hemipelagic interval at 184 mbsf was analyzed at high resolution with XRF scanning. It reveals that carbonate content varies between 18% and 60% with an average of ~40%. Sr/Ca ratio and carbonate content variations suggest a single binary mixing between marine biogenic carbonate and a clay end-member of supracrustal composition.

Site U1453

Site U1453 (proposed Site MBF-4A) is located in the center of the seven site, ~200 m penetration transect drilled during the expedition. Site U1453 is located at 8°0.42′N, 86°47.90′E in a water depth of 3690.5 m. Combined with the other transect sites, Site U1453 will document depocenter migration and quantify the overall sediment delivery to 8°N since the Pleistocene.

Site U1453 is located ~1 km south and ~5 km east of a prominent surficial channel. The channel exhibits pronounced meandering point bars and internal terraces. Sediment transported by this channel has therefore significantly influenced deposition at this site during the channel's lifetime. A prominent buried point bar is located <1 km west of the site. The overall seismic reflectivity at the drill site is relatively high, indicating coarse material throughout most of the drilled section, except for the lower portion of the drill hole. Distinct and variable local spillover deposits were expected at the site in response to the channel and meander evolution. Toward the base of the hole, lower seismic reflectivity and distinct layering is inferred to reflect hemipelagic or distal levee deposition.

In addition to coring, downhole logging was introduced as an important objective of Site U1453 after attempts to log at Sites U1450 and U1451 were unsuccessful. Logging data are considered to be essential for determining the inventory of lithofacies and structures in the fan given the limitations in recovery of unconsolidated coarse material and for measuring in situ physical properties and imaging fine-scale sedimentary structures. Therefore, we decided to log Hole U1453A despite its shallow penetration to only ~215 m CSF-A to increase chances that we could acquire this critical in situ log data. This was particularly important for characterizing the in situ properties of thick sandy intervals that HLAPC cores returned as loose and liquefied sand.

Principal results

Site U1453 contributes to the overall seven site transect drilled by Expedition 354. When integrated with the seismic profile and refined chronostratigraphic data from the rest of the transect, this site will document the fan construction processes and depocenter migration time frame. More particularly, Site U1453 provides an almost completely recovered succession of silt- and/or sand-dominated sheeted units, which are related to the formation and evolution of a large meandering channel system lacking a distinct levee unit. Intercalation of these sheets with thinner levee units either from the large channel or from nearby smaller channels may help us to understand why the channel has been apparently main-

tained in this position for a relatively long time period. This type of configuration is part of the different processes that influence interlevee deposition. A few thin hemipelagic layers are also observed between sandy turbiditic units, which may indicate that sheeted sedimentation may be restricted to short time periods only and is not always followed by an erosional and levee formation phase. The interval cored between 144 and 159 m CSF-A represents an expanded hemipelagic unit, dated to the time interval between 0.8 and 1.2 Ma. Fan sedimentation intensified between 800 and 300 ka, the basal age of the surface hemipelagic unit. Accordingly, fan deposits grew by 100 m in 500 ky, equivalent to an average sedimentation rate of 20 cm/ky.

Acquisition of the expedition's only downhole log data will allow detailed comparison of how well the fine-scale (centimeter to decimeter) structure in the formation has been preserved in cores. Particularly, the proportion of sand in the formation versus the amount recovered by coring is of interest to calibrate the sedimentary records from other sites.

Analyzing some graded variations within the sandy units using magnetic susceptibility data from both cores and downhole data shows that despite the HLAPC coring process and curatorial procedures (vertical settling of sands), the average physical properties still match with in situ data and can be used to characterize the formation. This match confirms that cored structureless sand truly reflects, on average, the sand unit at depth even though several meter thick sand cores were recovered with the HLAPC system that apparently did not fully penetrate the formation.

Operations

In Hole U1453A, APC and HLAPC coring penetrated the seafloor to 172.9 m CSF-A, except for one 5 m interval advanced without coring. Most of the coring was done with the HLAPC system. However, the APC system was used for the uppermost four cores and one deeper core around 145 m CSF-A when we attempted to recover a hemipelagic layer in a single core. From 172.9 to 215.7 m CSF-A, the hole was deepened with HLAPC cores alternating with five 4.8 m advances without coring. Hole U1453 penetrated 186.7 m, and 164.8 m was cored, 88% recovery.

After coring was completed, we collected downhole logging data with two tool strings (triple combo and FMS-sonic). Logging was very successful with good hole conditions and reached the full depth of the hole.

Lithostratigraphy

The overall lithology of Site U1453 is similar to the other Expedition 354 sites, in that it is dominated by mica- and quartz-rich sand, silt, and clay turbidites separated by bioturbated nannofossil-rich calcareous oozes and occasional glassy volcanic ash layers. Turbidite sequences at Site U1453 represent cycles of channel-levee activity and abandonment that constructed the fan. The base of the section contains thick sand units, which are most likely sheet deposits from nearby channels. Above these sands, a moderately thick (~15 m) section of calcareous clay indicates a time when channel activity was reduced. The middle of the section contains a 127 m thick interval of fine sand interbedded with mud turbidites and occasional calcareous clay beds, suggesting onset and waxing and waning of proximal channel activity and levee building. The stratigraphic section is topped with 10 m of calcareous clay, indicating reduced siliciclastic input.

Biostratigraphy

Calcareous nannofossil and planktonic foraminiferal biostratigraphic analyses were conducted at Site U1453 on 37 samples and resulted in the identification of 4 biomarker events. The sedimentary succession at Site U1453 extends to the early Pleistocene. As with other sites, planktonic foraminiferal assemblages are characteristic of tropical–subtropical environments. Foraminiferal preservation ranges from poor to good in samples where they occur, and fragmentation of planktonic foraminifers ranges from light to severe. As at Site U1452, the last occurrence of the foraminiferal biomarker *Globorotalia tosaensis* (0.61 Ma) was found at a shallower depth than the nannofossil biomarkers *Emiliania huxleyi* (0.29 Ma) and *Pseudoemiliania lacunosa* (0.44 Ma), indicating that this foraminifer was either reworked or has a longer duration in the Indian Ocean. Foraminiferal biostratigraphy was limited at this site because of the large section of sands recovered from Cores 354-U1453A-10F through 28F, in which samples are either barren of foraminifers or have a very rare occurrence (<0.1%). The last occurrence of the nannofossil *Helicosphaera sellii* (1.26 Ma) is found at approximately 116 m CSF-A. However, the Brunhes/Matuyama boundary (0.781) is found at 152 m CSF-A, indicating that either *H. sellii* was reworked or has a longer duration in the Indian Ocean. This discrepancy was observed at several Expedition 354 sites and will be further studied in postexpedition work.

Paleomagnetism

The Brunhes/Matuyama boundary and both boundaries of the Jaramillo and Cobb Mountain Subchrons were identified at Site U1453 in hemipelagic calcareous clay units between ~142 and 160 m CSF-A. A ~180° change in declination associated with a thin ash layer is interpreted as the Brunhes/Matuyama boundary (152.59 m CSF-A). Changes in declination also clearly delineate the Jaramillo and Cobb Mountain Subchrons (155.76–156.71 and 157.59–158.23 m CSF-A, respectively) in calcareous clay deposits at Site U1453.

Physical properties

Physical property data were acquired on all Hole U1453A cores, including density, magnetic susceptibility, *P*-wave velocity, NGR, and thermal conductivity. Physical property data at Site U1453 are mostly of good quality and reflect lithologic variations. Using the principal lithologic name from the core description to assign five lithologies (sand = ~73 m, silt = ~11 m, clay = ~45 m, calcareous clay = ~23 m, and volcanic ash), we calculated their minimum, maximum, and average physical properties. Wet bulk densities are rather uniform for terrigenous sediment (sand, silt, and clay), ranging from 1.89 to 1.96 g/cm^3. Calcareous clay has the lowest densities (1.62 g/cm^3), followed by volcanic ash (1.68 g/cm^3). *P*-wave velocities are highest in sand (1666 m/s on average) and lowest in silt and clay (~1530 m/s). Magnetic susceptibilities are also highest in sand (109×10^{-5} SI), followed by silt (90×10^{-5} SI) and clay (56×10^{-5} SI). The lowest values occur in calcareous clay (20×10^{-5} SI). NGR is high throughout the terrigenous components sand, silt, and clay (around 70 counts/s) and low in calcareous clay (43 counts/s). Thermal conductivity is highest in sand (1.82 W/[m·K]) and lowest in calcareous clay (1.17 W/[m·K]).

Downhole logging

The triple combo (magnetic susceptibility, NGR, and resistivity) and FMS-sonic velocity tool strings were run in Hole U1453A. The

hole was filled with 12 lb/gal heavy viscous mud to inhibit borehole wall collapse. In contrast to our previous logging attempts, logging was successful with a single run of the triple combo tool string and two runs of the FMS-sonic tool string to the bottom of the hole at 220 m wireline log depth below seafloor (WSF). The hole diameter varied between 9 and 14 inches with only a few washout zones.

The downhole measurements of magnetic susceptibility and NGR match the equivalent core measurements well and permit preliminary interpretation of lithology based on the log data in the intervals where core was not recovered. The FMS resistivity images in particular provide a good record of the depth and thickness of the sand beds in the hole. Sand-rich cores were sometimes fluidized when recovered, but the log data could confirm that the sands in the 9.5 m core came from the same 9.5 interval in the hole, and compositional trends over several cores were similar in core and log data. Additionally, downhole *P*-wave velocities are higher than those measured in the laboratory, reflecting in situ conditions in the borehole.

Geochemistry

The close proximity of a channel incising deeper than 100 m CSF-A, associated with the variable dip angle of the formations, provided the opportunity to investigate a subseafloor hydrology that is potentially affected more by lateral flow than other drill sites. A well-defined boundary between two hydrologic units is observed at Site U1453 around 30 m CSF-A, defined by depth profiles of sulfate content and alkalinity. This is very similar to what was observed at Sites U1449 and U1452, implying only a limited local hydrological effect related to the close proximity of a channel.

Other similarities include (1) Pleistocene turbidites characterized by carbonate content of 0.8 to 5.9 wt% and (2) hemipelagic deposits that have an average carbonate content of 25.9 wt%. For turbidites, these characteristics are similar to what is observed in modern Ganga-Brahmaputra river sediments, as well as the uppermost 150 m at Sites U1449–U1452 and DSDP Site 218. TOC content in turbidites averages 0.7 wt%, and the maximum TOC values of hemipelagic lithologies (2.5 wt%) is identical to maximum values for turbiditic sediments. TOC covaries with bulk sediment Al/Si ratios, reflecting the preferential association of organic matter with clays that is documented in both the modern Ganga-Brahmaputra river system and in active channel-levee sediments in the Bay of Bengal deposited over the past 18 ky. Bulk geochemical trends closely track those observed at Sites U1449–U1452 and in modern sediments in the Ganga-Brahmaputra river system. Samples offset from the main trends are from hemipelagic units and suggest the occurrence of Fe-rich clays and/or a low K/Al subpopulation, possibly suggesting a different terrigenous input or sorting effect.

Site U1454

Site U1454 (proposed Site MBF-7A) is the westernmost site of the transect of seven shallow penetration holes drilled in the Bengal Fan at 8°N during Expedition 354. The site was introduced during the expedition as an alternate site to capture the most recent and Upper Pleistocene fan deposition. Expedition 354 sites in the eastern and central part of the transect revealed that fan deposition above and below the Toba ash layer (~75 ka) was remarkably low, marking the migration of turbidite channel activity to the west of the 85°East Ridge for probably the last 300 ky.

Site U1454 is located ~50 km west of Site U1455 (DSDP Site 218) at 08°0.39′ N, 85°51.00′E, in a water depth of 3721.4 m. It is situated on the western levee of a channel-levee system that is believed to be the modern active channel of the fan (Hübscher et al., 1997). The levee surface rises ~50 m above the thalweg of the meandering channel that is well imaged with multibeam bathymetry. Site U1454 is intended to provide a sequence through a channel-levee system that can be dated by ^{14}C and $\delta^{18}O$ and which can thereby be related to global climatic and sea level cycles as well as other proxies for sediment flux and weathering. The general objective of the Pleistocene transect at 8°N is to document depocenter migration and overall accumulation rates since the Pliocene, and Site U1454 completes this approach by focusing on the Late Pleistocene and Holocene fan deposition. Obtaining a high-resolution levee record that could extend into the Holocene will allow comparison of this middle fan deposition to an upper fan levee likely constructed across the same channel levee at 16°N since 18 ka (Hübscher et al., 1997; Weber et al., 1997). The levee at 16°N records consistent changing weathering and vegetation conditions since the Last Glacial Maximum (Galy et al., 2008; Lupker et al., 2013), which can be further correlated at Site U1454.

Principal results

Site U1454 provides a key expanded section to the overall understanding of depositional processes in the Pleistocene Bengal Fan. This site was added during the expedition because of the inferred Holocene age of the channel with sediments suitable for dating with oxygen isotopes and radiocarbon on foraminiferal tests and on terrestrial organic, in addition to high-resolution nannofossil biostratigraphic work. Accordingly, we will be able to determine the time spans over which the levee units have formed. Also, the surficial calcareous clay unit will shed light on the episodicity and absence of turbidites at this location. Furthermore, we expect to be able to link channel activity with sea level and glacial–interglacial climatic cycles.

Beneath the levee unit, coring recovered a sand-rich section comparable to Site U1452 and likely representing the progradational facies of early channel formation and erosion. Several other smaller channel systems in the vicinity contributed to sediment accumulation at Site U1454, and it will be interesting to investigate their temporal relationships with the active channel. Mud turbidites, silt, and sand beds are intercalated between hemipelagic units, indicating rare episodic activity.

An organic-rich turbidite was recovered at ~34 m CSF-A in the sand-rich section. It comprises an 18 cm thick layer of organic debris deposited at the base of a sand layer. The base of the organic layer contains centimeter-sized pieces of wood. Unlike the Miocene and Pliocene, organic debris is not frequently found in Pleistocene turbidites, and this one represents certainly an unusual transport from delta or floodplain to the fan. Identification of wood species may allow relating this deposit more precisely to an event and a vegetation zone.

Site U1454 also completes the recovery of the Middle Pleistocene hemipelagic interval to the westernmost position and allows detailed study of the transition to intensified fan activity over a lateral distance of 300 km. This will shed light on the distances over which the active channel can deliver the fine particles in particular and contribute to the dilution of pelagic accumulation.

Operations

Four holes were cored at Site U1454. Hole U1454A was a single mudline core to 7.5 mbsf for microbiology and geochemical studies. Hole U1454B was cored with the APC and HLAPC systems to 161.8 mbsf and recovered 129.51 m of sediment (88%). This hole also in-

cluded three 4.8 m advances without coring. The four upper cores utilized the APC system with an orientation tool and nonmagnetic hardware. Holes U1454C and U1454D were shallow penetrations (37.2 and 37.1 mbsf, respectively) and recovered 30.16 and 24.46 m of sediment (81% and 66%, respectively). The later were cored to fully record the uppermost levee, provide sufficient samples for high-resolution studies, and avoid gaps. Cores from Holes U1454C and U1454D were not split.

Lithostratigraphy

Coring at Site 1454 recovered a full levee sequence thought to be associated with the modern active channel of the Bengal Fan, well represented by the 25 m sequence of mud turbidites in Unit II. Intervals of calcareous clay occur in the top 20 cm of Hole U1454B and are rare to about 110 m CSF-A. Deeper calcareous and clastic units alternate to 139.14 mbsf, where an 18 m thick interval of mottled calcareous clay with occasional color banding appears. Plant fragments occur in several silt intervals, including large (~2 cm) woody pieces. In the lower hemipelagic interval, one 8 cm thick volcanic ash layer is present at 145.5 m CSF-A. It is much thinner than the shallowest ash layers recovered at other 354 sites (~20 cm) and is likely related to the Toba eruption before the Brunhes/Matuyama boundary (790 ka).

Overall, siliciclastic units (silt, clay, and sand) at Site U1454 are compositionally classified as mica rich (muscovite and biotite) and quartz rich. Sand occurs mostly in fine to medium grain size ranges, with rare occurrences of coarse-grained particles. Feldspars and heavy minerals (e.g., amphibole, garnet, clinozoisite, zoisite, tourmaline, zircon, rutile, epidote, sillimanite, chloritoid, pyroxene, staurolite, and opaque minerals) are common in silt- and sand-rich layers and occasionally contain euhedral carbonate minerals and carbonate aggregate grains. Lithic fragments (e.g., biotite-gneiss, amphibole-mica schist, sillimanite-biotite-gneiss, and phyllite fragments) appear in sand. These minerals are consistent with a general provenance from Himalayan river sands (e.g., Garzanti et al., 2010).

Biostratigraphy

The levee system targeted for drilling at Site U1454 was expected to be of Pleistocene age. Biostratigraphic age control within the Pleistocene is limited to three nannofossil zonations and two foraminiferal biomarkers (at 0.61 and 1.88 Ma). Calcareous nannofossil assemblages were observed in 44 samples from Site U1454, and the sediments contain a recent to early Pleistocene sequence. Foraminiferal assemblages were observed in 19 samples, and 19 samples were barren of foraminifers because of the recovery of turbidite sands in the core catcher samples. Postexpedition work on nannofossils may further constrain sediment ages, as there are an additional potential 20 biostratigraphic markers that can be used to refine the Pleistocene age model.

Paleomagnetism

We identified the Brunhes/Matuyama boundary and the Jaramillo and Cobb Mountain Subchrons in hemipelagic calcareous clay at 145–151 m CSF-A at Site U1454; they can be correlated with similar intervals in other holes within the Expedition 354 transect based on both magnetostratigraphy and seismic stratigraphy. The Brunhes/Matuyama boundary occurs at 145.83 m CSF-A, roughly similar to the depth of the same transition at Site U1453; as at Site U1453, the transition is associated with an ash layer. The upper boundary of the Jaramillo Subchron is likely in an interval that was not recovered between Cores 354-U1454B-29F and 30F. Core 30F contains the lower boundary of the Jaramillo Subchron (148.63 m CSF-A) and both boundaries of the Cobb Mountain Subchron (149.86–150.20 m CSF-A).

Physical properties

Physical property data were acquired on all Hole U1453A cores, including density, magnetic susceptibility, *P*-wave velocity, NGR, and thermal conductivity. The physical property data at Site U1453 are mostly of good quality and reflect lithologic variations. For five principal lithologies based on visual core description, average physical properties were determined: the most common principal lithology is sand (~73 m), followed by clay (~45 m), calcareous clay (~23 m), and silt (~11 m), with volcanic ash occurring in traces. The physical property average values are as follows. Wet bulk densities are rather uniform for terrigenous sediment (sand, silt, and clay), ranging from 1.89 to 1.96 g/cm^3. Calcareous clay has the lowest density (1.62 g/cm^3), followed by volcanic ash (1.68 g/cm^3). *P*-wave velocities are highest in sand (average = 1666 m/s) and lowest in silt and clay (~1530 m/s). Magnetic susceptibilities are also highest in sand (109×10^{-5} SI), followed by silt (90×10^{-5} SI) and clay (56×10^{-5} SI). The lowest values occur in calcareous clay (20×10^{-5} SI). NGR is high throughout the terrigenous components sand, silt, and clay (around 70 counts/s) and low in calcareous clay (43 counts/s). Thermal conductivity is highest in sand (1.82 W/[m·K]) and lowest in calcareous clay (1.17 W/[m·K]).

Geochemistry

At Site 1454, interstitial water measurements were conducted only in the top 7 m. As at other sites studied during this expedition, the hydrochemistry in this upper section is dominated by biogenic processes that release dissolved phosphate, ammonium, and CO_2 (leading to a rise in alkalinity) and consume sulfate.

Carbonate content of turbidites analyzed throughout Site U1454 have $CaCO_3$ contents between 2 and 5 wt%, except for four samples from the upper 16 m of the levee that have 6 to 7.4 wt%. These higher values are significantly higher than all turbidite carbonate contents measured in the seven Pleistocene sections cored during Expedition 354 (0.5 to 6 wt%). It is, however, identical to carbonate content recorded in the levee sediments at 17°N during the last deglaciation stage (Lupker et al., 2013). This could indicate a match between the 17° and 8° levee records; however, the pattern of K/Al appears different between Site U1454 and 17°N.

Site U1455

Site U1455 (proposed Site MBF-1A) is the last site drilled during Expedition 354 in the Bengal Fan. It is a reoccupation of DSDP Site 218 (von der Borch, Sclater, et al., 1974), which was the first attempt to drill the Bengal Fan and was only spot cored with the RCB system to 773 mbsf. The site is above the eastern flank of the 85°E Ridge at 8°0.42′N, 86°16.97′E at 3743 m water depth. Site U1455 is one of the three deep-penetration sites of the Expedition 354 transect located to reveal Neogene fan evolution and Himalayan erosion. The site will also document the Pleistocene fan architecture when integrated into the complete seven site transect of the expedition. Coring to 900 m was planned to determine Miocene to Pliocene accumulation rates and changes related to Himalayan erosion and environment. The deeper part of the site will extend the existing Site 218 record back into the middle Miocene. Because of time constraints at the end of Expedition 354, we focused coring on three objectives: the Pleistocene (0–122 mbsf), the late Miocene terrestrial vegetation

(C_3 to C_4 plants) transition (360–431 mbsf), and the middle Miocene (773–949 mbsf) to extend the existing core record of Site 218.

Because Site U1455 is above the 85°E Ridge, which has undergone deformation since the Miocene (Schwenk and Spiess, 2009), accumulation rates at this site are lower than at Site U1450 in the axial part of the fan transect and similar to those at Site U1451. The overall thickness of the fan is less than 4 km in this location according to Curray et al. (2003). These lower accumulation rates offer the possibility to capture a longer stratigraphic range within an achievable depth of penetration. Site U1455 is intended to help establish a representative accumulation history from the middle Miocene to recent, which is essential to complete the 8°N transect of the Bengal Fan.

Principal results

Site U1455, located above 85°E Ridge, is a key location for the transect approach, particularly for investigating Miocene fan deposition. A comparison between the easternmost Site U1451 and this site should elucidate whether depocenter migration occurred in a similar manner as in the Pliocene and Pleistocene. Because of the absence of major channel-levee systems, addressing these objectives can only be achieved by integrating core and seismic data. This integration will require good chronostratigraphic control to be able to compare the same time periods. This has to await postexpedition work.

Site U1455 cored critical intervals that will address different objectives. In the upper section, in Core 354-U1455C-1H, the Toba ash layer is found at 5.6 mbsf instead of being consistently around 2 m deep as at other eastern Expedition 354 sites. The vicinity of the most recently active channel (see Site U1454, ~50 km west) is the likely explanation for this increased sedimentation, and indeed discrete turbiditic deposition is observed above the Toba ash layer at this site. This site will further document deposition of clay and silt in the context of a distant channel.

Second, the deeper late Miocene interval cored between 360 and 431 mbsf returned a relatively continuous record across the terrestrial vegetation change from the C_3 to C_4 photosynthetic type of plants, known to occur around 380 mbsf at Site 218. A number of short hemipelagic intervals are present in this section and should provide good chronological constraint for this transition. They may also document variability on shorter timescales.

Coarser grained deposition has been found deeper than 770 mbsf, even though recovery of sand is limited. Coarser grained material suitable to study Himalayan erosion was found, although it was not recovered at Site U1451 for the same period. In this particular depth interval, further detailed sedimentologic analyses may shed light on the causes for the depositional facies being different from Pliocene and Pleistocene times and determine whether the absence of levees originates from a change in sediment supply or in the lifetime of transport pathways or from other factors.

Operations

We cored three holes at Site U1455 (proposed Site MBF-1A; DSDP Site 218). Holes U1455A and U1455B each consists of a single mudline core penetrating to 0.9 and 6.9 mbsf, respectively. Hole U1455C consists of coring in three intervals from 0 to 122.3 m CSF-A (APC and HLAPC), 359.8 to 431.4 mbsf (HLAPC), and 773.0 to 949.0 mbsf (RCB). The uppermost interval consists of APC and HLAPC coring and four 4.8 m advances without coring (19.2 m). Cores 354-U1455C-1H through 24F cored 103.1 m in this interval and recovered 89.82 m of sediment (87%). We drilled 237.5 m without coring from 122.3 to 359.8 mbsf and then resumed continuous HLAPC coring. Cores 354-U1455C-26F through 41F penetrated from 359.8 to 431.4 mbsf (71.6 m) and recovered 48.82 m of sediment (68%). After retrieving the drill string to switch to the RCB system, we reentered Hole U1455C and drilled ahead without coring from 431.4 to 773.0 mbsf. We RCB cored from that depth to 949.0 mbsf. Cores 354-U1455C-43R through 60R penetrated 176.0 m and recovered 59.36 m of sediment (34%). Coring ended on 28 March 2015 at 1435 h when the operational time for the expedition expired.

Lithostratigraphy

As at other Expedition 354 sites, lithologic differences between units and variations in grain size and bed thickness reflect cycles of proximal turbidity current channel activity and abandonment. Sand intervals may represent interlevee sheet flows (e.g., Curray et al., 2003), whereas finer grained fractions are more likely preserved in leveed sections. Calcareous clay units reflect cessation of proximal channel activity, but the intervals also resemble episodes of minor increase in siliclastic depostion.

Coring in Hole U1455C was divided into three segments. The uppermost segment (from the seabed to 120.51 m CSF-A) is principally composed of micaceous quartz-rich siliciclastic sediments, many containing turbiditic structures and/or parallel laminations. In this segment, sand units are overlain by 13.5 m of calcareous clay covered by a 45.86 m thick section of sand and mud turbidites. There are two glassy volcanic ash layers at 5.68–5.75 and 82.80–82.89 m CSF-A. The second recovered segment of Hole U1455C (431.39–359.80 m CSF-A) is also predominantly micaceous and quartz-rich sand, silt, and clay, although fewer turbiditic structures are present. Calcareous clay units alternate with siliciclastic sediments. The lowermost segment (773.0 m CSF-A to base of the hole at 942.35 m CSF-A) contains claystone and siltstone intervals with preserved turbiditic structures, as well as a ~4 m thick unit of calcareous claystone. Organic fragments are prevalent in this lower section.

Overall, siliciclastic units (silt, clay, and sand) at Site U1455 are compositionally classified as micaceous (muscovite and biotite) and quartz rich. Sand occurs mostly in fine to medium grain size ranges, with rare coarse-grained particles. Feldspars and heavy minerals (e.g., amphibole, garnet, clinozoisite, zoisite, tourmaline, zircon, rutile, sphene, epidote, sillimanite, chloritoid, pyroxene, staurolite, and opaque minerals) are common in silt and sand layers and occasionally contain euhedral carbonate minerals and carbonate aggregate grains. Lithic fragments (e.g., biotite-gneiss, amphibole-mica schist, sillimanite-biotite-gneiss, and phyllite fragments) appear in sand. From previous sites (see **Principal results** from Site U1450), we know that siliciclastic sediments in the fan contain between ~3% and 10% of detrital carbonate as well. Calcareous clays contain clay minerals, foraminifers, diatoms, and radiolarians.

Biostratigraphy

Calcareous nannofossil and planktonic foraminiferal biostratigraphic analyses were conducted at Site U1455 on 113 samples and resulted in the identification of 14 biomarker events. These events were used to construct 3 foraminiferal and 10 nannofossil biozones, providing good age control extending back to the middle Miocene. The age model reconstruction is limited to the drilled intervals from

120 to 360 mbsf and between 430 and 770 mbsf as well as by the very low abundance and barren intervals from 360 mbsf to the bottom of Hole U1455C. Foraminiferal species diversity decreased with depth, which could be due to preservation changes in the sediments or could reflect a change in environmental conditions of the overlying water column.

Paleomagnetism

We identified the Brunhes/Matuyama boundary and the Jaramillo Subchron in a calcareous clay interval at Site U1455 that was correlated with similar intervals in other holes within the Expedition 354 transect based on both magnetostratigraphy and seismic stratigraphy. The Brunhes/Matuyama boundary occurs at 82.83 m CSF-A in Core 354-U1455C-6F and, as at all other sites where the Brunhes/Matuyama boundary is identified, the transition is associated with an ash layer. Core 354-U1455C-17F contains the Jaramillo Subchron (86.40–87.92 m CSF-A). Unlike all other sites, the Cobb Mountain Subchron was not recorded at Site U1455 and is likely located between Cores 354-U1455C-17F and 18F.

Physical properties

Physical property data were acquired on all Hole U1455C cores, including density, magnetic susceptibility, *P*-wave velocity, NGR, and thermal conductivity. The physical property data at Site U1455 are mostly of good quality. For Hole U1455C, average physical property values are as follows: GRA densities are 1.88 g/cm^3, *P*-wave velocities are 1697 m/s for the *P*-wave logger and 1712 m/s for caliper measurements, magnetic susceptibilities are 53 × 10^{-5} SI for whole-round measurements and 62 × 10^{-5} SI for point sensor measurements. Average NGR is 61 counts/s, and average thermal conductivity is highest in sand at 1.64 W/(m·K). The physical property data reflect lithologic variations, compaction, and lithification with depth. The following unlithified principal lithologies are present: the most common is sand (~56 m), followed by claystone (~38 m), calcareous clay (~40 m), silt (~22 m), clay (21 m), calcareous claystone (~10 m), and siltstone (~6 m), with volcanic ash occurring in traces.

Geochemistry

Interstitial water chemistry in the upper section of Hole U1455 suggests active biotic processes releasing dissolved phosphate and ammonium and influencing pore water alkalinity and sulfate concentrations. Phosphate and ammonium contents covary, and the rise in alkalinity in the upper section of the core is associated with the drop in calcium and magnesium contents.

Bulk sediment major, minor, and trace element concentrations correspond closely to sediment lithology and are consistent with observations made at other sites cored during Expedition 354 and within the Ganga-Brahmaputra river system. The increase in carbonate content in turbiditic sediments deeper than 360 m CSF-A is consistent with a similar increase at Sites U1450 and U1451 and DSDP Site 218 and indicates a regional change in the delivery of detrital carbonate to the fan. TOC content in Pleistocene turbiditic sediments covaries with Al/Si, a proxy for grain size and mineral composition, reflecting preferential association of organic matter with clay. This behavior is consistent with similar observations in the Ganga-Brahmaputra river system and modern (18 ka) fan deposits and at all sites along the 8°N transect across the Bengal Fan. The organic carbon content of pelagic and hemipelagic sediments broadly decreases with depth, consistent with organic carbon concentrations observed at Site 218.

Preliminary assessment

Expedition 354 was planned to core the sedimentary record of erosion of the Himalayan mountain range for paleoerosion studies, to determine associated accumulation rates at the scale of one section across the sedimentary fan in the Bay of Bengal, and to ultimately constrain fluxes of erosion. To meet these objectives, a transect approach perpendicular to the axis of the fan at 8°N was adopted. One challenge was to cover the Neogene and late Paleogene at several sites where these objectives could be achieved within a reasonable depth of penetration. Another challenge was to be able to recover cores in sandy formations, which are very difficult to sample with most coring techniques. Recovering sand samples, however, is essential for paleoerosion studies, which are based on single grain measurements. Sand recovery was also an issue for reconstructing fan depositional processes. As core recovery in sand was expected to often be incomplete, downhole logging was a key element in the expedition planning. With these constraints, our original objective was to core and log the three deep sites and to core three additional shallower sites to increase the level of resolution of the Pleistocene transect to the scale of 50 km.

Figure **F10** compares our original drilling plans with the operations conducted during the expedition. Figures **F3** and **F4** show the locations of the drill sites. The sites we occupied and coring totals are presented in Table **T1**.

Following our first coring experience at Site U1449, it appeared that the APC system would be limited to the uppermost 3–5 cores in these formations and that the HLAPC would be the best compromise to recover the firm material. The HLAPC was efficient in providing excellent recovery of the sedimentary record in unconsolidated silts and sand but resulted in much longer coring times. In order to meet time constraints for the full expedition, HLAPC coring was often alternated with 4.8 m advances without coring, particularly in deeper sections of the holes. Deep drilling in the fan revealed that lithification did not increase much with depth and was highly variable depending on lithology. Even 10–20 m thick sand layers remained essentially unconsolidated even at 900 mbsf. This significantly limited our ability to obtain downhole log data, as sand collapse prevented logging in all deep holes. Logging was finally achieved only in a single 220 m deep hole at Site U1453. This logging operation was very successful and is critical for documenting the different lithologic facies and guiding the interpretation of core and seismic data throughout the drilling transect. Because of the lack of recent (<300 ka) deposition at all Expedition 354 transect sites, Site U1454 was added to the western end of the transect to core through a levee unit supplied by the presently active channel.

Given these adaptations to the initial strategy, during Expedition 354 we drilled at all of the originally planned sites plus one additional and succeeded in establishing (1) a seven site transect to cover Pleistocene deposition and fan architecture, (2) a three site deep transect (Sites U1450, U1451, and U1455) to record complete Miocene and Pliocene accumulation, and (3) one deeper site to 1180 mbsf (Site U1451) to reach the oldest fan deposition possible to drill in the Paleogene. Logging mostly failed because of borehole conditions, but shallow logging at one site (U1453) provided valuable characterization of sand deposition. Although logging was a very important objective to reconstruct the full succession of lithologies, the excellent match between the cored sediments and seismic data indicates that correlation across the transect sites can be achieved and will reliably document fan sedimentation processes and help reconstruct overall fan growth rates. The expedition was able to suc-

cessfully address most of the research objectives originally planned. Core and log data, along with their preliminary results, provide excellent material and a strong scientific foundation for postexpedition research. In the following sections, we briefly review how Expedition 354 science objectives were addressed.

1. Fan architecture and depocenter variability

Expedition 354 pursues in a sedimentary fan for the first time the approach to systematically drill along a transect a larger number of holes, an approach intended to account for the lateral shifting of depocenters on relatively short timescales and an incomplete documentation of fan activity at any single hole. Altogether seven sites were drilled, all with an almost full recovery of the upper 150 to 220 m of the sedimentary section. This limit in continuous coring penetration was constrained by the capabilities of the APC technology for coring sequences with minor or major amounts of silt and sand. APC coring (9.7 m) was only possible within the upper 20 to 50 m, deeper, barrels did not penetrate sufficiently because of frictional forces and significant drilling disturbance, and low recovery was the consequence. Only the HLAPC (4.7 m) was able to penetrate the formation, and it provided cores with limited disturbance and up to 100% recovery. However, coring time increased significantly with the HLAPC, and the original depth targets (300 mbsf) had to be adjusted to ~200 mbsf. Accordingly, Pliocene fan sediments were recovered at Site U1450 with coring gaps and were completely cored at Site U1451, but with minor fan representation, and the primary objective was adjusted to focus on the Pleistocene.

The primary stratigraphic framework for constraining Pleistocene sedimentation across the seven site transect was provided by two units of calcareous clay and ooze with carbonate content varying between >2 wt% and 80 wt% (average = 21 wt%). These sediments provide sufficient biostratigraphic age constraints. The most recent unit is surficial calcareous clay and oozes dating back to ~0.2–0.3 Ma. It is present across the eastern part of the transect with a thickness of ~5 m at Sites U1449–U1453 and >10 m at Site U1455 and is replaced at Site U1454 by the active turbidite channel of the modern Bengal Fan. The absence of any indication of turbiditic activity at distances >100 km from the active channel clearly indicates that channels in the Bengal Fan act as a line source of sediment supply for the fine-grained fraction. They only supply material for the buildup of levees perpendicular to the channel axis to a limited distance away from the channel but do not appear to release unchannelized turbidite clouds across the fan area as a whole. Detection of fan activity would have in this case only been possible closer than 100 km to the channel axis—a strong support of our transect approach to document Pleistocene fan activity and ensure continuous recovery of material delivered to the fan. As a confirmation, pelagic calcareous deposition is diluted at Site U1455, which is located closer (~30 km southeast) to the active channel.

The second stratigraphically important calcareous clay and ooze unit dates back to the Middle Pleistocene to ~1.2 to 0.8 Ma and is well constrained by magnetostratigraphy. Some combination of the Brunhes/Matuyama boundary and the Jaramillo and Cobb Mountain Subchrons were repeatedly recovered within this unit at all seven sites. This is of particular interest, as it marks another longer interval of absence of fan deposition in this segment of the Bengal Fan, which likely shifted farther to the west than today. Thus, it allows investigation of a very well constrained time slice of fan activity. Overlying this unit, the most intense fan deposition of all cored time periods occurred, with overall growth rates on the order of 20 cm/ky. Across the transect, mid-Pleistocene growth rates are relatively uniform, which in turn indicates a highly dynamic system. Given the large number of larger and smaller channels imaged in seismic data, the lifetime of a single channel-levee system is likely short. Accordingly, the intercalation of units from different channels has to be reconstructed to generate a channel stacking succession from each site first, which is then integrated into the fan perspective.

It is astonishing that despite the rapid shifts of depocenters, the overall fan growth rate is relatively uniform, at all sites in the same order of magnitude, which in turn ensures that the fan maintains a relatively smooth surface, and depressions between channel-levee systems will eventually be leveled. As a consequence, although seismic data indicated tectonic activity that has faulted the fan sediments and has influenced topography, the rapid fan deposition maintained the average surface of the fan. In uplifting areas, average growth rates are documented to be less, but not on short timescales as, for example, the Late Pleistocene time slice.

Expedition 354 sites were strategically placed so that different elements of the fan architecture could be studied with coring the upper 100–200 m. Among the dedicated coring attempts, several larger levee units were fully recovered at Site U1449, or even with duplicate coverage at Sites U1452 and U1454, the latter representing the active Holocene channel. Although the finer material is known to be well recovered with the APC coring technique, silty and sandy units were surprisingly well cored with the HLAPC system. Large volumes of unconsolidated sand and massive silt beds were retrieved. These sediments will allow study of the progradational phase of early channel formation; these are found at the base of all levees (Sites U1449, U1452, and U1454). However, sheeted sand and silt deposits were also observed in areas where seismic data show no associated channel-levee structure. These indicate "interlevee sedimentation," which may spread over wider distances than the latter levees and may result from readjustments within terminal lobes or short-lived episodes of avulsion followed by the reoccupation of an older channel. Interlevee sediments of particular interest were cored at almost all sites, with an emphasis on the shallow section of Site U1449, on Sites U1451 and U1455 situated above 90°E and 85°E Ridges, and Site U1453, which reveals a succession of sheeted sand deposits next to a large channel.

The core material is of excellent quality to achieve the objective of understanding the depositional processes by utilizing high-resolution sedimentological imaging and scanning (e.g., with XRF, computed tomography [CT], or physical properties) and for the purpose of building an inventory of units, lithologies, and sedimentologic properties.

Site U1453 has apparently provided a complete succession of lobe progradation, channel incision, and levee buildup, as has Site U1454 for the active channel. Dating of those sequences will be challenging, as most of the Late Pleistocene deposits are older than 300 ka and therefore out of the reach of radiocarbon dating. As a consequence, Site U1454 was added to the transect during the expedition to provide age constraints on different elements of the channel formation and levee growth and to distinguish between changes in sediment delivery and geometrical changes of the channel. The active channel model from Site U1454 can then be applied to the other older sequences.

Site U1451 is unique in the sense that accumulation has been reduced since the early Pliocene, leading to a prevalent hemipelagic carbonate-rich deposition that can be dated with oxygen isotopes or perhaps cycle stratigraphy. Furthermore, the transition from hemipelagic sedimentation to fan activity is important in analyzing the spatial scales and the rates at which the delivery changes. This tran-

sition may be particularly interesting for the end of the Middle Pleistocene hemipelagic interval, where intercalations of mud turbidites were found, as well as thicker silty and sandy beds, in various places and to various degrees of mixing into the calcareous clay units. As this transition marks a major shift in the depositional system, likely from west to east, we will be able to determine the succession of these depocenter shifts and the trends in time and space. In that respect, the transition is also of interest when studying the surficial sediments, which may have received material from the active channel (Site U1454). At Site U1455, the Toba ash occurs at 5.6 mbsf, compared to more easterly sites, where the ash layer is constantly found at around 2 mbsf. Site U1453, ~100 km away, will be used for reference and to clarify the question of how much clay material is dispersed in the water column and contributes to the hemipelagic units, which often contain carbonate content significantly lower than that of pelagic oozes.

Coring has provided large volumes of coarser grained sediment to study the provenance of the turbiditic material on both the scale of single events and the scale of single channel-levee systems or sand beds, which may still represent snapshots in time. The variability of sources of turbidite release must be carefully studied, as well as how representative measurements on single turbiditic events are for the reconstruction of Himalayan erosional processes. This material will also be important in analyzing how erosion and transport respond to the intense and well-documented climatic changes over the last 1 My. Comprehensive analyses of provenance, weathering, low-temperature exhumation, and exposure ages will be used to study climate-erosion interactions.

2. Calibration of Neogene to present changes

Three sites drilled during Expedition 354 were intended to document Neogene fan activity. Only Site U1451, east of our transect, captured a full record of the Neogene back to 23 Ma. Sites U1450 and U1455 penetrated to the late and middle Miocene, respectively. Although Site U1451 retrieved a complete Miocene succession, a transect approach was chosen to account for lateral variations in deposition rate and sedimentologic characteristics associated with depocenter variability. For instance, the Pliocene section at Site U1451 is mainly represented by hemipelagic deposition with minor turbidite events. In contrast, Pliocene fan activity is well documented at Site U1450 with ~200 m of turbiditic material. Coring only Site U1451 would have significantly biased most sedimentological and geochemical studies. Also, the overall fan growth rate on the transect is variable because of ongoing deformation throughout Neogene on the Ninetyeast and 85°E Ridges (Schwenk and Spiess, 2009), and accumulation must be integrated on the transect scale. As drilling during Expedition 354 provided valuable constraints on the interpretation of nature of reflectors, seismic facies, and associated sediment characteristics, it will be possible to correlate and extrapolate properties, measurements, and volumes throughout the fan transect. Of particular interest will be identifying and dating the various hemipelagic intervals and correlating them between sites, using Site U1451 as an anchor to model Neogene growth rates of this fan segment.

Although each site bears different lithologies and time periods because of its location and paleobathymetry, shipboard observations and analysis of sediments recovered during Expedition 354 show consistent characteristics that reflect ubiquitous processes throughout the Neogene but also reveal an evolution at the Neogene timescale. The overall Neogene fan appears constructed by turbidite units interlayered with hemipelagic units of varying thickness. This results in contrasting accumulation rates (1–2 cm/ky vs. 10–100 cm/ky, respectively) and reflects the migration of turbiditic channels at the fan scale.

Pleistocene, Pliocene, and late Miocene sediments show common characteristics. Turbidite sand, silt, and clay have mineralogical and geochemical characteristics remarkably similar to those of the modern Ganges and Brahmaputra Rivers. Hemipelagic intervals show highly variable proportions of clay and calcareous ooze. The mineralogical and geochemical signature of the hemipelagic clay varies from (1) identical to the illite-chlorite rich clays of turbidites, characteristic for Himalayan rivers, to (2) smectite-rich assemblages enriched in iron and depleted in potassium, representing either more extreme sorting of the same material or input from another source. Sediments reveal increasing lithification downhole, represented by claystones, calcareous claystones, and limestones. Sand and silt beds usually remain unlithified. In terms of sand deposition, differences exist between the three sites. The earliest occurrence of thick Miocene sand beds was recovered at Site U1451 at around 530 m CSF-A (~9 Ma). Sand deposition at Site U1450 is very common from the late Miocene to Pleistocene, but the record extends only to 7.5 Ma. Site U1455 demonstrates the persistent presence of 10 m thick sand units over the last 12 My, although these units could only be deduced from high–penetration rate RCB coring with low sand recovery. Because large parts of the Miocene at all three sites are characterized by comparable parallel seismic reflection patterns (indicating sheet-like turbidites), the three sites should show comparable large-scale lithologies. In this case, the occurrence of major sand beds shallower in Site U1450 may be related to different coring techniques between the RCB and HLAPC systems. Nevertheless, higher recovery and lower accumulation rates in the early Miocene at Site U1451 suggest finer sediments in earlier fan deposits. This could be related to changes in the source region or to the paleobathymetry and tectonic deformation linked to the evolution of Ninetyeast Ridge.

Petrographic investigations on sand-sized particles reveal that high-grade metamorphic rock fragments and heavy minerals are present since the late Miocene and are not present during the early Miocene and late Oligocene. Throughout the Neogene succession, the sands can be divided into three types on the basis of the heavy mineral assemblage: (1) tourmaline-rich sands, (2) garnet-rich sands, and (3) amphibole-rich sands. Early and middle Miocene intervals mainly contain tourmaline-rich sands. The late Miocene interval primarily contains both amphibole-rich and garnet-rich sands, both showing high-temperature metamorphic minerals, such as sillimanite, kyanite, and staurolite. The Pliocene and Pleistocene are characterized by a predominance of amphibole-rich sands. The presence of detrital carbonate is also persistent through the Neogene but appears to show a consistent trend from 3%–6% in the Pleistocene and Pliocene to 8%–10% during the Miocene. Finally, a prominent feature in Miocene silt and sand beds is the higher abundance of plant fragments compared to younger sediments. Hence, changes occurred during the Miocene that will reveal changes in the eroded sources and erosion conditions.

Aside from these changes, the Expedition 354 record of the Bengal Fan at 8°N shows less variability than the distal fan record of Leg 116 (Cochran, 1990; Stow et al. 1990). There, middle Miocene turbidites have mineralogical and geochemical signatures very similar to those of most of the 8°N transect. From 7 Ma on and through the Pliocene, sedimentation changes to mud turbidites with smectite-rich clay assemblages and high organic carbon content (Bouquillon et al., 1990). This change is associated with a reduced accumulation

rate at the three Leg 116 sites and linked to the C_4 photosynthetic plant expansion (Galy et al., 2010). However, the transect record at 8°N differs from the evolution of the distal fan, although the C_4 plant expansion is also recorded at Site 218 and the provenance traced by radiogenic isotopes is consistent at both locations. This difference implies that the evolution recorded in the distal fan does not record a simple evolution in the source but rather relates to changes in sediment transport in the fan.

Unraveling the full image of the Himalayan erosion and Bengal Fan growth will rely on postexpedition multidisciplinary studies on core material. Expedition 354 clearly represents a substantial basis to undertake this research for several reasons:

- Expedition 354 data and cores will provide a robust stratigraphic framework of the sedimentary evolution at the Neogene timescale. Dating of beds with biogenic carbonate content that is higher than is typically observed in turbiditic sequences will provide biostratigraphic age constraints and act as tie points for the seismic correlation. Further investigations on the scale of sediment beds, such as grain size and composition and the thickness and frequency of beds, will help determine the sedimentary variability between the three sites. The lower recovery of sand beds by XCB and RCB coring in deeper parts of the sites might be addressed by microscopic investigations of maximum grain size as a function of transport energy rather than grain-size spectrum measurements on specific sand beds. These observations, when integrated with seismic correlation, will provide a model at the scale of the transect and may elucidate the implications of varying sediment properties for the evolution of sediment transport, sedimentary facies, and the dawn of channel-levee systems in the late Miocene.
- Collectively, Sites U1450, U1451, and U1455 sampled a complete record of Neogene turbiditic deposition that will permit in-depth petrological, mineralogical, geochemical, biogeochemical, and geochronological studies to decipher the geological and environmental evolution of the Himalayan basin. This includes sand in sufficient quantities to extract heavy minerals necessary for single-grain provenance and geochronological studies, unconsolidated sediments that will allow full application of isotopic biomarkers usually not applicable in Miocene sediments because of diagenesis, and organic fragments that will further refine paleoenvironmental reconstructions. The latter may provide information on the monsoon evolution and will be compared to other independent monsoon proxies. Other samples will allow more classic bulk analyses of sediment provenance and weathering.
- Combined investigations of the fan stratigraphic framework with petrologic and geochemical tracing will allow us not only to characterize the evolution of the Himalayan basin but also to link observed changes in geological sources and environmental conditions to accumulation rates and changes of transport in the Bengal Fan. Comparison of erosion rates derived from metamorphic minerals and integrated accumulation rates will allow testing the regional consistency between sources and sink. On this basis, the fan record can be used to decipher past fluxes of erosion and assess impact of the Himalayan erosion at the global scale.

3. *Sampling the oldest sediments of the fan*

The importance of recovering a Paleogene record of erosion of the eastern side of the Himalaya lies in the uniqueness of the resulting archive. The deepest previous drilling of the Bengal Fan achieved penetration to the early Miocene (≈18 Ma) (Cochran and Stow, 1989). Onshore, a late Eocene–late Oligocene unconformity stretches across the foreland basin; thus, the onland archive of Paleogene erosion of the eastern side of the Himalaya is restricted to sparse early to mid-Eocene foreland basin material (e.g., DeCelles et al., 2004) and one near-complete but poorly exposed Paleogene record in the Bengal remnant ocean basin, Bangladesh (e.g., Najman et al., 2008).

During Expedition 354, the site intended to reach to the base of the fan (Site U1451; proposed Site MBF-3A) is located above the western flank of Ninetyeast Ridge. This location was chosen to access the fan where its sediment thickness was less and older sediment could be recovered at shallower depths. Site U1451 achieved the objective to drill to the base of the fan in this location, encountering pelagic limestones of Oligocene age at 1103.40 m CSF-A.

The fan succession shows a clear trend to finer lithologies downhole, although the effects of XCB and RCB coring most likely have influenced percentage recovery of loose sand. Late Miocene (10–11 Ma) is the oldest time interval in which sand, as either a major or minor lithology, was recorded at Site U1451. Downhole from that time period, the turbidite successions are mud turbidites, composed of silt and clay.

Mud turbidites continue down to the Oligocene–Miocene transition. The deepest turbidite was observed at ~1085 m and was most likely deposited before 26–28 My ago. A deeper short interval (late Oligocene) composed of claystone, calcareous claystone, and siltstone was recovered, different from the overlying lithologies in its brown-gray rather than gray color. The deeper late Oligocene to late Eocene section comprises prefan limestones interbedded with intervals of claystone and, where the limestone is brecciated, infilling of the fractures by gray siltstone injectites. Postexpedition analyses will determine the provenance of the clastic units found associated with the basement limestone intervals. The deeper limestone was dated to the Paleocene, so there should be a hiatus with the overlying late Eocene limestone.

Sandstone compositional trends downhole involve the reduction in diversity of heavy mineral assemblage as the fan base is reached and the increasingly lower grade of lithic fragments. Schistose lithic fragments are present in the late Oligocene to middle Miocene interval, but lithic fragments contained in the injectites are no higher grade than claystone and phyllite.

From seismic data, the early history of fan deposition at Site U1451 is associated with a change in depositional style above a seismic unconformity. This unconformity was likely cored at the bottom of the hole, recovering Eocene and Paleocene limestones and containing a 16–18 My hiatus. The structurally disturbed unit immediately overlying the unconformity is an Oligocene/Eocene limestone and claystone unit injected by sand and silt (injectites). On top, parallel strata are onlapping, which clearly indicates turbiditic sedimentation. Tilting of these Miocene strata with respect to modern stratification indicates, however, tectonic deformation associated to the Ninetyeast Ridge, which has affected fan deposition to a minor degree at Site U1451 since the Miocene.

The recovered detrital record of the Himalaya from the early Miocene to late-Oligocene represents a unique archive of the Himalayan erosion. It does not cover the full Oligocene–Eocene direct deposition of the fan that probably lies in what represented deeper parts of the basin west of Site U1451 during the early and mid-Oligocene. Nevertheless, this record represents an essential source of information to document the structure and the composition of this

early stage of the Himalaya. Petrologic, geochemical, and geochronologic studies of this record will allow unraveling not only the geological formations that were exposed during the Oligocene but also the conditions of erosion. Provided postexpedition studies can resolve the exhumation age of the eroded formations, erosion rates may be derived from these sediments to put constraints on mountain building dynamics. These sediments will also allow us to further test the role of the Himalayan erosion on the observed global evolution of oceanic dissolved isotopic tracers such as Sr and Os, which are in part controlled by the Himalayan erosion (e.g., Richter et al., 1992). Beyond the silty turbiditic sediments that appear as relatively direct relicts of the Himalayan erosion, the claystone deposition that extends to the Eocene at Site U1451 is another clastic deposition that could be related to nearby fan activity. Study of these claystones may further document older Himalayan-derived material.

4. Forcing of the carbon cycle and climate

Coring along the Expedition 354 transect of seven drill sites at 8°N across the Bengal Fan recovered several extended records of Himalayan-derived material that will be further integrated in space and time to estimate carbon fluxes associated to the Himalayan erosion processes and carbon burial in the Bay of Bengal. Geochemical analyses of sediments allow estimation of the atmospheric CO_2 drawdown associated with silicate weathering and organic carbon burial (France-Lanord and Derry, 1997). Silicate weathering is estimated from the chemical difference between turbiditic sediment deposited in the Bengal Fan and its inferred unaltered bedrock counterpart. The loss of cations (Ca, Mg, Na, and K) per mass unit of deposited sediment is calculated and then converted into equivalent dissolved alkalinity (HCO_3^-), or moles of atmospheric CO_2 required to drive the weathering reactions. Therefore, it requires identifying the bedrock, and that can be achieved relatively well for the Pliocene and Pleistocene based on the knowledge of Himalayan geological formations and the modern river system (e.g., Lupker et al., 2012). Identification becomes is more tentative for the middle to early Miocene, when the exact nature of the source rocks might have been different. The use of an independent weathering isotopic tracer is then necessary. Organic carbon burial is more straightforward, as it is essentially derived from concentrations of TOC in the sediments and measurements of petrogenic organic carbon (i.e., refractory carbon recycled from the source rocks, e.g., Galy et al., 2008). The primary control on organic burial is the organic carbon loading of the sediment, which is largely a function of the clay content of the sediment. Shipboard analyses of TOC already provide insight into the magnitude of this process. It is therefore important to capture the average composition of the accumulated sediments for a given time slice or sedimentary unit.

Carbon budgets estimated from discrete samples and/or turbiditic sequences then need to be integrated at the spatial scale of site distribution. Combined either with measurements of erosion rates or in a stratigraphic framework including sedimentology and seismic stratigraphy at the scale of the transect, it will be possible to better constrain quantitative estimates of total fluxes of carbon related to Himalayan erosion.

Preliminary observations and shipboard analysis of turbiditic sediments recovered at each of the seven sites across the Bengal Fan allow us to formulate a set of hypotheses, which will be tested via higher resolution reconstructions and the use of state-of-the-art analytical techniques:

- Highly weathered, organic carbon-rich sediments recovered during periods of low accumulation rates in the distal Bengal Fan (ODP Leg 116, ~7 to 1 Ma) (France-Lanord and Derry, 1997) are clearly absent from the transect of drill sites at 8°N. This suggests that the tendency observed in the distal fan cannot be extrapolated to the entire fan but rather reflects changes in sediment routing and/or provenance occurring in the distal Bengal Fan.
- At first glance, the chemical composition of turbiditic sediments cored across the transect of drill sites at 8°N reveals a relatively stable and weak regime of chemical weathering throughout the Neogene. This needs to be coupled with insightful postexpedition studies but further supports the idea that Himalayan erosion has consumed atmospheric CO_2 through the burial of organic carbon, more than by silicate weathering (France-Lanord and Derry, 1997).
- Preliminary estimates of organic carbon loading and behavior—such as preferential association of organic matter with clays—resemble observations made in the modern Ganga-Brahmaputra river system, suggesting efficient terrestrial organic carbon burial in the Bengal Fan (Galy et al., 2007). The relationship reveals, however, larger dispersion than documented in modern rivers, which suggests either variable source conditions or preservation during transport/deposition processes. In addition, from the early to late Miocene, visible fragments of organic matter were observed to be almost ubiquitous in sand and silt turbidites. These fragments sometimes form organic layers at the base of turbidites. These independent wood particles can represent significant proportion of TOC, but likely do not respond to the same dynamics as discrete organic matter that is principally attached at the surface of fine particles. This may further alter the TOC and Al/Si relationship.
- Hemipelagic sedimentation was observed at all sites and represents periods of clay-rich deposition mixed with pelagic input. It appears from shipboard measurements that organic carbon loading of these particles is low. Nevertheless, the detrital fraction of the hemipelagic units needs to be taken into account in the general budget of the fan accumulation.
- The paucity of ooze-dominated sediments in the hemipelagic units (characterized by relatively low sedimentation rates of <3 cm/ky) suggests low primary productivity in the Bay of Bengal throughout the Neogene. This is also evident in prefan limestones of Eocene age with very low sedimentation rates, which are related to the connection of the equatorial Pacific Ocean to the equatorial Indian Ocean, suggesting that the closure of the Indonesian gateway and/or the nutrient supply by continental erosion are not the primary control of the marine biological carbon pump in that part of the Indian ocean.

Other objectives

1. Fan hydrology and hydrochemistry

The Bengal Fan is a major sedimentary reservoir filled by continental material, including clays and organic matter that are evolving during burial. Along the seven site Bengal Fan Expedition 354 transect, the interstitial water chemistry displays large and systematic changes found at every site. Most of the characteristics are also shared with the interstitial water chemistry in the distal part of the Bengal Fan at the Leg 116 sites (Cochran, Stow, et al., 1989). In the upper section of the sedimentary pile, a large rise in alkalinity is associated with the complete reduction of sulfate and the occurrence

of some dissolved phosphate. A consequence of the high alkalinity values is the consumption of calcium (and magnesium) induced by the precipitation of carbonate. These characteristics are typical of biological activity in young sediments. In detail, the depths of the maximum alkalinity values (or the complete reduction of sulfate) are different from site to site but restrict the buffering of the interstitial water chemistry by the biological activity to the upper 200 m. The rate of the rise in alkalinity with depth is greatest at the western end of the transect and slowest at the eastern end. When the uppermost 10 m is studied in detail (Sites U1449, U1454 and U1455), the rise in alkalinity with depth is fastest where the Toba ash layer is the deepest. This suggests a strong control of the biological activity by the mass accumulation rate and could narrow the effect of fertilization of the seabed by the sedimentary input to less than 100 ky. The deep profiles clearly establish diffusion as the prime process driving the interstitial water chemistry below the biologically active layer, particularly in the 200 m of sediments just above the prefan limestone lithology at Site U1451, where a strong calcium gradient is observed. The lack of fluid advection along the transect across the Bengal Fan is further supported by the lack of occurrence of low salinity. Beside salinity, and despite the large difference in heat flow between Expedition 354 and Leg 116 sites in the distal fan, the close agreement for most of the characteristics (especially sulfate, calcium, magnesium, and potassium) between 200 and 800 mbsf might also support the restrained thermoconvective conditions in the distal part of the fan. The lack of low-salinity fluids also suggests that dehydration reactions are unimportant at 8°N, supporting the occurrence of diverse diagenetic reactions in the fan that will be characterized by postexpedition research. This research will lead to refined estimates of geochemical fluxes from the fan to the ocean.

2. Paleoceanography and chronology

Marine and terrestrial records in Bengal Fan sediments are intimately linked through prevalent turbiditic deposition. In the upper section, two major periods of hemipelagic deposition have been recovered at all sites across the Expedition 354 transect. During these time intervals of reduced detrital input, reference sections can be analyzed for a suite of paleoceanographic proxies to reconstruct sea-surface temperature, sea-surface salinity, ice volume, marine biological productivity, nutrient supply, and deepwater circulation. For the eastern transect sites, these intervals can provide high-resolution reference chronostratigraphies through oxygen isotopes on foraminifers and orbital tuning based on various physical properties of the carbonate-rich intervals, whereas at western sites more intense fan deposition is interfingering with or diluting pelagic input. For example, for the last two glacial–interglacial cycles, time series of detrital fluxes are recorded at Site U1455, where accumulation is enhanced by ~200%, and at Site U1454, where in the levees of the active channel accumulation increases by several orders of magnitude. There, in conjunction with radiocarbon dating, a precise chronology can be developed and calibrated for predominantly terrigenous sediments.

A second major hemipelagic unit of mid-Pleistocene age represents an even longer time period of at least 400 ky, which is well constrained by magnetostratigraphy by the Brunhes/Matuyama boundary and the presence of the Jaramillo and Cobb Mountain Subchrons. Again, a high-resolution age model can be established to study paleoceanographic changes at the mid-Pleistocene transition and to provide a chronostratigraphic framework for embedded detrital units intercalated along the transect. Coupling with proxies for weathering and provenance changes may provide a better understanding between Northern Hemisphere climate dynamics and the strength of the monsoon during this critical time period.

As numerous intermittent hemipelagic units were recovered throughout the Neogene from different sites, a biostratigraphy-based lower resolution chronology may be established for the past 10 My. By assuming that the overlying water column is essentially the same at all transect sites, it may be possible to create a composite record from all sites, which concurrently provide age constraints and paleoceanographic measures of water column temperatures and salinity, productivity, and nutrient variability, providing independent proxies for variability in monsoonal strength through the last 10 My.

3. Deep biosphere

Deep biosphere studies are one of the complementary objectives of Expedition 354. Whole-round core sections were collected from the sediment/water interface to 1097 m CSF-A for the investigation of the subseafloor biosphere of the Bengal Fan. Three shallow-penetration mudline cores (Sites U1449, U1454, and U1455) were retrieved for high-resolution combined microbiological and geochemical investigations in the uppermost portion of the sediment column where high microbiological activity due to the input of fresh organic matter was expected. These three sites were selected based on the sediment age, type, and location, varying in sedimentation from hemipelagic sedimentation of 1–2 cm/ky through a factor of 3 dilution by detrital fine-grained input to a levee setting, where units typically accumulate at a rate of meters per thousand years.

These whole-round core sections were subsampled and prepared for a variety of postexpedition microbiologic investigations, including prokaryotic cell counts. Frozen samples will be analyzed for endospores, hydrogenase enzyme, DNA, and intact polar lipids to investigate microbial biomass, activity, and community structures. Other samples were kept in sterile glass bottles with a nitrogen atmosphere at 4°C for postexpedition cultivation experiments of microbial carbon metabolism pathways.

Headspace hydrocarbon gas profiles seem to indicate spatial trends in microbial activity. In conjunction with pore water geochemistry, these trends have to be confirmed by shore-based work on gases, carbon preservation, sedimentation rates, and prevalent lithologies. Collaborative work will focus on a better understanding of interrelationships between microbial habitat, grain size distribution, and mineral composition, as well as on microbial lipids as living and fossil biomarkers.

Operations

During Expedition 354, a seven site transect was drilled across the Bengal Fan at 8° N (Table **T1**; Figures **F4**, **F10**). An additional Bengal Fan site was drilled at 14°N during IODP Expedition 353, Indian Monsoon, as part of their contingency operations plan.

The seventeen holes drilled at Sites U1449–U1455 penetrated a total of 5167.2 m of formation. Coring spanned 2889.7 m of this penetration and recovered 1727.12 m of sediment and rocks (60%). Because the Bengal Fan sediments were deposited extremely rapidly, contained frequent silts and sands, and were poorly consolidated and unlithified, the APC and XCB coring systems were not often utilized. The APC could not adequately penetrate into the formation except for a few surficial cores and a few limited relatively soft, hemipelagic intervals deeper in some sections. The XCB system was unable to sufficiently recover unconsolidated silts and

sand, a high priority for investigating Himalayan evolution. The RCB system was useful in deeper, more lithified sections. We identified these formation challenges in the *Scientific Prospectus*.

The HLAPC system worked most effectively for achieving the primary expedition objectives. The HLAPC allowed recovery of good quality cores very deep in the formation—for example, as deep as 687 mbsf in Hole U1450A and 431 mbsf in Hole U1455C. The HLAPC also proved effective in recovering unconsolidated and unlithified silts and sands that proved to be unrecoverable with the other coring systems. We also used this system to obtain deep formation temperature measurements, including the deepest ever obtained in scientific ocean drilling: 406 mbsf in Hole U1451A.

One implication of using the HLAPC system was doubling the wireline time for coring compared to using the APC system. As a result, we extensively used a strategy of alternating 4.7 m HLAPC cores with 4.8 m advances without coring. Otherwise, we could not have sufficiently achieved the expedition science objectives.

Hole conditions were challenging and problematic for coring deeply and especially for downhole logging. A reentry cone with 400 m of casing was used to reach our deepest targets at Site U1451. At Site U1455, a reoccupation of DSDP Site 218, we cored three different widely spaced intervals along with a free-fall funnel (FFF) to obtain sediments from critical periods of Himalayan tectonic and climate evolution. Our only success in logging was a relatively shallow penetration in Hole U1453A. In this case, however, hole conditions were excellent. These data fully characterize the formation—especially in intervals that were coarse, poorly lithified silt/sand—and allow us to better interpret our core recovery in other sites.

All times in this report are reported in ship local time. During on site coring and logging operations this was UTC + 6. However, time changes made during the transit to and from the drilling area are documented in the report.

Singapore port call

The R/V *JOIDES Resolution* was scheduled to arrive at Loyang offshore terminal in Singapore in the early morning of 29 January 2015 but had to anchor outside the port. The ship occupying our intended berth had a mechanical problem, and the arrival had to be shifted to the next day (30 January). In the late afternoon, water taxis were used to disembark Expedition 353 (Indian Monsoon) scientists and *JOIDES Resolution* Science Operator (JRSO) staff. The Expedition 354 Co-Chief Scientists and JRSO staff also boarded the ship by water taxi.

At 0600 h on 30 January, the pilot boarded the ship and we started the short 9 nmi transit to Loyang port. The first line ashore at 0821 h marked the end of Expedition 353 and the start of Expedition 354. This first day of port call activities included boarding the Bengal Fan scientists, ship operator crew change, offloading Expedition 353 core and sample shipments, and a variety of shipments to and from the ship. The Bengal Fan scientists settled in their rooms, were introduced to life on board, and then were given an initial safety orientation, laboratory tours, and an introduction to information technology on the ship.

On 31 January, the scientists and JRSO technical staff were introduced to each other and the Co-Chief Scientists kicked off the expedition with a presentation of the expedition science objectives. In the afternoon, the Captain introduced key staff and gave the overall ship safety orientation. The IODP Expedition Project Manager then gave the scientists an orientation. Port call activities continued with loading drilling mud, fueling the ship, a variety of shipments to and from the ship, and tours for a group of Texas A&M alumni from Singapore and journalism students from Nanyang Technological University. Port call continued with activities at the Loyang Offshore Supply Base jetty. This included loading drilling equipment, expedition stores, and food. All public relation activities were concluded on 1 February. On 2 February, we conducted our first safety drills (fire and boat; anti-piracy security) and then all scientists and staff were given the afternoon off because our departure from Singapore was scheduled for the next day. In the afternoon, the final port call activities included loading life rafts and the remainder of fresh food and dry goods, securing the ship for heading out to sea, and preparing for the installation of a new core line.

Transit to Site U1449

At 0800 h on 3 February 2015, we were cleared by immigration for departure. The pilot arrived on board at 1020 h, and the last line was released at 1048 h. Our departure was assisted by two harbor tugs, and we proceeded to the pilot station, where the pilot departed the vessel (1202 h). We then began our transit through the Malacca Strait, into the Bay of Bengal, and to Site U1449. During the transit, we retarded the ship's clock 2 h to UTC + 6. All times from this point until the end of Expedition 354 coring operations are given in this ship local time (UTC + 6). During the transit, the Co-Chief Scientists, key IODP staff, and the ship's crew met to review the coring and logging plan for the expedition.

Site U1449

The original plan for Site U1449 (proposed Site MBF-6A) was to core a single hole with the APC and XCB systems to 300 mbsf. Instead, two holes were cored. Hole U1449A was cored with the APC, HLAPC, and XCB systems to only 213.5 m DSF. The nature of the formation (interbedded sands, silts, and muds) created coring challenges that reduced penetration rate and recovery. Hole U1449B consisted of a single mudline core for high-resolution microbiology and geochemistry.

Hole U1449A

After completing the transit from Singapore (1105 nmi; 3.9 days; 11.8 nmi/h), we arrived at Site U1449 at 0623 h on 7 February 2015. We assembled a bit and bottom-hole assembly (BHA), verified the correct space-out of the core barrel, and lowered it to the seafloor. The BHA included a nonmagnetic drill collar, and we used nonmagnetic core barrels throughout coring at Site U1449. We placed the bit at 3660 m DRF and prepared to spud Hole U1449A. After a failed first attempt APC core (the shear pins did not break), Hole U1449A was spudded at 2125 h on 7 February. Core 1H recovered 6.27 m and established the seafloor at 3652.7 meters below sea level (mbsl; 3663.3 m drilling depth below rig floor [DRF]). We used the APC, HLAPC, and XCB systems to penetrate and recover core in Hole U1449A.

Core orientation started with Core 2H, but after it only penetrated 3.72 m the orientation tool was removed from the system. After Core 2H, we drilled 1 m without coring through a hard layer (9.9–10.9 m DSF) and then XCB cored to 17 m without any recovery. We then used both piston coring systems and penetrated 22.5 m (17.0–39.5 m CSF-A; Cores 5H, 6F, 7H, and 8H) and recovered 18.3 m of core (82%). Orientation was attempted on Cores 8H and 9H with poor results; Core 8H was also the only time we deployed the APCT-3 to obtain a formation temperature measurement. Core 9H did not penetrate the formation, so we switched to XCB coring and Cores 10X–12X extended from 39.5 to 68.4 m CSF-A but recov-

ered only 0.86 m (3%). We switched back to the HLAPC system, and Cores 13F–17F penetrated 19.6 m of formation (68.4–88.0 m CSF-A) and recovered 20.03 m (102%). Because we wanted to core deeply at this site, the formation appeared soft enough, and the HLAPC takes longer, we switched back to the APC. Cores 18H–21H extended from 88.0 to 113.4 m DSF and recovered 25.02 m of core (99%); however, all but the first were only partial strokes (7.6, 4.9, and 3.4 m) and were advanced by recovery.

We switched to the HLAPC, and Cores 22F–31F penetrated 43.1 m (113.4–156.5 m DSF) and recovered 45.33 m; the last two were only partial strokes. As the formation still appeared to be too firm for full APC coring and achieving our primary objective of obtaining deeper samples would take much longer with the HLAPC, we deployed the XCB coring system. Cores 32X–36X penetrated 48.5 m (156.5–205.0 m CSF-A) but only recovered 1.17 m of sediment (2%). We then switched back to APC coring, first with HLAPC Core 37F, which penetrated from 205.0 to 209.7 m DSF and recovered 4.79 m (102%). The final core of Hole U1449 was another attempt at APC Core 38H that only partially stroked out from 209.7 to 213.5 m CSF-A and recovered 3.87 m of core.

Because we (1) had achieved a substantial part of this site's objectives, (2) had exceeded the operational time allocated for this site, and (3) had many high-priority expedition objectives remaining, we decided to not to spend any more time attempting to sample to the full 300 m originally planned.

The APC system penetrated a total of 57.1 m of formation and recovered 52.37 m (91%, but includes advance by recovery and one core that did not penetrate the formation). The HLAPC system penetrated 71.9 m of formation and recovered 74.98 m (104%). The XCB system penetrated a total of 83.5 m of formation and recovered only 2.03 m (2%). Ten barrels of sepiolite mud was circulated during or shortly after cutting Cores 10X and 33X.

Hole U1449B

After finishing coring in Hole U1449A, we offset the ship 20 m east and obtained a single mudline core in Hole U1449B for high-resolution microbiological and geochemical sampling. The bit was spaced out to 3661.0 m DRF in an attempt to recover approximately 7.0 m with the mudline core. Core 1H extended from the seafloor to 7.9 mbsf. We then retrieved the drill string, secured the rig floor, and started the short transit to Site U1450 at 1530 h on 10 February.

Site U1450

Site U1450 (proposed Site MBF-2A) consists of two holes. Hole U1450A (10–17 February 2015) was cored to 687.4 mbsf using primarily the HLAPC system alternating with short (4.8 m) advances without coring. The APC and XCB systems were used in the shallow and deepest portions of the hole, respectively. Hole U1450B (7–11 March) was drilled without coring to 608.0 mbsf and RCB cored continuously from there to 811.9 mbsf, and then downhole logging was attempted.

Hole U1450A

After the short 26 nmi transit from Site U1449, we arrived at Site U1450 at 1830 h on 10 February and lowered the bit to the seafloor. We spudded Hole U1450A at 0255 h on 11 February, and the mudline core established the seafloor at 3655.3 mbsl. This hole was drilled to a total depth of 687.4 mbsf using a combination of coring (APC, HLAPC, and XCB systems) and short (mostly 4.8 m) advances without coring. Nonmagnetic core barrels were used for all APC and HLAPC cores, and the nonmagnetic drill collar was in the BHA.

We used the APC system for the first three cores (1H–3H, 0–11.7 m DSF; 20.2 m cored; 18.63 m recovered). Because the latter two cores were partial strokes, we switched to the HLAPC system. Cores 4F–8F extended from 20.2 to 43.7 m DSF with a range of recoveries (0%–72%); despite this change we did not advance by recovery but rather the full 4.7 m barrel length each core.

From 43.7 to 132.9 m DSF (after Core 8F to Core 27F), we took a series of HLAPC cores interspersed with six 4.8 m long advances without coring. These HLAPC cores were taken consecutively when fine-grained intervals (e.g., without sand/silt) were encountered. Two cores with the APC system (Cores 22H and 24H) were taken in this section, but these recovered only 3.35 m of sediment. These were the only two cores where core orientation was attempted.

Based on our experiences in the upper portion of this hole and at Site U1449, we decided to deepen the hole by an alternating series of 4.7 m long HLAPC cores followed by 4.8 m advances without coring. The full APC coring system could not sufficiently penetrate/recover this formation, and the XCB system, although it could penetrate it, would not recover core from this type of formation. In addition, the science objectives required deep penetration sampling at multiple sites, which could not be accomplished in time if the HLAPC was used continuously. This alternating pattern penetrated 428.4 m of formation from 132.9 to 561.3 m DSF (Cores 28F–119F). The only exception to this pattern occurred in a few intervals where HLAPC cores were taken consecutively (Cores 80F–84F, 114F, 115F, and 117F–119F). The HLAPC cores taken from this interval (Cores 28F–119F) penetrated 226.8 m of formation and recovered 176.7 m of core (77%). Forty-two 4.8 m advances without coring penetrated 201.6 m of formation.

Because we had some difficulty getting Core 119F to penetrate the formation, we cored the rest of the hole with the XCB system, except for five HLAPC cores and three 4.8 m advances without coring. Cores 120X–123X cored 37.7 m (561.3–599.0 mbsf) and recovered 8.89 m (24%). Because the penetration rate substantially increased while cutting the last part of Core 123X, we inferred that the formation had likely changed back to sand. We switched back to HLAPC coring, as it was the most likely system to be able to recover sands. We then cored an alternating series of HLAPC cores (124F, 126F, and 128F) and 4.8 m advances without coring that penetrated 11.2 m of formation and recovered 8.89 m (85%).

The lowermost section of the hole consisted of mostly of XCB cores, with two HLAPC cores. Cores 129X and 132X–136X (619.8–628.2 and 637.7–686.3 mbsf) penetrated 57.0 m and recovered 6.47 m of core (11%). Two HLAPC cores (130F and 137F; 628.2–632.9 and 686.3–687.4 mbsf) penetrated 5.8 m and recovered 4.05 m (70%). The deepest core in this hole (HLAPC Core 137F) set the record for the deepest penetration piston core in scientific ocean drilling.

We decided to terminate operations in Hole U1450A after this last HLAPC core. We felt that recovering core to the 900 m target objective and obtaining good wireline logs would be better achieved by drilling a new RCB hole at this site later in the expedition. We pulled the drill string out of Hole U1450A, and the bit cleared the seafloor at 2035 h on 16 February and was back on the rig floor at 0235 h the next day. After the drill floor was secured and the thrusters raised, we started the transit to Site U1451 at 0418 h on 17 February.

Five APCT-3 formation temperature measurements were conducted in Hole U1450A at 86.3, 118.7, 156.6, 175.6, and 318.1 m DSF (while taking Cores 17F, 24H, 32F, 36F, and 66F, respectively).

The last of these measurements is the deepest APC formation temperature measurement ever obtained.

In Hole U1450A, we cored a total of 444.7 m and recovered 282.73 m of core (64%). This included 71 HLAPC cores (318.3 m cored; 245.39 m recovered; 77%), 5 APC cores (31.7 m cored; 21.98 m recovered; 69%), and 10 XCB cores (94.7 m cored; 15.36 m recovered; 16%).

Hole U1450B

After a 64 nm transit from Site U1451, we arrived back at Site U1450 at 1342 h on 7 March. Hole U1450A was cored to 687.4 mbsf, so we decided to drill without coring to 608 m and then RCB core below that depth and attempt to log the hole. This RCB coring has a 79.4 m overlap with the deepest cores from Hole U1450A. We assembled an RCB with a mechanical bit release (MBR), lowered it to the seafloor, and started drilling in Hole U1450B at 2305 h on 7 March. We continued drilling without coring in Hole U1450B from 0 to 465.0 mbsf. At this point (1945 h on 8 March), the low penetration rate led us to retrieve the center bit for inspection. No problems were observed. The center bit was redeployed, and drilling resumed at 2100 h on 8 March. At 0414 h on 9 March, the bit reached 608.0 m. After retrieving the center bit, RCB coring started at 0515 h on 9 March. Nonmagnetic core barrels were used for all RCB cores. Cores 2R–11R penetrated from 608.0 to 705.1 mbsf (97.1 m) and recovered 15.77 m of core. Because of poor recovery for Cores 3R–6R (3.72 m; 8%), a slow penetration rate, and sediment jammed in the core catchers, we ran a bit deplugger after Core 6R to clear the bit. After the bit deplugger was recovered, Cores 12R–22R penetrated from 705.1 to 811.9 mbsf (106.8 m) and recovered 15.77 m of core (29%). RCB coring in Hole U1450B sampled 203.9 m of formation (608.0–811.9 mbsf) and recovered 46.66 m of sediment (23%).

After the last core arrived on deck (1715 h on 10 March), we decided our primary coring objectives had been mostly achieved, so we prepared the hole for downhole logging. We circulated 35 barrels of mud to clear cuttings out of the hole (before retrieving the last core), deployed the rotary shifting tool (RST) to release the bit in the bottom of the hole, filled the hole with weighted mud, and raised the bottom of the drill string to 82.7 m. At 2300 h, we started assembling the first logging tool string (triple combo). We finished assembling and testing the triple combo at 0115 h on 11 March. We lowered it through the drill string and out of the open end of the drill string at 82.7 mbsf. The bottom of the tool string encountered an obstruction in the hole at 133.7 mbsf. The tool string was raised and lowered a few times in an attempt to pass through this obstruction, but the tool became stuck in the hole. After applying the maximum amount of force to the logging wireline, the tool string was freed from the formation. The tool string was recovered on the rig floor at 0615 h on 11 March. We decided logging was not possible because of the hole conditions. After the rig floor was cleared of the logging setup, the driller started to pull the string out of the seafloor. However, the pipe had become stuck, and the drillers had to apply 40,000 lb of overpull to extract the BHA out of the seafloor. After the drill string was retrieved, the rig floor secured, the thrusters raised, and the seafloor positioning beacon recovered, we departed for Site U1452 at 1430 h on 11 March.

Site U1451

We drilled two holes at Site U1451 (proposed Site MBF-3A). Hole U1451A extended from the seafloor to 582.1 m DSF and was advanced by the APC, HLAPC, and XCB systems, as well as short (4.8 m) intervals drilled without coring. A reentry cone with 401.76 m of 10¾ inch casing was installed in Hole U1451B and then was cored with both the XCB and RCB systems to a total depth of 1181.3 m DSF. Unfavorable hole conditions in Hole U1451B precluded collecting wireline log data.

Hole U1451A

After the 64 nmi transit from Site U1450, we arrived at Site U1451 at 1018 h on 17 February 2015. We assembled the APC/XCB BHA, lowered it to the seafloor, and started coring in Hole U1451A at 1810 h. Cores 1H–9H extended to 55.6 mbsf and were advanced by recovery; they were also oriented. The last of these cores recovered only 3.3 m, so we switched to HLAPC cores. Cores 10F–21F extended from 55.6 to 112.0 mbsf (56.4 m) and recovered 58.78 m of core (104%).

Based on the nature of the core material recovered, we decided to switch back to APC coring. Cores 22H–30H extended from 112.0 to 197.5 mbsf (85.5 m) and recovered 73.99 m of core (74%). Each of these cores was not advanced by recovery but by the full 9.5 m barrel length. Core orientation was conducted on Cores 23H–30H. The core liner of the last two APC cores failed, so we switched back to the HLAPC system.

The hole was then deepened from 197.5 to 573.7 mbsf with an alternating series of HLAPC cores and 4.8 m advances without coring. The 41 HLAPC cores from this interval (31F–110F) cored 189.0 m and recovered 144.3 m (76%); thirty-nine 4.8 m long intervals were drilled without coring. The majority of the HLAPC cores in this section were partial strokes. Recovery for the last four HLAPC cores was poor (only 0.55–1.30 m), and up to 40,000 lb was required to pull the core barrel out of the formation, despite only having penetrated a short distance into the formation. We decided further HLAPC coring would not work. Before stopping coring operations in Hole U1451A, we took one XCB core (111X; 573.7–582.1 mbsf; 4.75 m recovered; 57%). After this last core from Hole U1451A arrived on deck at 1750 h on 21 February, we started pulling the drill string out of the hole. The bit cleared the seafloor at 2130 h on 21 February. After taking a break from tripping pipe to slip and cut the drill line, we continued to retrieve the drill string, and the bit arrived back on the rig floor at 0600 h on 22 February.

Formation temperature measurements (APCT-3) were made while taking Cores 4H, 7H, 10H, 13H 29H, 52F, and 74F (28.9, 46.3, 60.3, 74.4, 188.0, 301.9, and 406.4 mbsf, respectively). The latter of these broke the record for the deepest piston core formation temperature measurement ever obtained. The previous record was set at our last site.

We cored 394.9 m in Hole U1451A and recovered 337.80 m of core (86%). The breakdown by coring system is as follows:

- 18 APC cores penetrated 141.1 m and recovered 129.96 m of core (92%).
- 53 HLAPC cores penetrated 245.4 m and recovered 203.1 m of core (83%).
- 1 XCB core penetrated 8.4 m and recovered 4.75 m of core (57%).
- Thirty-nine 4.8 m long intervals were drilled without coring for a total length of 187.2 m.

Hole U1451B

After finishing Hole U1451A, we started preparing and assembling the Hole U1451B reentry system to facilitate our deep coring and logging objectives at this site. The preassembled reentry cone was moved over the moonpool, and 401.75 m of 10¾ inch casing was assembled and latched into the reentry cone. To drill this casing

into the seafloor with a bit and underreamer, we made up a drilling assembly consisting of a 9⅞ inch tricone bit, an underreamer set to 12¾ inches, a mud motor, two stands of drill collars, and 328.57 m of drill pipe. The casing running tool was attached to the top of the drilling assembly and then latched into the reentry system. At 0315 h on 23 February, we opened up the moonpool and started lowering the reentry system to the seafloor. After deploying the camera system at 1000 h, we started to drill the reentry system into the seafloor at 1205 h.

At 0430 h on 24 February, we finished drilling in the 401.76 m of 10¾ inch casing with the reentry cone. The reentry cone landed on the mound of cuttings from drilling the hole ~1 m above the seafloor. The bottom of the casing was at ~400.76 mbsf. The casing running tool was detached from the reentry system, and we started to retrieve the camera system and drilling assembly. By 1600 h on 24 February, all parts of the drilling assembly had arrived back on the rig floor and been taken apart, cleaned, and stored. We assembled an APC/XCB BHA with a 9⅞ inch polycrystalline diamond compact (PDC) bit and started lowering it to seafloor at 1830 h on 24 February. We planned to drill without coring to ~540 mbsf (Hole U1451A was cored to 582.1 mbsf) and then XCB core as far as possible. We decided on the APC/XCB system so we had the option to deploy the APC to recover any loose sands, a high-priority science objective, not likely to be recovered by our other coring systems (XCB/RCB).

We reentered Hole U1451B at 0255 h on 25 February, retrieved the camera system, lowered the bit to 396 mbsf (~5 m above the bottom of the casing), dropped a center bit, and then washed to 404.7 mbsf. At 0645 h on 25 February, we started drilling ahead without coring from that depth to 542 mbsf; the previous hole was cored to 582.1 mbsf and we wanted to attempt to recover core from this overlapping interval. We retrieved the center bit and started XCB coring. Eleven XCB cores and a single 6.7 m interval drilled without coring penetrated from 542.0 to 640.8 mbsf (98.8 m). Cores 2X–13X sampled 92.1 m and recovered 19.05 m of core (21%).

Several XCB cutting shoe failures occurred while coring. When Core 7X arrived back on the rig floor, the lower part of the XCB cutting shoe was missing; it had been left in the hole. The inner flow diverter was still in place, so we inferred that the bit became overheated and failed after coring as the bit was pulled off the bottom of the hole. We deployed an XCB barrel with a center bit, advanced 6.7 m to push the pieces of the broken XCB bit out of the path of our coring bit, and then resumed XCB coring (Cores 9X–12X). On the last of these cores (12X), the XCB cutting shoe was recovered with substantial cracks in it; it fell apart on deck when the core was hydraulically extracted from the throat of the cutting shoe. Once again, we inferred that the bit was overheating. For the next core, we decided to reduce the weight on the bit, lower the rotation rate, and increase the fluid being pumped. However, while cutting Core 13X the penetration was substantially reduced, so we retrieved it after only a 3 m advance. When Core 13X was recovered on the rig floor, the lowermost part of the XCB cutting shoe was missing, and we decided that XCB coring was no longer viable. At 1930 h on 26 February, we started pulling out of the hole so we could switch to an RCB coring assembly, reenter Hole U1451B, and continue coring to our target depth.

After the APC/XCB bit arrived back on the rig floor (0340 h on 27 February), we started assembling an RCB bit and BHA. After the bit was spaced out, we picked up three additional drill collars, finished assembling the BHA, and started lowering it to the seafloor at 0800 h on 27 February. We deployed the camera and reentered Hole U1451B at 1642 h. The bit was lowered through the 10¾ inch casing that extends to 400.76 mbsf and then into the open hole below. At 578 mbsf, the bit encountered an obstruction in the hole, so it was raised up to 569 mbsf to install the top drive. At this time, the drill string became stuck in the hole. The drill string was freed after 2 h of working the drill string by applying overpull, torque, and circulation. We raised the bit back up to 549 mbsf, installed two knobbies beneath the top drive, and started washing and reaming back to the bottom of the hole (640.8 mbsf). After reaching the bottom of the hole, we drilled ahead 5 m (640.8–645.8 mbsf) with a center bit to ensure any pieces of the failed XCB cutting shoe were cleared to the side of the hole. Two wireline runs were needed to retrieve the center bit, as the first run came up without the core barrel and center bit. We started RCB coring at 0645 h on 28 February.

Cores 15R–36R penetrated from 645.8 to 860.2 mbsf (214.4 m) and recovered 49.51 m of core (23%). The drill string became stuck after retrieving Core 35R, and 30 min was needed to work the pipe free. Because of poor hole conditions, we decided to conduct a wiper trip after Core 36R arrived on the rig floor. While raising the bit back up into the 10¾ inch casing that extends to 401 mbsf, the drill string encountered significant torque and up to 30,000–40,000 lb of drag. After slipping and cutting the drill line with the bit inside the casing, the bit was lowered to 637 mbsf, where it encountered a bridge. We washed and reamed from this depth back down to the bottom of the hole (860.2 mbsf) and resumed RCB coring at 0145 h on 3 March. After a few fast-penetration, low-recovery cores (Cores 38R–41R; presumably loose sands) with high drill string torque and some overpull, we conducted a short wiper trip by raising the bit from 908.9 to 869.6 mbsf and then washing back to bottom. RCB coring resumed at 1115 h on 3 March.

Cores 42R–73R cored from 908.9 to 1181.3 mbsf (272.4 m) and recovered 104.28 m of core (38%). Because of the nature of the rocks being recovered, we decided to stop further coring at 1440 h on 6 March and conduct wireline logging. We started to raise the bit back up to the base of the 10¾ inch casing (401 m), two joints of drill pipe at a time (doubles) with the top drive in place, because of the poor hole conditions. While raising the bit, the drill string experienced torque and overpull and then became stuck at 963 mbsf. We also observed up to 250 psi of overpressure in the drill pipe. After the drill string was freed, we had to rotate, apply overpull, and circulate to be able to raise the bit up to 529 mbsf. We then removed the top drive but still had 20,000–25,000 lb of overpull until the bit was up inside the casing. Based on hole conditions, we decided it was not reasonable to log the hole. At the end of 6 March, we started reassembling the drill pipe doubles back into stands so that we could resume recovery of the drill string. After the bit was back on board, the rig floor was secured, and the seafloor positioning beacon was recovered, we departed for Site U1450 at 0806 h on 7 March.

Site U1452

Three holes were cored at Site U1452 (proposed Site MBF-5A). Hole U1452A was a single mudline core for high-resolution studies around the Toba ash layer. Hole U1452B penetrated a total of 217.7 m; 174.5 m of this interval was cored and 140.33 m of core was recovered (64%). Hole U1452C was continuously cored from the seafloor to 41.3 mbsf to obtain a more complete sampling of the uppermost levee sequence.

Hole U1452A

After a 29 nmi transit, we arrived at Site U1452 at 1700 h on 11 March 2015, prepared an APC/XCB BHA, and lowered it to the sea-

floor. After lowering the drill string to the seafloor, we attempted to take the mudline APC core in Hole U1452A at 0315 h on 12 March, but the system would not fire (shear pins did not fail). After recovering the APC core barrel and diagnosing/fixing the problem, we redeployed the APC core barrel and started coring Hole U1452A at 0540 h on 12 March. Core 1H penetrated 8 m. This core is dedicated to high-resolution studies around the Toba ash layer, so it was only run through the whole-round logging systems and then stored for postexpedition splitting and sampling. Nonmagnetic hardware (drill collar and core barrels) was used for all APC and HLAPC cores at Site U1452.

Hole U1452B

We then offset the ship 20 m east and started coring Hole U1452B at 0700 h on 12 March. Cores 1H–5H penetrated to 41.4 mbsf and recovered 33.51 m of sediment (80%). All of these cores were oriented. Core 5H was a partial stroke and inferred to have only penetrated ~4.7 m based on the amount of competent material recovered in the top of the core. We then switched to the HLAPC system. Cores 6F–12F penetrated from 41.4 to 71.1 mbsf (29.7 m) and recovered 23.32 m of core (79%). Based on evidence on the outside of the core barrel (rusty steel scrubbed clean by the formation), Core 6F only penetrated 1.5 m into the formation, so it was advanced this amount; all other cores were advanced 4.7 m. From 71.1 to 142.4 mbsf, we started alternating 4.7 m long HLAPC cores with 4.8 m intervals drilled without coring. In this interval, seven HLAPC cores (14F–26F) penetrated 32.9 m and recovered 21.41 m of core (65%). The eight 4.8 m advances without coring penetrated 38.4 m. Nearly continuous HLAPC coring (Cores 28F–43F, except for a single 4.8 m advance without coring) penetrated from 142.4 to 217.7 mbsf and recovered 62.49 m of core (89%). Although we had originally planned to core to 300 mbsf, we decided our primary coring objectives at this site had been achieved. We pulled out of Hole U1452B, and the bit cleared the seafloor at 0030 h on 14 March. Hole U1452B penetrated a total of 217.7 m; 174.5 m of this interval was cored and 140.33 m of core was recovered (64%). The majority of cores were partial strokes.

Hole U1452C

After the ship was offset 20 m south of Hole U1452B, Hole U1452C was continuously cored from the seafloor to 41.3 mbsf to obtain a more complete sampling of the uppermost levee sequence. APC coring in Hole U1452C started at 0245 h on 14 March. After a successful mudline core (1H), we used the XCB system to core from 7.0 to 11.0 mbsf; in Hole U1452B, this interval had poor recovery and appeared to be a hard layer. Unfortunately, this core came back empty. APC coring resumed and Cores 3H–6H extended from 11.0 to 41.3 mbsf (30.3 m) and recovered 30.3 m of core (87%). All APC cores were oriented. When the last core recovered sand, our objective for this hole was reached (we had passed below the targeted levee section), so we pulled out of the hole and recovered the drill string. After the bit was back on board, we secured the rig floor, raised the thrusters, and departed for Site U1453 at 1900 h on 14 March.

Site U1453

At Site U1453 (proposed Site MBF-4A), we cored with the APC and HLAPC systems to 215.7 mbsf. In this interval, 37 cores penetrated 186.7 m and recovered 164.78 m of sediment (88%). Six short (4.8 or 5.0 m) intervals were advanced without coring. After coring was completed, we collected downhole logging data with two tool strings (triple combo and FMS-sonic). Logging was very successful with good hole conditions and reached the full depth of the hole.

Hole U1453A

After a short 23 nmi transit, we arrived at Site U1453 at 2145 h on 14 March 2015. We assembled an APC coring BHA and lowered it to the seafloor. We used an 9.875 inch PDC coring bit with a lockable float valve (LFV) so that we would have a smaller diameter hole for improved log data if hole conditions would allow. Nonmagnetic hardware was used for all cores (drill collar and core barrels). We finished lowering the drill string to the seafloor and started coring in Hole U1453A at 1020 h on 15 March. Except for one 5 m interval advanced without coring, APC and HLAPC coring penetrated from the seafloor to 172.9 mbsf (Cores 1H–34F) and recovered 148.84 m of core (89%). The HLAPC system was used for all cores except for the first four cores (1H–4H) and one deeper core (29H; 142.4–149.4 mbsf) that targeted a hemipelagic layer; these were cored with the APC system. The rest of the coring in Hole U1453A (172.9–215.7 mbsf) consisted of four HLAPC cores alternating with five 4.8 m advances without coring. Cores 36F–42F penetrated 18.8 m and recovered 15.94 m of sediment (85%). The majority of piston cores at this site were partial strokes. Orientation was attempted on all of the APC cores.

After the primary coring objectives were achieved, at 0715 h on 17 March we started preparing the hole for downhole logging. We circulated 25 barrels of mud to clean cuttings out of the hole. To ensure the LFV was functioning properly for logging, we also activated it with a go-devil and an XCB barrel. After filling the hole with 180 barrels of 12.0 lb/gal mud, we raised the bit up to logging depth (78.5 mbsf). The triple combo logging string was assembled, and we began lowering it down the drill string at 1200 h on 17 March. At ~2170 m DRF with the drill pipe well above the seafloor, the string began losing weight. We inferred it had encountered the weighted mud, so we circulated the mud down to the seafloor and resumed lowering the logging tool string. Log data were collected to the full depth of the hole and indicated good hole conditions. After the triple combo was recovered, we ran the FMS-sonic tool string, which also reached the bottom of the hole. The tool string was back on the rig floor just before midnight on 17 March, and the rig floor was cleared of all equipment by 0055 on 18 March. It took us ~45 min to free the pipe from the formation, and the bit cleared the seafloor at 0200 h. We retrieved the drill string, secured the rig floor, raised the thrusters, and departed for Site U1454 at 1130 h on 18 March.

Site U1454

We cored four holes at Site U1454 (proposed Site MBF-7A). Hole U1454A was a single mudline core to 7.5 mbsf for microbiology and geochemical studies. Hole U1454B was cored with the APC and HLAPC systems to 161.8 mbsf and recovered 129.51 m of sediment (88%). This hole also included three 4.8 m advances without coring. Holes U1454C and U1454D were shallow penetrations (37.2 and 37.1 mbsf, respectively) and recovered 30.16 and 24.46 m of sediment (81% and 66%), respectively. Core orientation was attempted for all APC cores, nonmagnetic hardware was used, and many of the cores were only partial strokes.

Hole U1454A

After a 56 nmi transit, we arrived at Site U1454 at 1706 h on 18 March 2015, assembled an APC/XCB BHA, and lowered it to the seafloor. At 0115 h on 19 March, we took a single mudline core in Hole U1454A (1H; 0–7.5 mbsf) for microbiologic and geochemical studies.

Hole U1454B

We offset the ship 20 m east and started coring in Hole U1454B at 0255 h on 19 March. The APC penetrated from the seafloor to 32.1 mbsf (Cores 1H–4H; 30.28 m recovered; 94%). We switched to the HLAPC and cored from 32.1 to 161.8 mbsf. This 129.7 m interval included three 4.8 m advances without coring. Cores 5F–32F sampled 129.7 m of formation and recovered 99.23 m of sediment (86%). Coring was interrupted for 2 h (1400–1600 h on 19 March) when a broken strand on the coring line snagged in the top drive; ~1500 m of coring line had to be cut off and the coring line reterminated. A single temperature measurement was obtained while recovering Core 30F.

Holes U1454C and U1454D

Having achieved our depth objectives, we decided to core two more holes to obtain a more complete section in the upper ~37 m. We pulled the bit out of Hole U1454B, offset the ship 20 m south, and started coring in Hole U1454C at 1650 h on 20 March. Cores 1H–6F penetrated to 37.2 mbsf and recovered 30.16 m (81%). We pulled the bit out of Hole U1454C, offset the ship 20 m west, and started coring in Hole U1454D at 0020 h on 21 March. Cores 1H–5F penetrated to 37.1 mbsf and recovered 24.46 m (66%). We pulled the bit out of the seafloor (0630 h) and retrieved the drill string. Once the bit was back on the rig floor, we secured the rig floor, raised the thrusters, and departed for Site U1455 at 1336 h.

Site U1455

We cored three holes at Site U1455 (proposed Site MBF-1A; DSDP Site 218). Holes U1455A and U1455B each consisted of single mudline core penetrating to 0.9 and 6.9 mbsf, respectively. Hole U1455C consisted of coring in three intervals: from 0 to 122.3 mbsf (APC and HLAPC), from 359.8 to 431.4 mbsf (HLAPC), and from 773.0 to 949.0 m (RCB). The uppermost interval consisted of APC and HLAPC coring and four 4.8 m advances without coring (19.2 m). Cores 1H–24F cored 103.1 m in this interval and recovered 89.82 m of sediment (87%). We drilled 237.5 m without coring from 122.3 to 359.8 mbsf and then resumed continuous HLAPC coring. Cores 26F–41F penetrated from 359.8 to 431.4 mbsf (71.6 m) and recovered 48.82 m of sediment (68%). After retrieving the drill string to switch to the RCB system, we reentered Hole U1455C and drilled ahead without coring from 431.4 to 773.0 mbsf. We RCB cored from that depth to 949.0 mbsf. Cores 43R–60R penetrated 176.0 m and recovered 59.36 m of sediment (34%). Coring ended when the operational time for the expedition expired.

Hole U1455A

After the 26 nmi transit, we arrived at Site U1455 at 1640 h on 21 March. We assembled an APC BHA with a 9⅞ inch PDC bit and a LFV (in case logging became an option) and lowered it to the seafloor. Coring in Hole U1455A started at 0105 h on 22 March. This hole was intended to be a single mudline core for microbiologic and geochemical studies. Because Core 1H recovered only 0.9 m, we decided to offset the ship and start another hole.

Hole U1455B

After the ship was offset 20 m east, coring started in Hole U1455B at 0225 h on 22 March. Core 1H recovered 6.88 m and was considered sufficient for microbiologic and geochemical studies.

Hole U1455C

We offset the ship 20 m south and started coring in Hole U1455C at 0350 h on 22 March. Cores 1H–3H penetrated from the seafloor to 23.2 mbsf and recovered 22.42 m of sediment (97%). Because Core 3H was only a partial stroke and the core liner cracked, we switched to the HLAPC system. The hole was deepened to 122.2 mbsf with 17 HLAPC cores and four 4.8 m advances without coring. Cores 1H–24F cored 103.1 m in this interval and recovered 89.82 m of sediment (87%). We then drilled from 122.3 to 359.8 mbsf (237.5 m) without coring; this lasted from 0230 to 1345 h on 23 March. Continuous HLAPC coring resumed, and Cores 26F–41F penetrated from 359.8 to 431.4 mbsf (71.6 m) and recovered 48.82 m of sediment (68%).

Because the formation was getting quite firm and we had obtained suitable cores from this section, we decided to stop piston coring. We decided that we would reenter this hole with the RCB system to core our deep objectives below ~770 mbsf. We circulated 30 barrels of mud to clear cuttings out of the hole and started raising the bit back up the hole at 1530 h on 24 March. After pulling a couple stands of pipe, we removed the top drive and continued pulling out of the hole. When the bit reached 77.4 m, we assembled a FFF around the drill string and dropped it through the moonpool at 1850 h on 24 March. We waited 1 h to allow the FFF to land, pulled the bit out of the hole at 1955 h, and retrieved the drill string. The APC bit arrived back on the rig floor at 0145 h on 25 March. After a couple of hours servicing the rig (drill line slip and cut; lubricating crown sheave and main blocks; 0230 to 0445 h), we assembled an RCB BHA with a MBR (to allow for any potential logging) and lowered it to the seafloor. The camera system was deployed and we reentered the Hole U1455C FFF after only ~15 min of maneuvering at 1540 h on 25 March. The camera system was retrieved, and we lowered the bit to 219.4 mbsf before it encountered any resistance. The top drive was installed, and we washed and reamed back down to the bottom of the cored part of the hole (431.4 m). We deployed a center bit and started to drill ahead without coring at 2215 h on 25 March.

At 0945 h on 26 March, we finished penetrating to 773 mbsf (DSDP Site 218 had cored to 773 mbsf). The center bit was retrieved and then redeployed in the middle of this drilled interval to ensure it could be removed and to tighten all connections in the core barrel. When the bit reached 773 mbsf, we retrieved the center bit, circulated mud to clean cuttings out of the hole, and started RCB coring at 2030 h on 26 March. Cores 43R–60R penetrated 176.0 m (773.0 to 949.0 mbsf) and recovered 59.36 m of sediment (34%). Coring ended when the operational time for the expedition expired; the last core of Expedition 354 arrived on deck at 1435 h on 28 March. We pulled the drill string out of the formation with the top drive in place until hole conditions were good enough to remove the top drive. The bit cleared the seafloor at 2120 h on 28 March, and it arrived back on the rig floor at 0640 h on 29 March. The BHA was taken apart, the rig floor was secured, the thrusters were raised, and we started our transit to Colombo, Sri Lanka, at 0645 h on 29 March.

Transit to Colombo, Sri Lanka

After the 513 nmi transit, we arrived at Colombo at 0600 on 31 March 2015.

References

Acharyya, S.K., Ray, K.K., and Sengupta, S., 1991. The Naga Hills and Andaman ophiolite belt, their setting, nature and collisional emplacement history. *Physics and Chemistry of the Earth,* 18(1):293–315. **http://dx.doi.org/10.1016/0079-1946(91)90006-2**

Aitchison, J.C., Ali, J.R., and Davis, A.M., 2007. When and where did India and Asia collide? *Journal of Geophysical Research: Solid Earth,* 112(B5):B05423. **http://dx.doi.org/10.1029/2006JB004706**

Avouac, J.P., and Burov, E.B., 1996. Erosion as a driving mechanism of intracontinental mountain growth. *Journal of Geophysical Research: Solid Earth,* 101(B8):17747–17769. **http://dx.doi.org/10.1029/96JB01344**

Beerling, D.J., and Royer, D.L., 2011. Convergent Cenozoic CO_2 history. *Nature Geoscience,* 4(7):418–420. **http://dx.doi.org/10.1038/ngeo1186**

Bender, F., 1983. *Geology of Burma:* Berlin (Gebrüder Borntraeger).

Boulègue, J., and Bariac, T., 1990. Oxygen and hydrogen isotope ratios of interstitial waters from an intraplate deformation area: Bengal Fan, Leg 116. *In* Cochran, J.R., Stow, D.A.V., et al., *Proceedings of the Ocean Drilling Program, Scientific Results,* 116: College Station, TX (Ocean Drilling Program), 127–133. **http://dx.doi.org/10.2973/odp.proc.sr.116.133.1990**

Boos, W.R., and Kuang, Z., 2010. Dominant control of the South Asian monsoon by orographic insulation versus plateau heating. *Nature,* 463(7278):218–222. **http://dx.doi.org/10.1038/nature08707**

Bouquillon, A., France-Lanord, C., Michard, A., and Tiercelin, J.-J., 1990. Sedimentology and isotopic chemistry of the Bengal Fan sediments: the denudation of the Himalaya. *In* Cochran, J.R., Stow, D.A.V., et al., *Proceedings of the Ocean Drilling Program, Scientific Results,* 116: College Station, TX (Ocean Drilling Program), 43–58. **http://dx.doi.org/10.2973/odp.proc.sr.116.117.1990**

Brunnschweiler, R.O., 1966. On the geology of Indoburman ranges. *Journal of the Geological Society of Australia,* 13(1):137–194. **http://dx.doi.org/10.1080/00167616608728608**

Burbank, D.W., Derry, L.A., and France-Lanord, C., 1993. Reduced Himalayan sediment production 8 Myr ago despite an intensified monsoon. *Nature,* 364(6432):48–50. **http://dx.doi.org/10.1038/364048a0**

Cande, S.C., and Kent, D.V., 1995. Revised calibration of the geomagnetic polarity timescale for the Late Cretaceous and Cenozoic. *Journal of Geophysical Research: Solid Earth,* 100(B4):6093–6095. **http://dx.doi.org/10.1029/94JB03098**

Cerling, T., 1997. Late Cenozoic vegetation change, atmospheric CO_2, and tectonics. *In* Ruddiman, W.F. (Ed.), *Tectonic Uplift and Climate Change:* New York (Plenum), 313–327.

Clift, P.D., 2006. Controls on the erosion of Cenozoic Asia and the flux of clastic sediment to the ocean. *Earth and Planetary Science Letters,* 241(3–4):571–580. **http://dx.doi.org/10.1016/j.epsl.2005.11.028**

Clift, P.D., Hodges, K.V., Heslop, D., Hannigan, R., Long, H.V., and Calves, G., 2008. Correlation of Himalayan exhumation rates and Asian monsoon intensity. *Nature Geoscience,* 1(12):875–880. **http://dx.doi.org/10.1038/ngeo351**

Cochran, J.R., 1990. Himalayan uplift, sea level, and the record of Bengal Fan sedimentation at the ODP Leg 116 sites. *In* Cochran, J.R., Stow, D.A.V., et al., *Proceedings of the Ocean Drilling Program, Scientific Results,* 116: College Station, TX (Ocean Drilling Program), 397–414. **http://dx.doi.org/10.2973/odp.proc.sr.116.144.1990**

Cochran, J.R., Stow, D.A.V., et al., 1989. *Proceedings of the Ocean Drilling Program, Initial Reports,* 116: College Station, TX (Ocean Drilling Program). **http://dx.doi.org/10.2973/odp.proc.ir.116.1989**

Contreras-Rosales, L.A., Jennerjahn, T., Tharammal, T., Meyer, V., Lückge, A., Paul, A., and Schefuß, E., 2014. Evolution of the Indian Summer Monsoon and terrestrial vegetation in the Bengal region during the past 18 ka. *Quaternary Science Reviews,* 102:133–148. **http://dx.doi.org/10.1016/j.quascirev.2014.08.010**

Copeland, P., and Harrison, T.M., 1990. Episodic rapid uplift in the Himalaya revealed by $^{40}Ar/^{39}Ar$ analysis of detrital K-feldspar and muscovite, Bengal Fan. *Geology,* 18(4):354–357. **http://dx.doi.org/10.1130/0091-7613(1990)018<0354:ERUITH>2.3.CO;2**

Copley, A., Avouac, J.-P., and Royer, J.-Y., 2010. India-Asia collision and the Cenozoic slowdown of the Indian plate: implications for the forces driving plate motions. *Journal of Geophysical Research: Solid Earth,* 115(B3):B03410. **http://dx.doi.org/10.1029/2009JB006634**

Corrigan, J.D., and Crowley, K.D., 1992. Unroofing of the Himalayas: a view from apatite fission-track analysis of Bengal fan sediments. *Geophysical Research Letters,* 19(23):2345–2348. **http://dx.doi.org/10.1029/92GL02743**

Curray, J.R., 1994. Sediment volume and mass beneath the Bay of Bengal. *Earth and Planetary Science Letters,* 125(1–4):371–383. **http://dx.doi.org/10.1016/0012-821X(94)90227-5**

Curray, J.R., Emmel, F.J., and Moore, D.G., 2003. The Bengal Fan: morphology, geometry, stratigraphy, history and processes. *Marine and Petroleum Geology,* 19(10):1191–1223. **http://dx.doi.org/10.1016/S0264-8172(03)00035-7**

Curray, J.R., Emmel, F.J., Moore, D.G., and Raitt, R.W., 1982. Structure, tectonics and geological history of the northeastern Indian Ocean. *In* Nairn, A.E.M., and Stehli, F.G. (Eds.), *The Ocean Basins and Margins* (Vol. 6): New York (Plenum), 399–450.

Curray, J.R., and Moore, D.G., 1974. Sedimentary and tectonic processes in the Bengal deep-sea fan and geosyncline. *In* Burk, C.A., and Drake, C.L. (Eds.), *The Geology of Continental Margins:* New York (Springer-Verlag), 617–627.

DeCelles, P.G., Gehrels, G.E., Najman, Y., Martin, A.J., Carter, A., and Garzanti, E., 2004. Detrital geochronology and geochemistry of Cretaceous–early Miocene strata of Nepal: implications for timing and diachroneity of initial Himalayan orogenesis. *Earth and Planetary Science Letters,* 227(3–4):313–330. **http://dx.doi.org/10.1016/j.epsl.2004.08.019**

DePaolo, D.J., and Ingram, B.L., 1985. High-resolution stratigraphy with strontium isotopes. *Science,* 227(4689):938–941. **http://dx.doi.org/10.1126/science.227.4689.938**

Derry, L.A., and France-Lanord, C., 1996. Neogene Himalayan weathering history and river $^{87}Sr/^{86}Sr$: impact on the marine Sr record. *Earth and Planetary Science Letters,* 142(1–2):59–74. **http://dx.doi.org/10.1016/0012-821X(96)00091-X**

Derry, L.A., and France-Lanord, C., 1997. Himalayan weathering and erosion fluxes: climate and tectonic controls. *In* Ruddiman, W.F. (Ed.), *Tectonic Uplift and Climate Change:* New York (Plenum), 289–312. **http://dx.doi.org/10.1007/978-1-4615-5935-1_12**

Dettman, D.L., Kohn, M.J., Quade, J., Ryerson, F.J., Ojha, T.P., and Hamidullah, S., 2001. Seasonal stable isotope evidence for a strong Asian monsoon throughout the past 10.7 m.y. *Geology,* 29(1):31–34. **http://dx.doi.org/10.1130/0091-7613(2001)029<0031:SSIEFA>2.0.CO;2**

Duplessy, J.-C., 1982. Glacial to interglacial contrasts in the northern Indian Ocean. *Nature,* 295(5849):494–498. **http://dx.doi.org/10.1038/295494a0**

Dupont-Nivet, G., Lippert, P.C., Van Hinsbergen, D.J.J., Meijers, M.J.M., and Kapp, P., 2010. Palaeolatitude and age of the Indo–Asia collision: palaeomagnetic constraints. *Geophysical Journal International,* 182(3):1189–1198. **http://dx.doi.org/10.1111/j.1365-246X.2010.04697.x**

Edmond, J.M., 1992. Himalayan tectonics, weathering processes, and the strontium isotope record in marine limestones. *Science,* 258(5088):1594–1597. **http://dx.doi.org/10.1126/science.258.5088.1594**

Fluteau, F., Ramstein, G., and Besse, J., 1999. Simulating the evolution of the Asian and African monsoons during the past 30 Myr using an atmospheric general circulation model. *Journal of Geophysical Research: Atmospheres,* 104(D10):11995–12018. **http://dx.doi.org/10.1029/1999JD900048**

France-Lanord, C., and Derry, L.A., 1994. $\delta^{13}C$ of organic carbon in the Bengal Fan: source evolution and transport of C3 and C4 plant carbon to marine sediments. *Geochimica et Cosmochimica Acta,* 58(21):4809–4814. **http://dx.doi.org/10.1016/0016-7037(94)90210-0**

France-Lanord, C., and Derry, L.A., 1997. Organic carbon burial forcing of the carbon cycle from Himalayan erosion. *Nature,* 390(6655):65–67. **http://dx.doi.org/10.1038/36324**

France-Lanord, C., Derry, L., and Michard, A., 1993. Evolution of the Himalaya since Miocene time: isotopic and sedimentological evidence from the Bengal Fan. *In* Treloar, P.J., and Searle, M. (Eds.), *Himalayan Tectonics.* Geological Society Special Publication, 74(1):603–621. **http://dx.doi.org/10.1144/GSL.SP.1993.074.01.40**

France-Lanord, C., Schwenk, T., and Klaus, A., 2014. Bengal Fan: Neogene and late Paleogene record of Himalayan orogeny and climate: a transect across the Middle Bengal Fan. *International Ocean Discovery Program Scientific Prospectus,* 354. **doi:10.14379/iodp.sp.354.2014**

Freeman, K.H., and Colarusso, L.A., 2001. Molecular and isotopic records of C_4 grassland expansion in the late Miocene. *Geochimica et Cosmochimica Acta,* 65(9):1439–1454. **http://dx.doi.org/10.1016/S0016-7037(00)00573-1**

Galy, A., and France-Lanord, C., 2001. Higher erosion rates in the Himalaya: geochemical constraints on riverine fluxes. *Geology,* 29(1):23–26. **http://dx.doi.org/10.1130/0091-7613(2001)029<0023:HERITH>2.0.CO;2**

Galy, A., France-Lanord, C., and Derry, L.A., 1996. The late Oligocene–early Miocene Himalayan belt constraints deduced from isotopic compositions of early Miocene turbidites in the Bengal Fan. *Tectonophysics,* 260(1–3):109–118. **http://dx.doi.org/10.1016/0040-1951(96)00079-0**

Galy, A., France-Lanord, C., and Derry, L.A., 1999. The strontium isotopic budget of Himalayan rivers in Nepal and Bangladesh. *Geochimica et Cosmochimica Acta,* 63(13–14):1905–1925. **http://dx.doi.org/10.1016/S0016-7037(99)00081-2**

Galy, V., Beyssac, O., France-Lanord, C., and Eglinton, T., 2008. Recycling of graphite during Himalayan erosion: a geological stabilization of carbon in the crust. *Science,* 322(5903):943–945. **http://dx.doi.org/10.1126/science.1161408**

Galy, V., Eglinton, T., France-Lanord, C., and Sylva, S., 2011. The provenance of vegetation and environmental signatures encoded in vascular plant biomarkers carried by the Ganges–Brahmaputra rivers. *Earth and Planetary Science Letters,* 304(1–2):1–12. **http://dx.doi.org/10.1016/j.epsl.2011.02.003**

Galy, V., France-Lanord, C., Beyssac, O., Faure, P., Kudrass, H., and Palhol, F., 2007. Efficient organic carbon burial in the Bengal Fan sustained by the Himalayan erosional system. *Nature,* 450(7168):407–410. **http://dx.doi.org/10.1038/nature06273**

Galy, V., France-Lanord, C., Peucker-Ehrenbrink, B., and Huyghe, P., 2010. Sr-Nd-Os evidence for a stable erosion regime in the Himalaya during the past 12 Myr. *Earth and Planetary Science Letters,* 290(3–4):474–480. **http://dx.doi.org/10.1016/j.epsl.2010.01.004**

Galy, V., François, L., France-Lanord, C., Faure, P., Kudrass, H., Palhol, F., and Singh, S.K., 2008. C4 plants decline in the Himalayan basin since the Last Glacial Maximum. *Quaternary Science Reviews,* 27(13–14):1396–1409. **http://dx.doi.org/10.1016/j.quascirev.2008.04.005**

Gartner, S., 1990. Neogene calcareous nannofossil biostratigraphy, Leg 116 (central Indian Ocean). *In* Cochran, J.R., Stow, D.A.V., et al., *Proceedings of the Ocean Drilling Program, Scientific Results,* 116: College Station, TX (Ocean Drilling Program), 165–187. **http://dx.doi.org/10.2973/odp.proc.sr.116.122.1990**

Garzanti, E., Andò, S., France-Lanord, C., Vezzoli, G., Censi, P., Galy, V., and Najman, Y., 2010. Mineralogical and chemical variability of fluvial sediments: 1. Bedload sand (Ganga–Brahmaputra, Bangladesh). *Earth and Planetary Science Letters,* 299(3–4):368–381. **http://dx.doi.org/10.1016/j.epsl.2010.09.017**

Gasparotto, G., Spadafora, E., Summa, V., and Tateo, F., 2000. Contribution of grain size and compositional data from the Bengal Fan sediment to the understanding of Toba volcanic event. *Marine Geology,* 162(2–4):561–572. **http://dx.doi.org/10.1016/S0025-3227(99)00090-0**

Goddéris, Y., and Donnadieu, Y., 2009. Biogeochemistry: climatic plant power. *Nature,* 460(7251):40–41. **http://dx.doi.org/10.1038/460040a**

Goodbred, S.L., Jr., and Kuehl, S.A., 1999. Holocene and modern sediment budgets for the Ganges-Brahmaputra river system: evidence for highstand dispersal to flood-plain, shelf, and deep-sea depocenters. *Geology,* 27(6):559–562. **http://dx.doi.org/10.1130/0091-7613(1999)027<0559:HAMSBF>2.3.CO;2**

Gopala Rao, D., Bhattacharya, G.C., Ramana, M.V., Subrahmanyam, V., Ramprasad, T., Krishna, K.S., Chaubey, A.K., Murty, G.P.S., Srinivas, K., Desa, M., Reddy, S.I., Ashalata, B., Subrahmanyam, C., Mital, G.S., Drolia, R.K., Rai, S.N., Ghosh, S.K., Singh, R.N., and Majumdar, R., 1994. Analysis of multi-channel seismic reflection and magnetic data along 13°N latitude across the Bay of Bengal. *Marine Geophysical Research,* 16(3):225–236. **http://dx.doi.org/10.1007/BF01237515**

Gopala Rao, D., Krishna, K.S., and Sar, D., 1997. Crustal evolution and sedimentation history of the Bay of Bengal since the Cretaceous. *Journal of Geophysical Research: Solid Earth,* 102(B8):17747–17768. **http://dx.doi.org/10.1029/96JB01339**

Heezen, B.C., and Tharp, M., 1966. Physiography of the Indian Ocean. *Philosophical Transactions of the Royal Society, A: Mathematical, Physical & Engineering Sciences,* 259(1099):137–149. **http://dx.doi.org/10.1098/rsta.1966.0003**

Hodell, D.A., Mueller, P.A., McKenzie, J.A., and Mead, G.A., 1989. Strontium isotope stratigraphy and geochemistry of the late Neogene ocean. *Earth and Planetary Science Letters,* 92(2):165–178. **http://dx.doi.org/10.1016/0012-821X(89)90044-7**

Hübscher, C., Spieß, V., Breitzke, M., and Weber, M.E., 1997. The youngest channel-levee system of the Bengal Fan: results from digital sediment echosounder data. *Marine Geology,* 141(1–4):125–145. **http://dx.doi.org/10.1016/S0025-3227(97)00066-2**

Karunakaran, C., Ray, K.K., Sen, C.R., Saha, S.S., and Sarkar, S.K., 1975. Geology of the great Nicobar Island. *Journal of the Geological Society of India,* 16:135–142.

Kingston, J., 1986. Undiscovered petroleum resources of South Asia. *USGS Open-File Report,* 86-80. **http://pubs.er.usgs.gov/publication/ofr8680**

Koepnick, R.B., Burke, W.H., Denison, R.E., Hetherington, E.A., Nelson, H.F., Otto, J.B., and Waite, L.E., 1985. Construction of the seawater $^{87}Sr/^{86}Sr$ curve for the Cenozoic and Cretaceous: supporting data. *Chemical Geology: Isotope Geoscience section,* 58(1–2):55–81. **http://dx.doi.org/10.1016/0168-9622(85)90027-2**

Kottke, B., Schwenk, T., Breitzke, M., Wiedicke, M., Kudrass, H.R., and Spiess, V., 2003. Acoustic facies and depositional processes in the upper submarine canyon Swatch of No Ground (Bay of Bengal). *Deep Sea Research Part II: Topical Studies in Oceanography,* 50(5):979–1001. **http://dx.doi.org/10.1016/S0967-0645(02)00616-1**

Krishna, K.S., Bull, J.M., and Scrutton, R.A., 2001. Evidence for multiphase folding of the central Indian Ocean lithosphere. *Geology,* 29(8):715–718. **http://dx.doi.org/10.1130/0091-7613(2001)029<0715:EFMFOT>2.0.CO;2**

Krishna, K.S., Ramana, M.V., Gopala Rao, D., Murthy, K.S.R., Malleswara Rao, M.M., Subrahmanyan, V., and Sarma, K.V.L.N.S., 1998. Periodic deformation of oceanic crust in the central Indian Ocean. *Journal of Geophysical Research: Solid Earth,* 103(B8):17859–17875. **http://dx.doi.org/10.1029/98JB00078**

Krishnaswami, S., Trivedi, J.R., Sarin, M.M., Ramesh, R., and Sharma, K.K., 1992. Strontium isotopes and rubidium in the Ganga-Brahmaputra river system: weathering in the Himalaya, fluxes to the Bay of Bengal and contributions to the evolution of oceanic $^{87}Sr/^{86}Sr$. *Earth and Planetary Science Letters,* 109(1–2):243–253. **http://dx.doi.org/10.1016/0012-821X(92)90087-C**

Kroon, D., Steens, T., and Troelstra, S.R., 1991. Onset of monsoonal related upwelling in the western Arabian Sea as revealed by planktonic foraminifers. *In* Prell, W.L., Niitsuma, N., et al., *Proceedings of the Ocean Drilling Program, Scientific Results,* 117: College Station, TX (Ocean Drilling Program), 257–263. **http://dx.doi.org/10.2973/odp.proc.sr.117.126.1991**

Kudrass, H.R., Michels, K.H., Wiedicke, M., and Suckow, A., 1998. Cyclones and tides as feeders of a submarine canyon off Bangladesh. *Geology,* 26(8):715–718. **http://dx.doi.org/10.1130/0091-7613(1998)026<0715:CATAFO>2.3.CO;2**

Licht, A., van Cappelle, M., Abels, H.A., Ladant, J.-B., Trabucho-Alexandre, J., France-Lanord, C., Donnadieu, Y., Vandenberghe, J., Rigaudier, T., Lécuyer, C., Terry, D., Jr., Adriaens, R., Boura, A., Guo, Z., Soe, A.N., Quade, J., Dupont-Nivet, G., and Jaeger, J.-J., 2014. Asian monsoons in a

late Eocene greenhouse world. *Nature*, 513(7519):501–506. **http://dx.doi.org/10.1038/nature13704**

Lupker, M., France-Lanord, C., Galy, V., Lavé, J., Gaillardet, J., Gajurel, A.P., Guilmette, C., Rahman, M., Singh, S.K., and Sinha, R., 2012. Predominant floodplain over mountain weathering of Himalayan sediments (Ganga basin). *Geochimica et Cosmochimica Acta,* 84:410–432. **http://dx.doi.org/10.1016/j.gca.2012.02.001**

Lupker, M., France-Lanord, C., Galy, V., Lavé, J., and Kudrass, H., 2013. Increasing chemical weathering in the Himalayan system since the Last Glacial Maximum. *Earth and Planetary Science Letters,* 365:243–252. **http://dx.doi.org/10.1016/j.epsl.2013.01.038**

Lupker, M., France-Lanord, C., Lavé, J., Bouchez, J., Galy, V., Métivier, F., Gaillardet, J., Lartiges, B., and Mugnier, J.-L., 2011. A Rouse-based method to integrate the chemical composition of river sediments: application to the Ganga Basin. *Journal of Geophysical Research: Earth Surface,* 116(F4):F04012. **http://dx.doi.org/10.1029/2010JF001947**

Martinod, J., and Molnar, P., 1995. Lithospheric folding in the Indian Ocean and the rheology of the oceanic plate. *Bulletin de la Societe Geologique de France,* 166(6):813–821. **http://bsgf.geoscienceworld.org/content/166/6/813.extract**

Métivier, F., Gaudemer, Y., Tapponnier, P., and Klein, M., 1999. Mass accumulation rates in Asia during the Cenozoic. *Geophysical Journal International,* 137(2):280–318. **http://dx.doi.org/10.1046/j.1365-246X.1999.00802.x**

Michels, K.H., Kudrass, H.R., Hübscher, C., Suckow, A., and Wiedicke, M., 1998. The submarine delta of the Ganges-Brahmaputra: cyclone-dominated sedimentation patterns. *Marine Geology,* 149(1–4):133–154. **http://dx.doi.org/10.1016/S0025-3227(98)00021-8**

Molnar, P., Boos, W.R., and Battisti, D.S., 2010. Orographic controls on climate and paleoclimate of Asia: thermal and mechanical roles for the Tibetan Plateau. *Annual Review of Earth and Planetary Sciences,* 38(1):77–102. **http://dx.doi.org/10.1146/annurev-earth-040809-152456**

Moore, D.G., Curray, J.R., Raitt, R.W., and Emmel, F.J., 1974. Stratigraphic-seismic section correlations and implications to Bengal Fan history. *In* von der Borch, C.C., Sclater, J.G., et al., *Initial Reports of the Deep Sea Drilling Project,* 22: Washington, DC (U.S. Government Printing Office), 403–412. **http://dx.doi.org/10.2973/dsdp.proc.22.116.1974**

Najman, Y., Bickle, M., BouDagher-Fadel, M., Carter, A., Garzanti, E., Paul, M., Wijbrans, J., Willett, E., Oliver, G., Parrish, R., Akhter, S.H., Allen, R., Ando, S., Chisty, E., Reisberg, L., and Vezzoli, G., 2008. The Paleogene record of Himalayan erosion: Bengal Basin, Bangladesh. *Earth and Planetary Science Letters,* 273(1–2):1–14. **http://dx.doi.org/10.1016/j.epsl.2008.04.028**

Ormond, A., Boulègue, J., and Genthon, P., 1995. A thermoconvective interpretation of heat flow data in the area of Ocean Drilling Program Leg 116 in a distal part of the Bengal Fan. *Journal of Geophysical Research: Solid Earth,* 100(B5):8083–8095. **http://dx.doi.org/10.1029/95JB00072**

Pagani, M., Freeman, K.H., and Arthur, M.A., 1999. Late Miocene atmospheric CO_2 concentrations and expansion of C4 grasses. *Science,* 285(5429):876–879. **http://dx.doi.org/10.1126/science.285.5429.876**

Palamenghi, L., Schwenk, T., Spiess, V., and Kudrass, H.R., 2011. Seismostratigraphic analysis with centennial to decadal time resolution of the sediment sink in the Ganges–Brahmaputra subaqueous delta. *Continental Shelf Research,* 31(6):712–730. **http://dx.doi.org/10.1016/j.csr.2011.01.008**

Peirce, J., Weissel, J., et al., 1989. *Proceedings of the Ocean Drilling Program, Initial Reports,* 121: College Station, TX (Ocean Drilling Program). **http://dx.doi.org/10.2973/odp.proc.ir.121.1989**

Pierson-Wickmann, A.-C., Reisberg, L., France-Lanord, C., and Kudrass, H.R., 2001. Os-Sr-Nd results from sediments in the Bay of Bengal: implications for sediment transport and the marine Os record. *Paleoceanography,* 16(4):435–444. **http://dx.doi.org/10.1029/2000PA000532**

Quade, J., and Cerling, T.E., 1995. Expansion of C_4 grasses in the late Miocene of northern Pakistan: evidence from stable isotopes in paleosols. *Palaeogeography, Palaeoclimatology, Palaeoecology,* 115(1–4):91–116. **http://dx.doi.org/10.1016/0031-0182(94)00108-K**

Quade, J., Cerling, T.E., and Bowman, J.R., 1989. Development of Asian monsoon revealed by marked ecological shift during the latest Miocene in northern Pakistan. *Nature,* 342(6246):163–166. **http://dx.doi.org/10.1038/342163a0**

Ramstein, G., Fluteau, F., Besse, J., and Joussaume, S., 1997. Effect of orogeny, plate motion and land–sea distribution on Eurasian climate change over the past 30 million years. *Nature,* 386(6627):788–795. **http://dx.doi.org/10.1038/386788a0**

Raymo, M.E., and Ruddiman, W.F., 1992. Tectonic forcing of late Cenozoic climate. *Nature,* 359(6391):117–122. **http://dx.doi.org/10.1038/359117a0**

Richter, F.M., Rowley, D.A., and DePaolo, D.J., 1992. Sr isotope evolution of seawater: the role of tectonics. *Earth and Planetary Science Letters,* 109(1–2):11–23. **http://dx.doi.org/10.1016/0012-821X(92)90070-C**

Rowley, D.B., 1996. Age of initiation of collision between India and Asia: a review of stratigraphic data. *Earth and Planetary Science Letters,* 145(1–4):1–13. **http://dx.doi.org/10.1016/S0012-821X(96)00201-4**

Rowley, D.B., 1998. Minimum age of initiation of collision between India and Asia north of Everest based on the subsidence history of the Zhepure Mountain section. *Journal of Geology,* 106(2):229–235. **http://dx.doi.org/10.1086/516018**

Schwenk, T., and Spieß, V., 2009. Architecture and stratigraphy of the Bengal Fan as response to tectonic and climate revealed from high-resolution seismic data. *In* Kneller, B.C., Martinsen, O.J., and McCaffrey, B. (Eds.), *External Controls on Deep-Water Depositional Systems.* Special Publication - SEPM (Society of Sedimentary Geologists), 92:107–131.

Schwenk, T., Spieß, V., Hübscher, C., and Breitzke, M., 2003. Frequent channel avulsions within the active channel–levee system of the middle Bengal Fan—an exceptional channel–levee development derived from Parasound and Hydrosweep data. *Deep Sea Research Part II: Topical Studies in Oceanography,* 50(5):1023–1045. **http://dx.doi.org/10.1016/S0967-0645(02)00618-5**

Shipboard Scientific Party, 1974. Site 218. *In* von der Borch, C.C., Sclater, J.G., et al., *Initial Reports of the Deep Sea Drilling Project,* 22: Washington, DC (U.S. Government Printing Office), 325–338. **http://dx.doi.org/10.2973/dsdp.proc.22.109.1974**

Shipboard Scientific Party, 1989a. Site 717: Bengal Fan. *In* Cochran, J.R., Stow, D.A.V., et al., *Proceedings of the Ocean Drilling Program, Initial Reports,* 116: College Station, TX (Ocean Drilling Program), 45–89. **http://dx.doi.org/10.2973/odp.proc.ir.116.105.1989**

Shipboard Scientific Party, 1989b. Site 718: Bengal Fan. *In* Cochran, J.R., Stow, D.A.V., et al., *Proceedings of the Ocean Drilling Program, Initial Reports,* 116: College Station, TX (Ocean Drilling Program), 91–154. **http://dx.doi.org/10.2973/odp.proc.ir.116.106.1989**

Shipboard Scientific Party, 1989c. Site 719: Bengal Fan. *In* Cochran, J.R., Stow, D.A.V., et al., *Proceedings of the Ocean Drilling Program, Initial Reports,* 116: College Station, TX (Ocean Drilling Program), 155–196. **http://dx.doi.org/10.2973/odp.proc.ir.116.107.1989**

Spiess, V., Hübscher, C., Breitzke M., Böke, W., Krell, A., von Larcher, T., Matschkowski, T., Schwenk, T., Wessels, A., Zühlsdorff, L., and Zühlsdorff, S., 1998. Report and preliminary results of R/V *Sonne* Cruise 125, Cochin-Chittagong, 17.10–17.11.97. *Berichte aus dem Fachbereich Geowissenschaften der Universität Bremen,* 123. **http://elib.suub.uni-bremen.de/ip/docs/00010242.pdf**

Stow, D.A.V., Amano, K., Balson, P.S., Brass, G.W., Corrigan, J., Raman, C.V., Tiercelin, J.-J., Townsend, M., and Wijayananda, N.P., 1990. Sediment facies and processes on the distal Bengal Fan, Leg 116. *In* Cochran, J.R., Stow, D.A.V., et al., *Proceedings of the Ocean Drilling Program, Scientific Results,* 116: College Station, TX (Ocean Drilling Program), 377–396. **http://dx.doi.org/10.2973/odp.proc.sr.116.110.1990**

van Hinsbergen, D.J.J., Steinberger, B., Doubrovine, P.V., and Gassmöller, R., 2011. Acceleration and deceleration of India-Asia convergence since the Cretaceous: roles of mantle plumes and continental collision. *Journal of*

Geophysical Research: Solid Earth, 116(B6):B06101. **http://dx.doi.org/10.1029/2010JB008051**

von der Borch, C.C., Sclater, J.G., et al., 1974. *Initial Reports of the Deep Sea Drilling Project,* 22: Washington (U.S. Government Printing Office). **http://dx.doi.org/10.2973/dsdp.proc.22.1974**

Weber, M.E., Wiedicke, M.H., Kudrass, H.R., Hübscher, C., and Erlenkeuser, H., 1997. Active growth of the Bengal Fan during sea-level rise and high-stand. *Geology,* 25(4):315–318. **http://dx.doi.org/10.1130/0091-7613(1997)025<0315:AGOTBF>2.3.CO;2**

Weber, M.E., Wiedicke-Hombach, M., Kudrass, H.R., and Erlenkeuser, H., 2003. Bengal Fan sediment transport activity and response to climate forcing inferred from sediment physical properties. *Sedimentary Geology,* 155(3–4), 361–381. **http://dx.doi.org/10.1016/S0037-0738(02)00187-2**

Willenbring, J.K., and von Blanckenburg, F., 2010. Long-term stability of global erosion rates and weathering during late-Cenozoic cooling. *Nature,* 465(7295):211–214. **http://dx.doi.org/10.1038/nature09044**

Zachos, J., Pagani, M., Sloan, L., Thomas, E., and Billups, K., 2001. Trends, rhythms, and aberrations in global climate 65 Ma to present. *Science,* 292(5517):686–693. **http://dx.doi.org/10.1126/science.1059412**

Zhang, P., Molnar, P., and Downs, W.R., 2001. Increased sedimentation rates and grain sizes 2–4 Myr ago due to the influence of climate change on erosion rates. *Nature,* 410(6831):891–897. **http://dx.doi.org/10.1038/35073504**

Zhang, Q., Willems, H., Ding, L., Gräfe, K.-U., and Appel, E., 2012. Initial India-Asia continental collision and foreland basin evolution in the Tethyan Himalaya of Tibet: evidence from stratigraphy and paleontology. *Journal of Geology,* 120(2):175–189. **http://dx.doi.org/10.1086/663876**

Zhisheng, A., Kutzbach, J.E., Prell, W.L., and Porter, S.C., 2001. Evolution of Asian monsoons and phased uplift of the Himalaya–Tibetan plateau since late Miocene times. *Nature,* 411(6833):62–66. **http://dx.doi.org/10.1038/35075035**

Table T1. Operations summary. See Figure **F4** for location of drill sites. **Download table in .csv format.**

Hole	Proposed site	Location	Water depth (mbsl)	Total penetration (m)	Interval cored (m)	Interval drilled without coring (m)	Core recovery (m)	Core recovery (%)	Time on hole (d)	Cores (*N*)
354-										
U1449A	MBF-6A	8°0.4194′N, 88°6.5994′E	3652.7	213.5	212.5	1.0	129.38	61	2.9	37
U1449B		8°0.4206′N, 88°6.6091′E	3651.9	7.9	7.9	0	7.91	100	0.5	1
			Site U1449 totals:	221.4	220.4	1.0	137.29	62	3.4	38
U1450A	MBF-2A	8°0.4201′N, 87°40.2478′E	3655.3	687.4	444.7	242.7	282.73	64	6.4	86
U1450B		8°0.4192′N, 87°40.2586′E	3655.4	811.9	203.9	608.0	46.67	23	4.0	21
			Site U1450 totals:	1499.3	648.6	850.7	329.40	51	10.4	107
U1451A	MBF-3A	8°0.4195′N, 88°44.5012′E	3607.3	582.1	394.9	187.2	337.80	86	4.8	72
U1451B		8°0.4203′N, 88°44.4745′E	3607.2	1181.3	627.6	553.7	180.86	29	13.1	70
			Site U1451 totals:	1763.4	1022.5	740.9	518.66	51	17.9	142
U1452A	MBF-5A	8°0.4196′N, 87°10.9001′E	3670.5	8.0	8.0	—	8.03	100	0.6	1
U1452B		8°0.4191′N, 87°10.9128′E	3670.3	217.7	174.5	43.2	138.21	79	1.8	34
U1452C		8°0.4088′N, 87°10.9116′E	3671.5	41.3	41.3	—	33.30	81	0.8	6
			Site U1452 totals:	267.0	223.8	43.2	179.54	80	3.1	41
U1453A	MBF-4A	8°0.4193′N, 86°47.8973′E	3679.5	215.7	186.7	29.0	164.78	88	3.6	37
			Site U1453 totals:	215.7	186.7	29.0	164.78	88	3.6	37
U1454A	MBF-7A	8°0.4067N,′ 85°50.9882′E	3709.9	7.5	7.5	—	7.54	101	0.4	1
U1454B		8°0.4083′N, 85°51.0025′E	3710.3	161.8	147.4	14.4	129.51	88	1.6	29
U1454C		8°0.3968′N, 85°51.0033′E	3710.3	37.2	37.2	—	30.16	81	0.4	6
U1454D		8°0.3975′N, 85°50.9927′E	3710.7	37.1	37.1	—	24.46	66	3.4	5
			Site U1454 totals:	243.6	229.2	14.4	191.67	84	5.7	41
U1455A	MBF-1A	8°0.4189′N, 86°16.9983′E	3732.5	0.9	0.9	—	0.90	100	0.4	1
U1455B		8°0.4198′N, 86°17.0096′E	3733.0	6.9	6.9	—	6.88	100	0.1	1
U1455C		8°0.4081′N, 86°17.0090′E	3732.5	949.0	350.7	598.3	198.00	56	7.1	54
			Site U1455 totals:	956.8	358.5	598.3	205.8	57	7.56	56
			Expedition 354 totals:	5167.2	2889.7	2277.5	1727.12	60	51.6	462
353-										
U1444A	MBF-10	14°0.0057′N, 84°49.7405′E	3127.7	330.6	330.6	0.0	226.05	68	3.0	37
U1444B		13°59.9940′N, 84°49.7412′E	3131.8	128.6	81.1	47.5	74.16	91	1.0	9
			Expedition 353 totals:	459.2	411.7	47.5	300.21	73	3.9	46

Figure F1. Cenozoic changes: global cooling and glaciations (Zachos, 2001), Oligocene atmospheric PCO_2 drawdown (Beerling and Royer, 2011) possibly related to a change in the balance between erosion and volcanic input of CO_2, Oligocene rise of seawater $^{87}Sr/^{86}Sr$ (Koepnick et al., 1985) likely reflecting the erosion of radiogenic formations analog of the modern Himalaya, and Eocene slowdown of the Indian plate motion following the collision and Tibet Uplift (Copley et al., 2010). Right: extent of existing sedimentary records in the Bengal fan and Himalayan foreland.

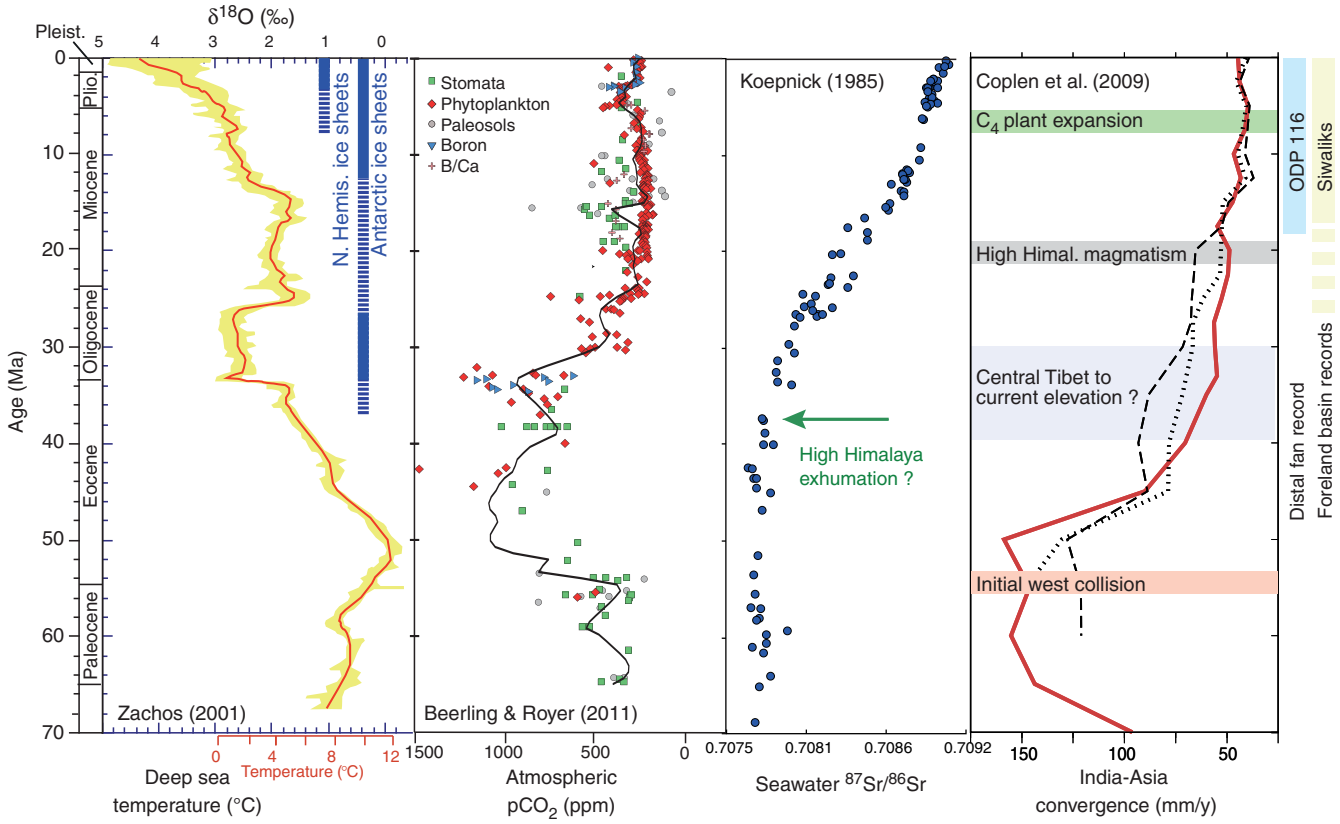

Figure F2. Map of the Himalayan erosion system showing the position of existing DSDP and ODP sites documenting the Bengal and Indus Fans or the monsoon history. Box = location of Expedition 354 Middle Bengal Fan (MBF) drill site transect at 8°N. Bengal Fan sediment isopachs (blue lines; in kilometers) are simplified from Curray et al. (2003) and represent the total sedimentary and metasedimentary rocks above the oceanic basalt as interpreted from seismic reflection and refraction data.

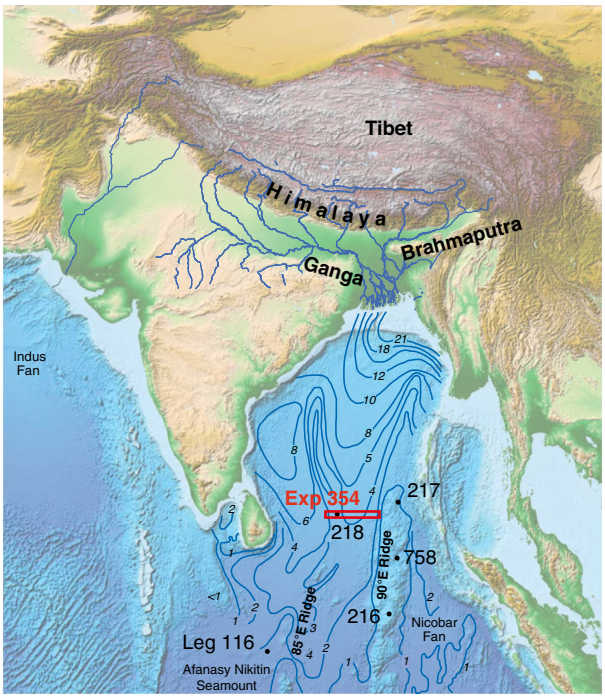

Figure F3. A. Seismic Profile GeoB097-020/027 showing the positions of Expedition 354 drill sites in relation to regional fan architecture. The tops of the Pliocene and Miocene, as well as the 10 Ma horizon, are traced through the profile based on results from DSDP Site 218 (Moore et al., 1974). The distinct unconformity in the east penetrated only by the deepest part of Site U1451 is inferred to represent the Eocene onset of fan deposition. CMP = common midpoint. B. Interpreted line drawing of Profile GeoB97-020/027 showing the later stage channel-levee systems, regional unconformities, and faults. Modified from Schwenk and Spiess (2009). VE = vertical exaggeration. Horizontal scale = CMP, CMP distance = 20 m. Naming of channels follows Curray et al. (2003).

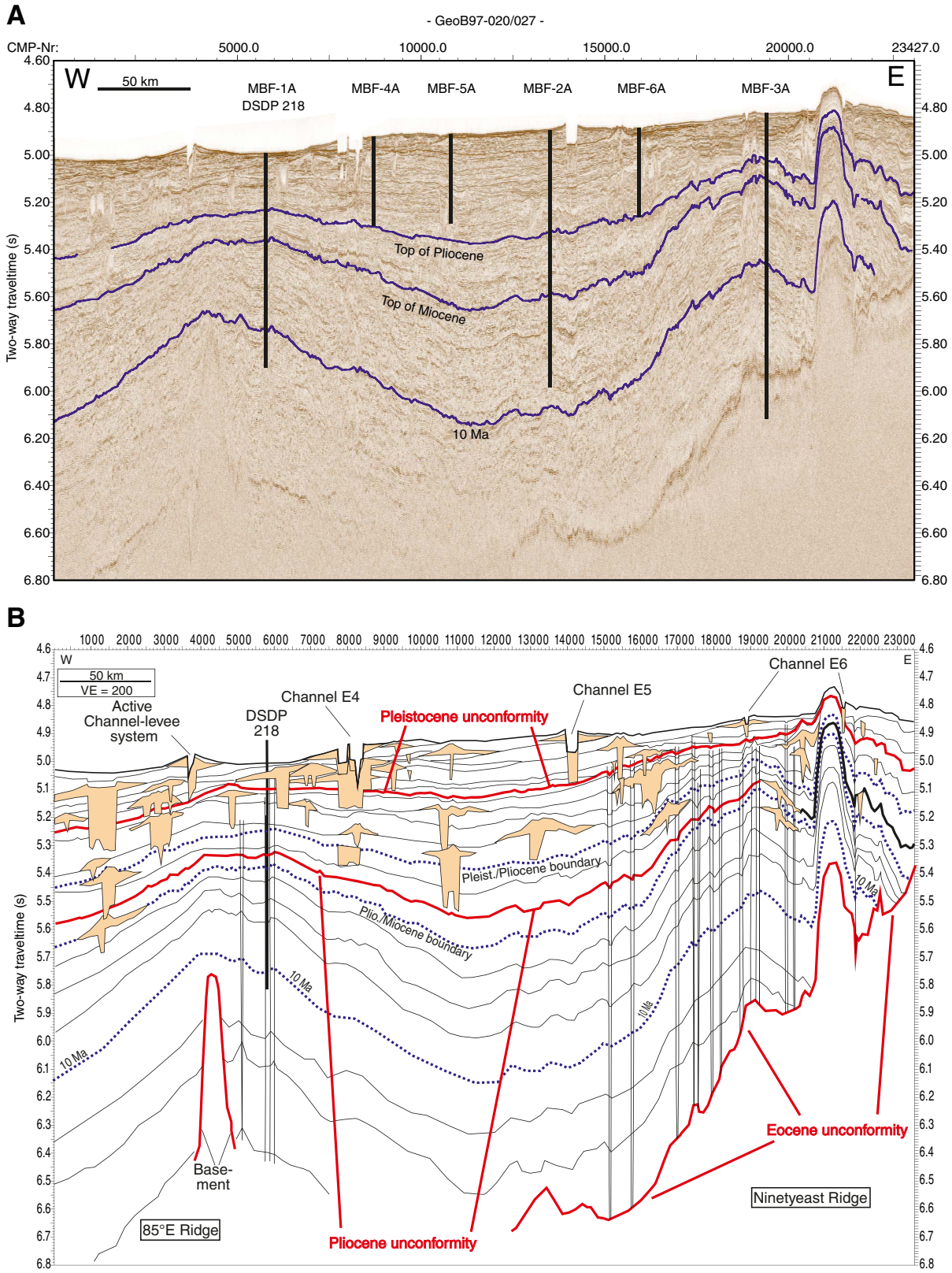

Figure F4. Location of Expedition 354 drill sites.

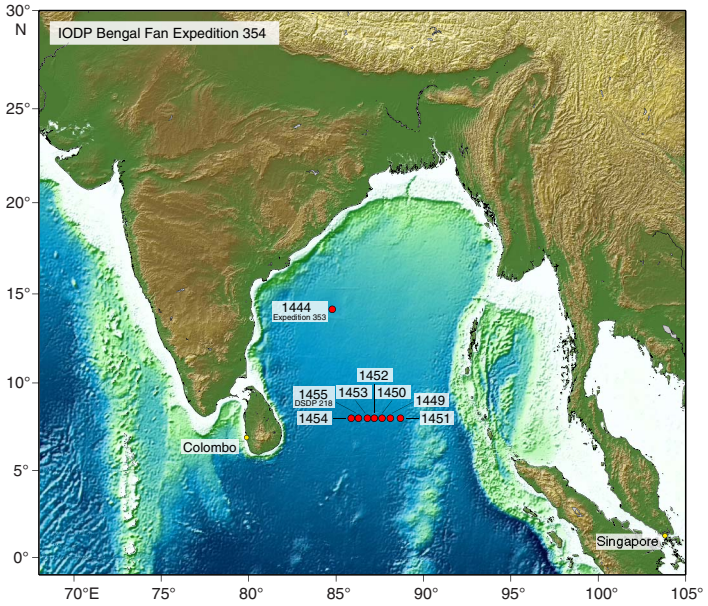

Figure F5. Compilation for the upper 250 m of the seven site drilling transect at 8°N from west to east, comprising subbottom depth axis, core numbers and recovery, and major and minor lithologies for the deepest hole at each site. Geographic longitude is given for each hole..

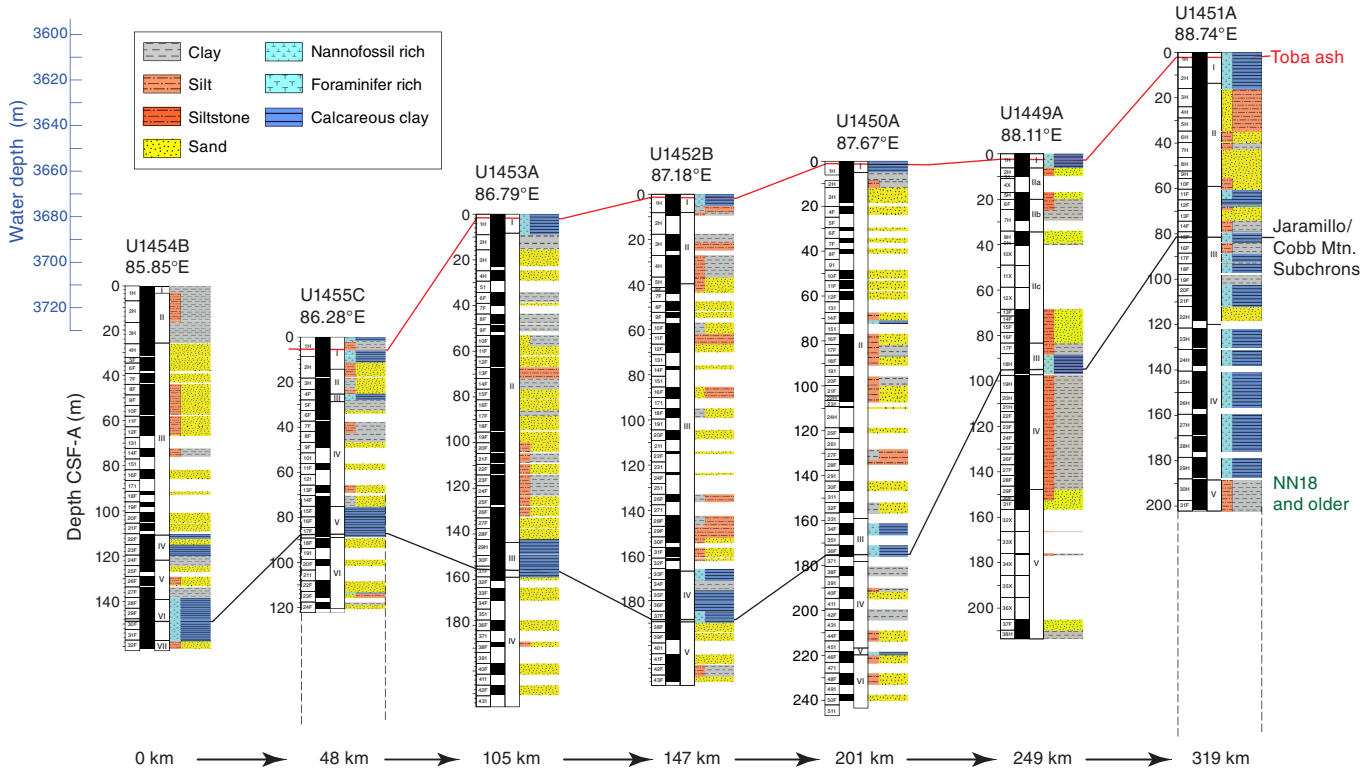

Figure F6. Compilation of the three deep holes of the drilling transect at 8°N from west to east, comprising subbottom depth axis, recovery, and major and minor lithologies for each site.

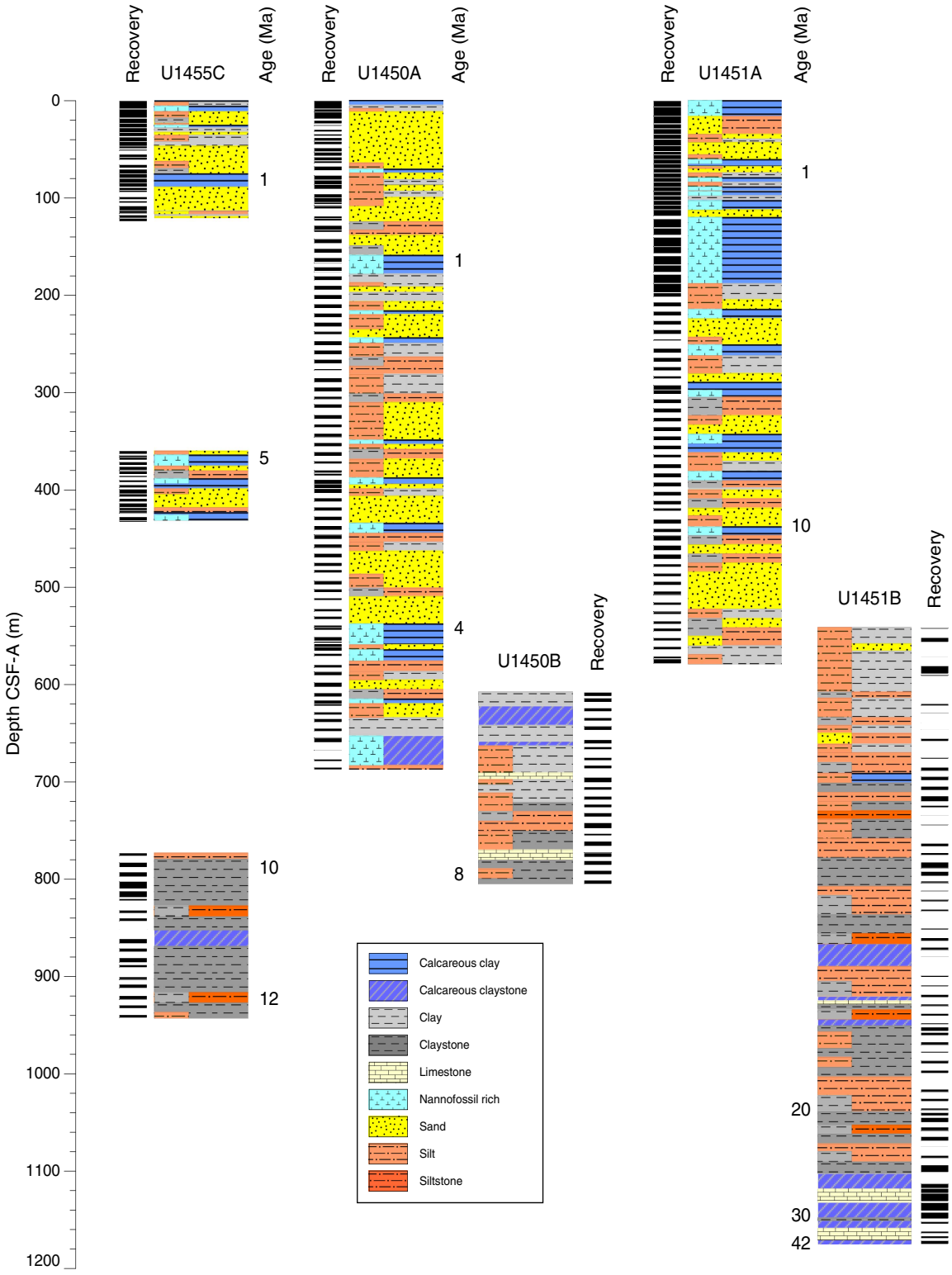

Figure F7. Estimated age span of Bengal Fan sedimentation vs. distance from the present apex or source of the fan. Shaded area at each site = known age span of fan sedimentation. The duration of the apparent hiatus was short near the source and long in the lower and distal fan. This plot is oversimplified because the distance from the fan apex changed through time with convergence of the Indian and Eurasian plates and with progradation of the delta in Bangladesh. IB ranges = Indo-Burman ranges, A-N Ridge = Andaman-Nicobar Ridge. DSDP and ODP numbers are sites.

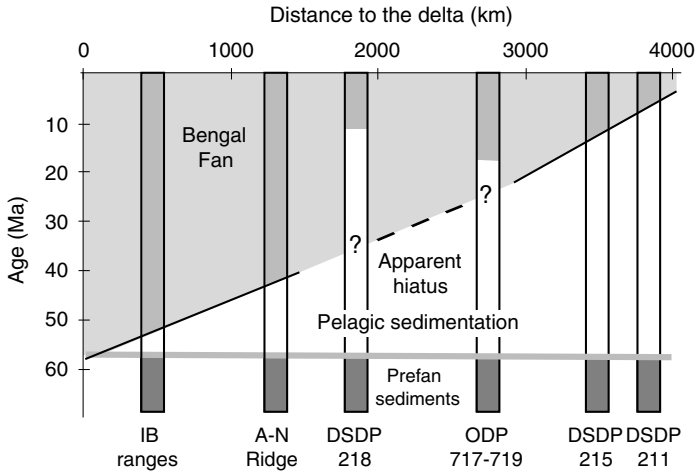

Figure F8. Map showing proposed Expedition 354 drill sites of on top of multibeam bathymetry. Available seismic lines from R/V *Sonne* Cruises SO125 (black) and SO188 (red) are indicated. Profiles crossing the sites are highlighted. See Site summaries and appendix figures in France-Lanord et al. (2014) for seismic data at each proposed site.

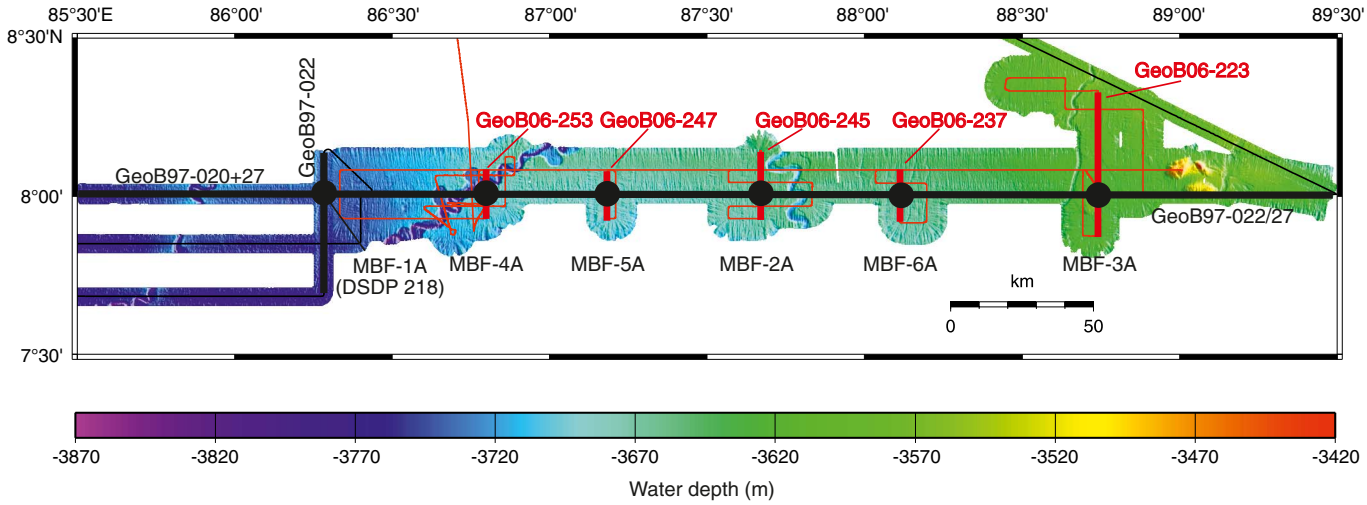

Figure F9. Accumulation rate (Gartner, 1990), clay mineralogy (Bouquillon et al., 1990), Nd isotopic data (Derry and France-Lanord, 1996; France-Lanord et al., 1993; Galy et al., 1996), and total organic carbon isotopic composition (France-Lanord and Derry, 1994), ODP Holes 717C and 718C. Ages recalculated using timescale of Cande and Kent (1995). Low sedimentation rates, smectite-kaolinite clays, and organic carbon derived from C_4 plants characterize the interval from 7.4 to 0.9 Ma. Nd isotopic composition does not change during the entire time recovered, suggesting the eroded source of material is not significantly changing. Biostratigraphic constraints on sediment accumulation are uncertain for the early Miocene. The apparent increase in sedimentation rate near 12 Ma could be an artifact of poor biostratigraphic control prior to that time.

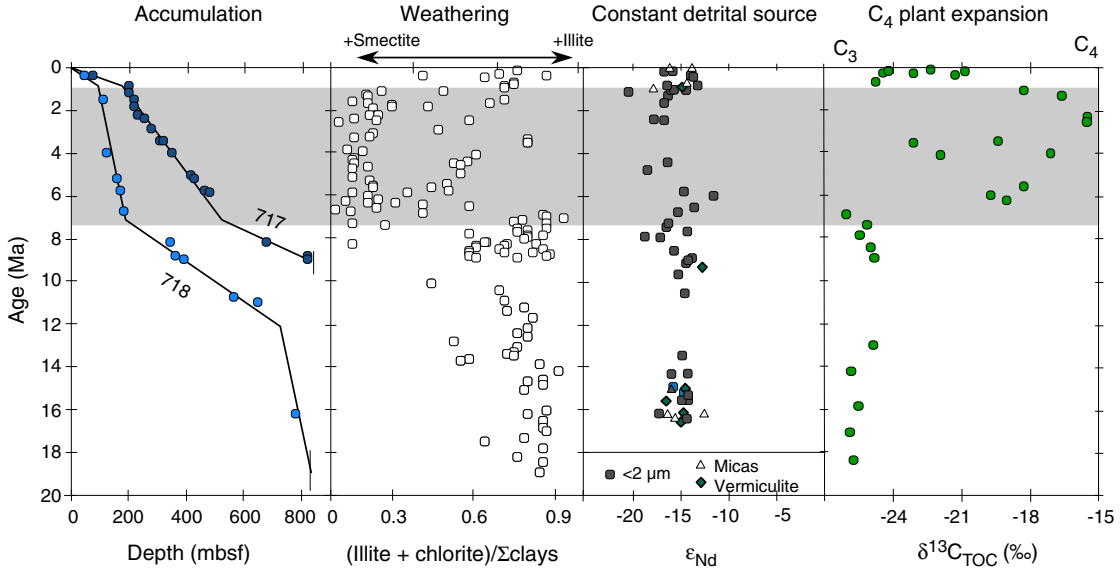

Figure F10. Actual and planned Expedition 354 operations.